ITALO ANTÔNIO FERNANDES

MOLECULAR DOCKING OF INDOLIN-2-ONE COMPOUNDS AS PROMISING DUAL AURORA B/FLT3 INHIBITORS AS ANTICANCER AGENTS

LAVRAS-MG

2018

ITALO ANTÔNIO FERNANDES

MOLECULAR DOCKING OF INDOLIN-2-ONE COMPOUNDS AS PROMISING DUAL AURORA B/FLT3 INHIBITORS AS ANTICANCER AGENTS

Tese apresentada à Universidade Federal de Lavras, como parte das exigências do Programa de Pós-Graduação em Agroquímica, área de concentração em Química/Bioquímica, para a obtenção do título de Doutor.

Orientadora

Prof. Dra. Elaine Fontes Ferreira da Cunha

LAVRAS-MG

2018

Ficha catalográfica elaborada pelo Sistema de Geração de Ficha Catalográfica da Biblioteca Universitária da UFLA, com dados informados pelo(a) próprio(a) autor(a).

Fernandes, Italo Antônio.
Molecular Docking of Indolin-2-one Compounds as Promising Dual Aurora B/FLT3 Inhibitors as Anticancer Agents / Italo Antônio Fernandes. - 2018.
105 p. : il.

Orientador(a): Elaine Fontes Ferreira da Cunha.
.
Tese (doutorado) - Universidade Federal de Lavras, 2018.
Bibliografia.

1. Docking. 2. Indolin-2-one derivatives. 3. Dual Aurora B/FLT3 inhibitors. I. Cunha, Elaine Fontes Ferreira da. . II. Título.

ITALO ANTÔNIO FERNANDES

ANCORAMENTO MOLECULAR DE COMPOSTOS INDOLIN-2-ONA COMO PROMISSORES INIBIDORES DUAIS DE AURORA B/FLT3 COMO AGENTES ANTICÂNCER

MOLECULAR DOCKING OF INDOLIN-2-ONE COMPOUNDS AS PROMISING DUAL AURORA B/FLT3 INHIBITORS AS ANTICANCER AGENTS

Tese apresentada à Universidade Federal de Lavras, como parte das exigências do Programa de Pós-Graduação em Agroquímica, área de concentração em Química/Bioquímica, para a obtenção do título de Doutor.

APROVADA EM 07 de dezembro de 2018

Dr. Teodorico de Castro Ramalho UFLA
Dra. Luciana Lopes Silva Pereira UFLA
Dr. Fernando Henrique Ferrari Alves UFLA
Dr. Alexandre Carvalho Bertoli UFMG

Prof. Dra. Elaine Fontes Ferreira da Cunha
Orientadora

LAVRAS-MG

2018

Aos meus pais por tornarem essa conquista possível

À Déborah, minha esposa, companheira, amiga, meu espelho...

DEDICO

AGRADECIMENTOS

A caminhada até aqui foi desafiadora, mas essa conquista não seria possível sem ela, muito mais que minha esposa, meu alicerce, meu tudo. Muito obrigado, meu amor, Déborah Braga Resende. Essa etapa não seria possível sem sua presença, certamente! Amo muito você! Obrigado por ser a pessoa que é!

Agradeço a Deus pela caminhada ao longo desses anos de muitos aprendizados. Nos momentos bons e ruins, por me conceder sabedoria, saúde e conduzir-me ao longo de toda minha vida.

Ao Luck, considerado e tratado como filho, por só momentos bons, pela sensibilidade que só um cachorro é capaz de ter, por "levantar-me" nos maus momentos e sempre me alegrar. Um verdadeiro companheiro. Só quem tem um cão é capaz de entender...

Àos meus pais, Antônio e Ismênia, que, apesar da distância, sempre me apoiaram e torceram pelo meu sucesso. Obrigado pelas orações. Por terem sempre me incentivado aos estudos e darem a mim, lá na graduação, a oportunidade de começar.

Aos meus sobrinhos, Elias e Natã, pelas visitas e momentos de descontração.

Ao meu sogro e minha sogra, Carlos e Pilar, por acreditarem e incentivarem ao longo desses anos. Desculpem-me os muitos finais de semana presente, "mas ausente".

À minha orientadora, Elaine, pela sua compreensão, paciência, conhecimento, alegria, fez com que todos esses anos fossem fluindo de uma forma mais leve e amigável, mas também de forma dedicada e compromissada. Obrigado por compartilhar seus ensinamentos e conhecimentos comigo.

Ao professor Evaristo Mauro pela compreensão, pelo incentivo e colaboração em todos os momentos.

Aos professores, Teodorico e Guerreiro, docentes do PPGAQ, pelos ensinamentos, pela atenção, comprometimento, exemplos de profissionais a serem seguidos.

Agradeço ao PPGAQ de uma forma geral, por todos aqueles que diretamente e indiretamente contribuíram nessa caminhada. À UFLA pela infraestrutura e oportunidade oferecidas.

“Nas grandes batalhas da vida, o primeiro passo para a vitória é o desejo de vencer”

Mahatma Ghandi

“Aqueles que se sentem satisfeitos sentam-se e nada fazem. Os insatisfeitos são os únicos benfeitores do mundo”

Walter Savage Landor

“A persistência é o menor caminho do êxito”

Charles Chaplin

“Talvez não tenha conseguido fazer o melhor, mas lutei para que o melhor fosse feito”

Marthin Luther King

RESUMO

Enzimas Aurora quinases desempenham importantes funções em mamíferos, principalmente no ciclo celular. A superexpressão dessas enzimas está relacionada ao desenvolvimento de tumores, sendo também indicativa de piora das condições clínicas dos pacientes diagnosticados com câncer. Aurora quinases são alvos promissores na busca de novos fármacos anticâncer, com destaque para Aurora B. Outra enzima relacionada a processos tumorais é a tirosina quinase FLT3 e intimamente relacionada à leucemia mieloide aguda (LMA). A enzima FLT3 é expressa em membranas de células hematopoiéticas precursoras e tem papel importante na diferenciação, proliferação e multiplicação celular. Na LMA ocorre normalmente hiperestimulação ou mutações na enzima FLT3, levando à proliferação celular exacerbada e menor resposta aos agentes citotóxicos padrões. Inibidores FLT3 e duais Aurora B/FLT3 têm se mostrado relevantes na busca por novos promissores compostos anticâncer, principalmente para a LMA. Este trabalho foi realizado para estudar e compreender as interações entre dois alvos diferentes, as enzimas Aurora B e FLT3, e vários derivados indolin-2-ona, estruturalmente semelhantes ao fármaco sunitinibe. O programa Molegro Virtual Docker foi utilizado nos cálculos de ancoramento molecular e as enzimas Aurora B e FLT3 obtidas a partir do PDB (4AF3 e 4XUF) com hesperadina e quizartinibe empregados como compostos referência, respectivamente. Os modelos matemáticos, realizados no programa Chemoface, alcançaram R^2 de 0,94 e 0,82, sugerindo que as conformações dos ligantes com Aurora B e FLT3 humana são cabíveis e os dados podem ser utilizados para prever o nível de interação de outros inibidores indolin-2-ona de Aurora B e FLT3 com padrões moleculares semelhantes. O composto **1**, mostrou as energias de interação mais estáveis, -225,90 kcal.mol^{-1} para Aurora B e -233,25 kcal.mol^{-1} para FLT3, entre todos os inibidores estudados com dados experimentais disponíveis, enquanto o sunitinibe foi o menos estável (-135,63 kcal.mol^{-1}) para a enzima Aurora B e um dos menos estáveis (-160,94 kcal.mol^{-1}) para FLT3. Quatro novos derivados indolin-2-ona propostos (**IAF61**, **IAF63**, **IAF66** e **IAF79**) foram destacados como promissores compostos para futura síntese e avaliação biológica visando a Aurora B, outros seis (**IAF70**, **IAF72**, **IAF75**, **IAF80**, **IAF84** e **IAF88**) visando a FLT3 e um composto (**IAF79**) como um promissor composto com atividade dual Aurora B/FLT3. Além disso, o padrão molecular evidenciado em nossos estudos deve ser explorado sinteticamente na busca de compostos mais efetivos que possam se tornar um fármaco utilizado no tratamento do câncer, incluindo LMA, validando e ratificando nossos estudos de docking.

Palavras-chave: Aurora B quinase. Inibidores de Aurora B quinase. Inibidores de FLT3. Derivados indolin-2-ona. Câncer. Inibidores duais Aurora B/FLT3. Leucemia mieloide aguda. Química medicinal. Compostos anticâncer. Química computacional. *Docking*.

ABSTRACT

Aurora kinase enzymes perform important roles in mammals, mainly in cell cycle. Overexpression of these enzymes is related to tumor development and indicative of worsening of clinical conditions of diagnosed patients with cancer. Aurora kinases are promising targets in the search for new anticancer drugs, highlighting Aurora B. Other enzyme related to tumoral processes is the tyrosine kinase FLT3 and closely related to the acute myeloid leukemia (AML). FLT3 enzyme is expressed in membranes of precursor hematopoietic cells and have important role in cellular differentiation, proliferation and multiplication. In AML disease, normally, occurs hyperstimulation or mutations of FLT3 enzyme, leading to exacerbated cellular proliferation and lower response to standard cytotoxic agents. FLT3 and dual Aurora B/FLT3 inhibitors have shown relevance in searching for promising new anticancer compounds, mainly to AML. This work was designed to study and understand the interactions between two different targets, Aurora B and FLT3 enzymes, and several indolin-2-one derivatives, structurally similar to sunitinib drug. Molegro Virtual Docker software was utilized in docking estimates and the human Aurora B and FLT3 structures obtained from PDB (4AF3 and 4XUF) with hesperadin and quizartinib used as reference compounds, respectively. The mathematical models, performed in Chemoface program, achieved R^2 of 0.94 and 0.82, suggesting that the binding conformations of the ligands with human Aurora B and FLT3 are reasonable and the data can be used to predict the level of interaction of other Aurora B and FLT3 indolin-2-one inhibitors with similar molecular patterns. Compound **1** showed more stable interaction energies, -225.90 $kcal.mol^{-1}$ to Aurora B and -233.25 $kcal.mol^{-1}$ to FLT3, among all studied inhibitors with experimental data available, while sunitinib was the least stable (-135.63 $kcal.mol^{-1}$) considering the Aurora B enzyme and one of the least stable (-160.94 $kcal.mol^{-1}$) to FLT3. Four new proposed indolin-2-one derivatives (**IAF61**, **IAF63**, **IAF66** and **IAF79**) were highlighted as promising compounds for future synthesis and biological evaluation against human Aurora B, other six (**IAF70**, **IAF72**, **IAF75**, **IAF80**, **IAF84** and **IAF88**) against FLT3 and one compound (**IAF79**) as a promising compound with dual Aurora B/FLT3 activity. Besides that, the molecular pattern evidenced in our studies must be exploited synthetically in searching for new compounds that may become a drug used in cancer treatment, including AML, thus validating and ratifying our docking studies.

Keywords: Aurora B kinase. Aurora B kinase inhibitors. FLT3 inhibitors. Indolin-2-one derivatives. Cancer. Dual Aurora B/FLT3 inhibitors. Acute myeloid leukemia. Medicinal chemistry. Anticancer compounds. Computational chemistry. Docking.

LISTA DE FIGURAS

Primeira parte

Segunda parte

Figure 3 – Overlapped conformations of FLT3 inhibitors. Quizartinib is shown in yellow, and Sunitinib in purple

Figure 4 – Overlapped conformations of compounds: 1, Quizartinib (yellow), and Sunitinib (purple)

Figure 5 – Promising indolin-2-one molecular pattern to dual Aurora B/FLT3 activity

LISTA DE TABELAS

Segunda parte

LISTA DE ABREVIATURAS

Å – ångström

Ala, A – alanina

AML – acute myeloid leukemia

Arg, R – arginina

Asn, N – asparagina

Asp, D – aspartato

CDKs – cyclin-dependent kinases

CPC – chromosome passenger complex

Cys, C – cisteína

DNA – deoxyribonucleic acid

EA – evolutionary algorithms

Eq – equação

FLT3 – FMS-like tyrosine kinase 3

FMS – feline McDonough sarcoma

GEMDOCK – generic evolutionary method for molecular dock

Glu, E – glutamato

Gly, G – glicina

H – hidrogênio

IC_{50} – half maximal inhibitory concentration

INCENP – inner centromere protein

ITD – internal tandem duplication

kcal – quilocaloria

Leu, L – leucina

Lig-Prot – ligante-proteína

LMA – leucemia mieloide aguda

Lys, K – lisina

Met, M – metionina

MVD – molegro virtual docker

PDGFR – platelet-derived growth factor receptor

Phe, F – fenilalanina

pIC_{50} – - logaritmo de IC_{50} ou colog de IC_{50}

pIC_{50exp} – pIC_{50} experimental

pIC_{50pred} – pIC_{50} predito

PLKs – polo-like kinases

PLP – Piecewise Linear Potential

Pro, P – prolina

RMN – ressonância magnética nuclear

RMSD – root mean square deviation

SD – standard deviation

TKD – tyrosine kinase domain

Tyr, Y – tirosina

UV – ultravioleta

Val, V – valina

VEGFR – vascular endothelial growth fator

LISTA DE SIGLAS

CAPES – Coordenação de Aperfeiçoamento de Pessoal de Nível Superior

CNPq – Conselho Nacional de Desenvolvimento Científico e Tecnológico

INCA – Instituto Nacional de Câncer

LABGQC – Laboratório de Modelagem Molecular

PDB – Protein Data Bank

PPGAQ – Programa de Pós-Graduação em Agroquímica

RQ-MG – Rede Mineira de Química

UFLA – Universidade Federal de Lavras

WHO – World Health Organization

SUMÁRIO

PRIMEIRA PARTE

1 INTRODUÇÃO

O câncer é considerado um grande problema de saúde pública, sendo uma das principais causas de mortalidade (SIEGEL; NAISHADHAM; JEMAL, 2012), com cerca de 9,6 milhões de mortes anuais mundialmente (WHO, 2018). A ausência de cura definitiva para o câncer em um elevado número de casos faz com que pesquisas sejam voltadas para a busca de novas alternativas terapêuticas que visam a descoberta de novos alvos terapêuticos e fármacos ou na melhoria das terapias já existentes. Os tratamentos atuais disponíveis são invasivos ou promovem uma série de efeitos colaterais graves nos pacientes, apesar dos avanços na área que melhoraram muito a qualidade e expectativa de vida dos portadores.

O processo de desenvolvimento de novos fármacos é complexo, demandando altos recursos financeiros e tempo, podendo um fármaco ser aprovado após décadas ou simplesmente ser descontinuado. O planejamento racional de novos protótipos a fármacos é uma ferramenta de suma importância que auxilia neste árduo processo, destacando-se as técnicas computacionais, que nos últimos anos ganharam espaço na área, contribuindo ainda nas diminuições de demandas financeiras e tempo, além de permitirem maiores possibilidades de sucesso (BARREIRO; FRAGA, 2008, GUIDO; OLIVA; ANDRICOPULO, 2008).

A enzima Aurora B quinase (EC: 2.7.11.1) está diretamente ligada a vários processos envolvendo a mitose, como condensação, segregação e alinhamento dos cromossomos, funcionamento do fuso mitótico e citocinese (DUCAT; ZHENG, 2004). Erros durante o processo mitótico levam à instabilidade genômica, podendo induzir à tumorgênese (ANDREWS et al., 2003). Uma vez que os níveis de Aurora B quinase encontram-se elevados em diferentes tipos de câncer, essa enzima é considarada um alvo efetivo e promissor na busca de novos protótipos à fármacos antitumorais (STOLS et al., 2007).

O *Feline McDonough Sarcoma-like* (FMS) tirosina-quinase 3 (FLT3) pertence à família de receptores tirosina-quinase classe III (BERENSTEIN, 2015). O FLT3 é expresso nas membranas das células hematopoiéticas e, em condições normais, possui relevante papel na diferenciação, proliferação e multiplicação celular. Blastos na leucemia mieloide aguda (LMA) expressam FLT3 e a desregulação dessa via de sinalização leva à proliferação celular

exacerbada, tanto hiperestimulação ou mutações, sendo que ambos processos contribuem para o surgimento da LMA (PORT et al., 2014). Mutações no gene relacionado à expressão do FLT3 são observadas em cerca de 40% dos casos de LMA (KAYSER et al., 2009). Mutações no domínio justamembranar levam ao alelo mutante FLT3/ITD (*internal tandem duplication*), sendo esse associado à uma diminuição da resposta terapêutica frente aos agentes quimioterápicos utilizados (PASTORE, 2016).

Estudos mostram que inibidores duais de FLT3 e Aurora B podem ser mais eficazes do que inibidores seletivos em casos de mutações (BAVETSIAS et al., 2012, MOORE et al., 2012). Muitos inibidores de proteínas quinases apresentam em sua estrutura o padrão indolin-2-ona, dentre eles o sunitinibe, que foi o primeiro inibidor multi-quinase em uso clínico e a hesperadina, inibidor de Aurora B (JAGTAP et al., 2014). Nesse sentido, estudos baseados no conceito “um fármaco – múltiplos alvos” (one drug – multiple targets) tendem a uma maior possibilidade de sucesso na busca de novos fármacos.

O *docking* molecular ou ancoramento molecular é uma técnica computacional utilizada na busca de novas entidades moleculares que possam ser promissores candidatos a fármacos empregados em diferentes patologias. Esta técnica se baseia na simulação das interações entre duas diferentes estruturas, mais comumente uma proteína e uma molécula orgânica de baixo peso molecular, onde são obtidas as melhores poses ou conformações quando no interior do sítio de ligação de uma determina proteína em estudo. Os resultados permitem estabelecer potenciais ligantes, buscando-se seletividade, além de possibilitar a otimização de compostos através de possíveis e permitidas modificações estruturais que elevem o nível de interações com os resíduos de aminoácidos no interior do sítio de interação (ANDRICOPULO; SALUM; ABRAHAM, 2009).

Diante dos fatos supracitados, o trabalho em questão baseou-se nos estudos computacionais, através de *docking* ou ancoramento molecular, de uma série de derivados indolinônicos frente às enzimas Aurora B e/ou FLT3 humanas, consideradas promissores alvos na busca de novos compostos com atividade antitumoral.

2 REVISÃO DE LITERATURA

2.1 Câncer: aspectos gerais

A *World Health Organization* (WHO) define o câncer como uma patologia onde ocorre crescimento desordenado de células, podendo ocorrer também invasão de outros tecidos do organismo diferentes da origem, conhecida como metástase. A palavra câncer é um termo genérico utilizado para um vasto grupo de doenças que podem afetar qualquer parte do corpo, sendo também utilizados os termos como neoplasias e tumores malignos. Dados mostram que, aproximadamente, 9,6 milhões de pessoas morrem anualmente em decorrência dessa doença, valor este estimado em cerca de 17% das mortes mundiais, sendo relatados mais de 100 tipos diferentes de câncer que requerem diagnósticos e tratamentos distintos. Expectativas indicam também um aumento de 70% no número de casos para as próximas duas décadas (WHO, 2016; WHO, 2018).

O Ministério da Saúde – INCA (BRASIL, 2018) estima, para o Brasil, biênio 2018-2019, a ocorrência de 600 mil casos novos de câncer, para cada ano. Essas estimativas refletem o perfil de um país que possui os cânceres de próstata, pulmão, mama feminina e cólon e reto entre os mais incidentes, entretanto ainda apresenta altas taxas para os cânceres do colo do útero, estômago e esôfago, como pode ser visto na Figura 1.

As Regiões Sul e Sudeste do Brasil concentram 70% da ocorrência de novos casos, sendo possível perceber uma variação nos tipos de câncer entre as diferentes Regiões do país. Nas Regiões Sul e Sudeste, predominam os cânceres de próstata e de mama feminina, bem como os cânceres de pulmão e de intestino. A Região Centro-Oeste, apesar de semelhante, incorpora em seu perfil os cânceres do colo do útero e de estômago entre os mais incidentes. Nas Regiões Norte e Nordeste têm como mais impactante a incidência dos cânceres do colo do útero e estômago (BRASIL, 2018).

Figura 1 – Distribuição dos dez tipos de câncer mais incidentes no Brasil em 2018.

Localização Primária	Casos	%
Próstata	68.220	31,7%
Traqueia, Brônquio e Pulmão	18.740	8,7%
Cólon e Reto	17.380	8,1%
Estômago	13.540	6,3%
Cavidade Oral	11.200	5,2%
Esôfago	8.240	3,8%
Bexiga	6.690	3,1%
Laringe	6.390	3,0%
Leucemias	5.940	2,8%
Sistema Nervoso Central	5.810	2,7%

Localização Primária	Casos	%
Mama Feminina	59.700	29,5%
Cólon e Reto	18.980	9,4%
Colo do Útero	16.370	8,1%
Traqueia, Brônquio e Pulmão	12.530	6,2%
Glândula Tireoide	8.040	4,0%
Estômago	7.750	3,8%
Corpo do Útero	6.600	3,3%
Ovário	6.150	3,0%
Sistema Nervoso Central	5.510	2,7%
Leucemias	4.860	2,4%

*Números arredondados para múltiplos de 10.

Fonte: Brasil (2018).

Diferentes fatores ou condições podem desencadear o processo tumoral no organismo, também chamados de carcinógenos, tais como radiação ultravioleta – UV (KIELBASSA; ROZA; EPE, 1997), radiação ionizante (CADET et al., 2012), diferentes carcinógenos químicos presentes no ambiente ou ingeridos na forma de medicamentos genotóxicos (ROOS; KAINA, 2013) e carcinógenos produzidos pelo próprio organismo por meio do metabolismo celular (VOULGARIDOU et al., 2011). Esses fatores são capazes de atacar o DNA e produzir uma variedade de lesões (DIPPLE, 1995) que podem dar início a mutações e danos cromossomais, sendo responsáveis pela transformação oncogênica e progressão tumoral (MILLER; MILLER, 1981).

O diagnóstico precoce torna-se importante devido a uma maior probabilidade de sucesso no tratamento, do contrário, quando tardiamente diagnosticada, na maioria dos casos, ocorre agravamento da doença e diminuição na expectativa de vida dos pacientes. O tratamento do câncer depende de fatores como histologia do tumor, estágio do câncer, preferência e aceitação da terapêutica pelo paciente, dentre outros (BYRNE; YEH; DESIMONE, 2018). As modalidades primárias de tratamento incluem cirurgia, quimioterapia e radioterapia. Outras modalidades podem ser combinadas à cirurgia, incluindo a quimio e

radioterapia. No entanto, estas terapias estão altamente associadas a fortes efeitos colaterais como fadiga, diarreia, xerostomia e tumores secundários (SUIT et al., 2007).

Muitas estratégias são desenvolvidas com a intenção de aprimorar a resposta imune às células tumorosas, o que leva ao aparecimento de diferentes agentes imunoterápicos como modalidade de tratamento anticâncer. As estratégias atuais que abrangem este tipo de tratamento incluem o estímulo não-específico de reações imunes, a imunização ativa por meio de vacinas e a transferência passiva de células imunes ativadas com atividade antitumoral (DUBBS, 2018).

Apesar dos grandes avanços na compreensão da base molecular do câncer, no progresso da detecção e tratamento, a mortalidade ainda é bastante elevada e não existe cura definitiva até o momento para um número bastante elevado de casos. Todas as terapias de câncer tradicionais, incluindo cirurgia, terapia hormonal, terapia antiangiogênese e imunoterapia mostram falta de eficácia em termos de resultados em longo prazo devido a sua incapacidade de atingir as células-tronco do câncer e à toxicidade por efeitos não específicos em células normais (HU; FU, 2012).

2.2 Família das Aurora Quinases

Durante a busca por genes de *Drosophila* reguladores do ciclo celular foi observado o gene chamado de *aurora* sofrendo mutação que bloqueou o ciclo (GLOVER et al., 1995). Tal nome foi escolhido devido à semelhança entre a morfologia do fuso mitótico defeituoso com o fenômeno “aurora boreal” observado nas regiões polares da Terra (MOUNTZIOS; TERPOS; DIMOPOULOS, 2008). Desde então, as Aurora quinases emergiram como reguladores essenciais da divisão celular. Juntamente com outras proteínas quinases, dentre elas as quinases ciclina-dependentes (CDKs) e as polo-like quinases (PLKs), as Aurora quinases controlam o fluxo mitótico e guiam uma divisão correta do material genético em duas células-filhas (CARMENA; RUCHAUD; EARNSHAW, 2009).

As Aurora quinases são importantes em diferentes etapas do processo de divisão celular. Estão envolvidas na organização dos centríolos, condensação de cromossomos,

organização de microtúbulos e citocinese. Em mamíferos, foram identificadas três Aurora quinases, Aurora A, Aurora B e Aurora C, todas apresentando papéis importantes no ciclo celular e a superexpressão está relacionada à desregulação nesse ciclo, podendo levar à tumorgênese (VADER; LENS, 2008).

As Aurora quinases A, B e C possuem em comum um domínio catalítico altamente conservado no carbono terminal e domínios curtos no nitrogênio terminal diferentes em comprimento, sendo que os domínios curtos regulam as diferentes localizações subcelulares e suas distintas funções na mitose (KEEN; TAYLOR, 2004).

A superexpressão do gene que codifica a Aurora A interfere em processos celulares levando a falhas na divisão celular e instabilidade genômica. A alta expressão está ainda relacionada com uma citocinese falha, sugerindo que o mesmo possa ser promotor de tumorgenêse (NIKONOVA et al., 2012). Os níveis aumentados de Aurora A estão relacionados a vários tipos de tumores malignos epiteliais, como mama, cólon, bexiga, ovário e pâncreas (TANNER et al., 2000; WATANABE et al., 2002).

O gene que codifica a Aurora B participa da orientação cromossômica. A proteína forma um complexo importante para a separação de cromátides e citocinese. A superexpressão de Aurora B tem sido demonstrada em vários tipos de tumores, com aumento da fosforilação de Histona H3 e poliploidia em tais células (KATAYAMA; BRINKLEY; SEM, 2003). Embora tal superexpressão não esteja relacionada à formação de tumores por si só, acredita-se que a Aurora B induza outros processos oncogênicos (POLLARD; MORTIMORE, 2009).

Aurora C e seu envolvimento na carcinogênese é a menos estudada da família de Aurora quinases. No entanto, alguns estudos mostram sua alta expressão em câncer colorretal, mama e próstata (TAKAHASHI et al., 2000).

A aneuploidia é uma alteração genômica prevalente em 90% dos tumores sólidos humanos (GORDON; RESIO; PELLMAN, 2012). Além dela, problemas relacionados aos centrossomos são encontrados em diversos tipos de câncer por afetarem a segregação cromossomal e produzirem células aneuploides (SATO et al., 2001). Aneuploidia e

anormalidades no centrossomo são detectadas também na superexpressão ou na inibição de genes da família das Aurora, o que caracteriza estas proteínas como importantes no surgimento e progressão do câncer (GAUTSCHI et al., 2008).

Estas enzimas são, portanto, consideradas alvos promissores na busca de novos candidatos a fármacos antitumorais, buscando-se novas substâncias com atividade inibitória ou na regulação da expressão destas enzimas (BEBBINGTON et al., 2009; QI et al., 2011; PRIME et al., 2011; KEREKES et al., 2011).

2.3 Aurora B como promissor alvo para o câncer

A enzima Aurora B quinase (EC 2.7.11.1) localiza-se no cromossomo 17p13 e forma um complexo cromossomal (CPC), associada a borealina, survivina e INCENP, essencial para a citocinese (ADAMS; CARMENA; EARNSHAW, 2001; GASSMANN et al., 2004; VADER et al., 2007). Cada proteína deste complexo é importante para a correta localização da Aurora B no processo mitótico. A Aurora B localiza-se nos centrômeros durante o início da mitose, transfere-se para a região central do fuso mitótico auxiliando na formação do anel contrátil durante a anáfase e, por fim, permanece no corpo central durante a citocinese (DESCAMPS; PRIGENT, 2001; SHANNON; SALMON, 2002). A Aurora B regula vários processos mitóticos, como condensação, segregação e alinhamento dos cromossomos, funcionamento do fuso mitótico, metáfase e citocinese (DUCAT; ZHENG, 2004; GOLDENSON; CRISPINO, 2015). Os substratos da Aurora B incluem INCENP, Survivina, Borealina, BubR1, Mad2, MCAK, NudC, Histona 2A e Histona H3, dentre outros (BOLANOS-GARCIA, 2005; WEIDERHOLD et al., 2016).

A fosforilação da Histona H3 é essencial para a correta conclusão da mitose e considerada um biomarcador da atividade quinase da Aurora B (PRIGENT; DIMITROV, 2003). A inibição da atividade da Aurora B pode diminuir a fosforilação da Histona H3, levando à incorreta condensação dos cromossomos e induzindo citocinese incompleta, tornando as células poliploides, gerando apoptose (CARVAJAL; TSE; SCHWARTZ, 2006; ZEKRI et al., 2015). Uma vez que a Aurora B está superexpressa em diferentes tipos de

câncer humano, especialmente colorretal, esta tem sido considerada como alvo efetivo e promissor na busca de novos fármacos anticâncer (LADYGINA; LATSIS; YEN, 2005; STOLS et al., 2007).

Aurora B é um componente central do complexo passageiro do cromossomo (CPC), que também contém a proteína do interior do centrômero (INCENP), Borealina e Survivina. Estes componentes não enzimáticos do CPC apresentam papel fundamental na regulação da atividade da quinase e sua localização (VADER; MEDEMA; LENS, 2006; RUCHAUD; CARMENA; EARSHAW, 2007). A estrutura de Aurora B foi previamente determinada em *Xenopus laevis*, em complexo com INCENP e seu inibidor hesperadin. Para fornecer um modelo de melhor compreensão sobre o mecanismo molecular de ativação, Elkins e colaboradores determinaram a estrutura da Aurora B humana (*Protein Data Bank* – 4AF3, Figura 2A), em complexo com INCENP humano e o inibidor de Aurora B, VX-680 (FIGURA 2B) (SESSA et al., 2005; ELKINS et al., 2012).

Figura 2 – Complexo proteína-ligante Aurora B/VX-680 e estrutura química do composto VX-680.

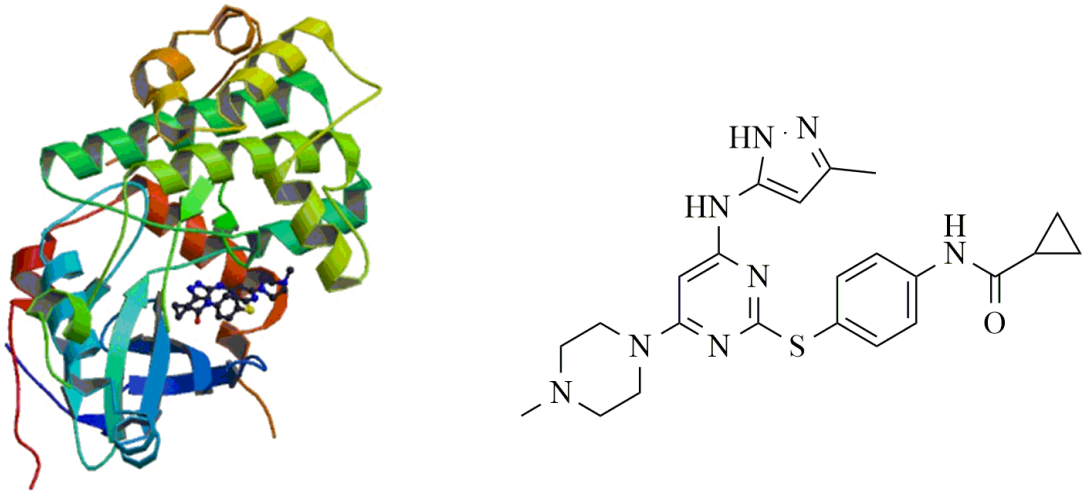

(A)
Aurora B Quinase Humana
(PDB: 4AF3)

(B)
VX-680

Fonte: Protein Data Bank (2017); do autor.

A Aurora B está superexpressa em diferentes tipos de tumores e tem sido relacionada a um mau prognóstico em pacientes com câncer (OTTO; SICINSKI, 2017). Com isso, diversos inibidores de Aurora B foram desenvolvidos ao longo do tempo (FIGURA 3), como barasertibe, Derrone, AT-9283, VX-680, PHA-680632, danusertibe, AMG-900, CYC-116 e os resultados das diferentes fases dos ensaios clínicos desses compostos têm mostrado que a inibição desta proteína possibilita estabilização da doença em muitos pacientes (ZIEMSKA; SOLECKA, 2016; TANG et al., 2017).

Figura 3 – Estruturas químicas de alguns inibidores de Aurora B.

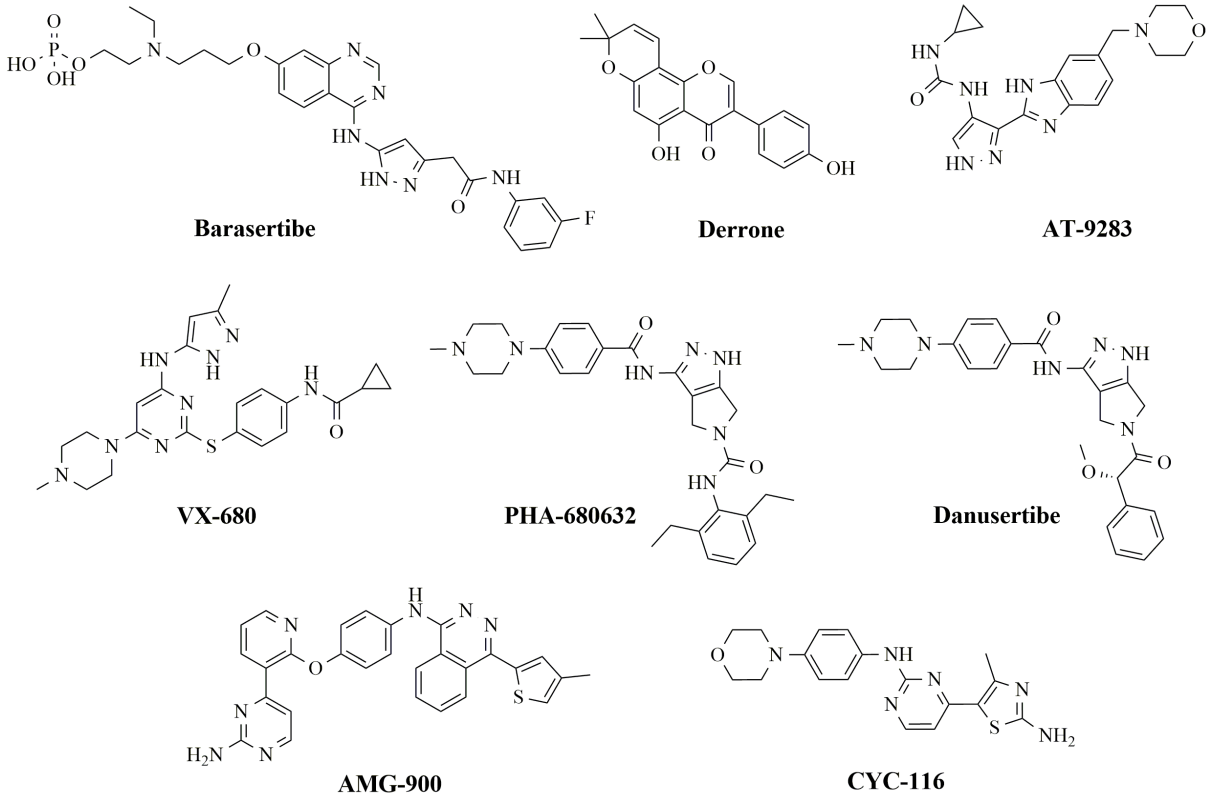

Fonte: Do autor.

2.4 FLT3 como alvo anticâncer

O *Feline McDonough Sarcoma* (FMS)-*like* tirosina-quinase 3 (FLT3) pertence à família de receptores tirosina-quinase classe III (FIGURA 4), sendo caracterizados pela

presença de cinco domínios imunoglobulina-*like* na porção extracelular, um domínio transmembranar na membrana plasmática da célula, um domínio justamembranar citoplasmático seguido de um domínio de tirosina-quinase citoplasmático, subdividido em dois – TKD I e TKD II, por uma zona de inserção de quinases, terminando a estrutura proteica com uma cauda C-terminal (BERENSTEIN, 2015).

Figura 4 – Composição molecular de receptores tirosina-quinase classe III.

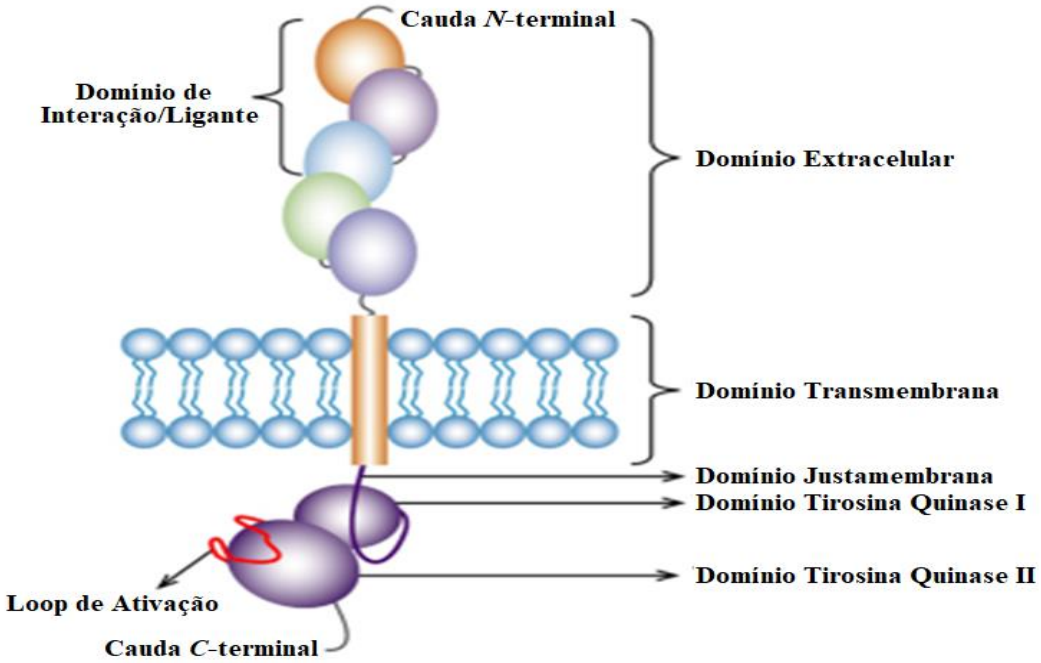

Fonte: Adaptado de Berenstein (2015).

Em condições normais, o FLT3 é expresso nas membranas das células hematopoiéticas precursoras, sendo importante para a sua diferenciação, proliferação e multiplicação. Demonstrou-se que os blastos de Leucemia Mieloide Aguda (LMA) expressam FLT3, sendo que a desregulação desta via de sinalização conduz à proliferação celular, seja por estimulação aberrante por FLT3 exógeno ou pela presença de mutações com ganho de função, sendo que ambos os processos contribuem para o surgimento da LMA (KAYSER et al., 2009, PORT et al., 2014).

O gene FLT3 está localizado no cromossomo 13q12 e é responsável por codificar um receptor com função de tirosina-quinase importante nos processos de proliferação e diferenciação celular (BERENSTEIN, 2015). Mutações no gene relacionado à expressão do FLT3 são observadas em cerca de 40% dos casos de LMA, tornando-o um dos genes mais frequentemente afetados em portadores dessa doença (KAYSER et al., 2009). Mutações no domínio justamembranar levam ao alelo mutante FLT3/ITD, que tem sido associado à uma diminuição da remissão da leucemia em pacientes tratados com quimioterapia, demonstrando que este alelo tem uma baixa resposta aos agentes citotóxicos padrões (PASTORE, 2016).

Independentemente do domínio da proteína afetado pela mutação, os mecanismos que contribuem para a carcinogênese parecem conduzir à ativação constitutiva do FLT3. Existem evidências de que as mutações na região justamembranar interferem com o mecanismo auto-inibitório, conduzindo a uma modificação conformacional da enzima, com ativação constitutiva da mesma (BERENSTEIN, 2015, KAYSER et al., 2009).

Diante da resistência aos agentes quimioterápicos convencionais, algumas moléculas têm sido exaustivamente estudadas como possíveis inibidores de FLT3, como sorafenibe, sunitinibe, midostaurina, lestaurtinibe e quizartinibe, mostrados na Figura 5. No entanto, muitas destas moléculas apresentaram problemas quanto à tolerabilidade e toxicidade nas doses eficazes, como o sunitibe (MA et al., 2017). Dentre os inibidores de 2ª geração, o quizartinibe demonstrou uma boa potência e seletividade pelo FLT3, no entanto, foi observado o desenvolvimento de pontos de mutação nos pacientes, conferindo resistência à molécula (SMITH et al., 2012). Já o crenolanibe se mostrou tão potente quanto o quizartinibe e foi eficaz contra as células resistentes a ele (ZIMMERMAN et al., 2013), enquanto o pexidartinibe se mostrou um potente inibidor da linhagem mutante FLT3/ITD (PASTORE, 2016).

Figura 5 – Estruturas químicas de alguns inibidores de FLT3.

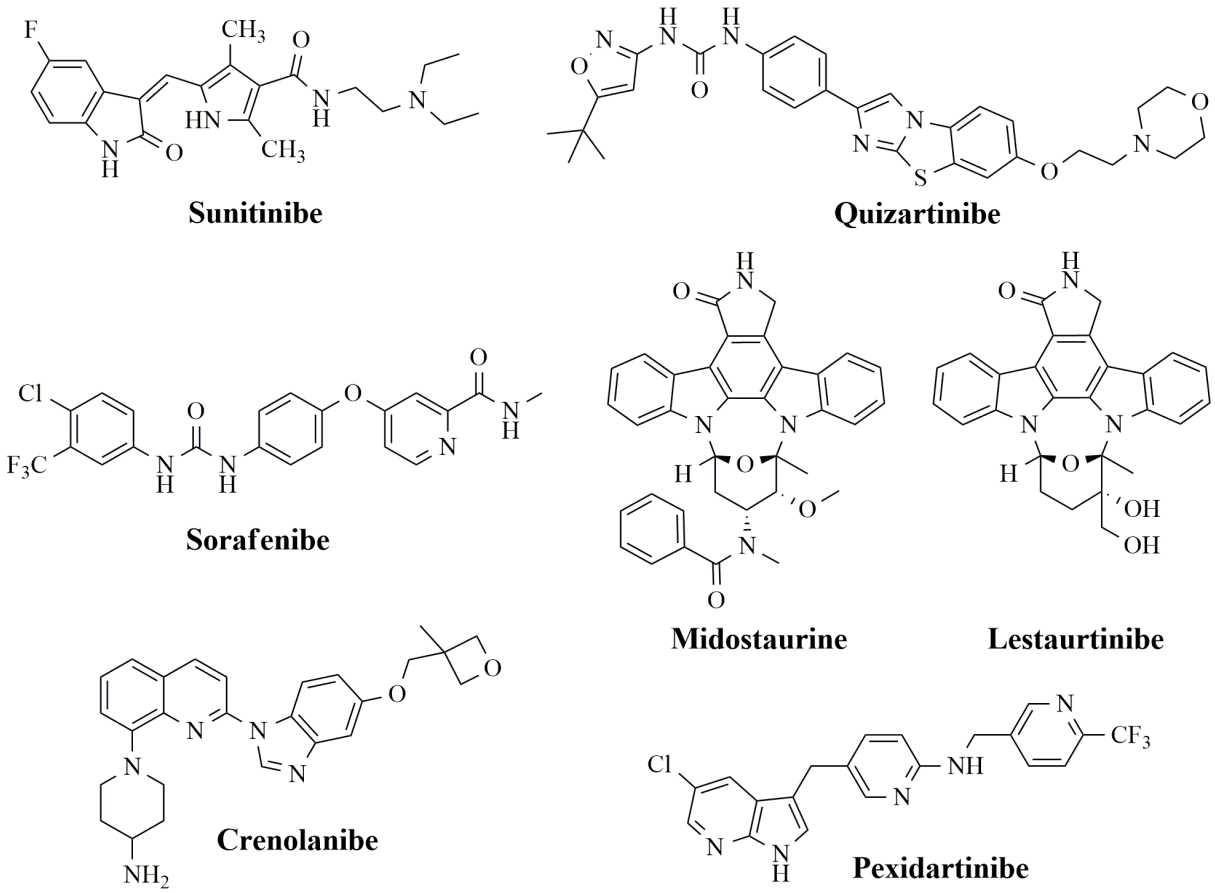

Fonte: Adaptado de Ma et al. (2017).

Estudos mostram que inibidores duais de FLT3 e Aurora B podem ser mais eficazes do que inibidores seletivos em casos de mutações (BAVETSIAS et al., 2012, MOORE et al., 2012). Muitos inibidores de proteínas quinases apresentam em sua estrutura o padrão indolin-2-ona, dentre eles o sunitinibe, que foi o primeiro inibidor multi-quinase em uso clínico e a hesperadina, inibidora de Aurora B (JAGTAP et al., 2014). Nesse sentido, estudos devem ser desenvolvidos com o objetivo de se focar no "one drug – multiple targets", buscando-se uma única molécula que seja eficaz frente a FLT3 e Aurora B.

2.5 Derivados indolin-2-ona como agentes anticâncer

O núcleo indol (FIGURA 6) é uma importante estrutura funcional de produtos naturais e sintéticos (GUPTA; TALWAR; CHAUHAN, 2007; ALVES; BARREIRO; FRAGA, 2009). Em particular, derivados indolin-2-ona (FIGURA 6), apresentam vários relatos de atividades biológicas, incluindo atividade antitumoral (ERKIZAN et al., 2009; PENTHALA et al., 2010; XIE et al., 2013). Da mesma forma, núcleos indolin-3-ona (FIGURA 6) também possuem propriedades farmacológicas, incluindo atividade antitumoral (LAYEK et al., 2011; PEJOVIC et al., 2012; BHEEMANAPALLI et al., 2012).

Figura 6 – Estrutura química evidenciando as subunidades indol, indolin-2-ona e indolin-3-ona.

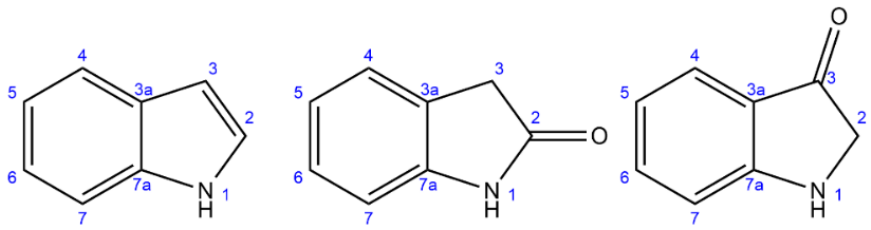

Indol **Indolin-2-ona** **Indolin-3-ona**

Fonte: do autor.

Derivados pertencentes à classe indolin-2-ona são estudados na busca de novos compostos anticâncer. Os compostos pertencentes a esta classe mostram interessantes atividades antitumorais (PRAKASH; RAJA, 2012), principalmente relacionados à capacidade de inibição de uma variedade de proteínas, principalmente da família das quinases (VINE et al., 2009). O primeiro composto inibidor de quinase pertencente à classe indolin-2-ona foi o sunitinibe (FIGURA 7), sendo esse utilizado como terapêutica em carcinoma metastático de células renais e tumor gastrointestinal (CHOW; ECKHARDT, 2007). O padrão indolin-2-ona é encontrado em alguns inibidores de Aurora como o inibidor seletivo de Aurora B, hesperadina (HAUF et al., 2003) e o inibidor multialvo de Aurora A e B, orantinibe (FIGURA 7) (GODL et al., 2005).

Modificações estruturais para a subunidade indolin-2-ona em diferentes compostos têm mostrado considerável progresso na atividade biológica, destacando-se alvos relacionados à atividade antitumoral (KAMMASUD et al., 2009; LV et al., 2011).

Figura 7 – Estrutura química do Sunitinibe, Hesperadina e Orantinibe.

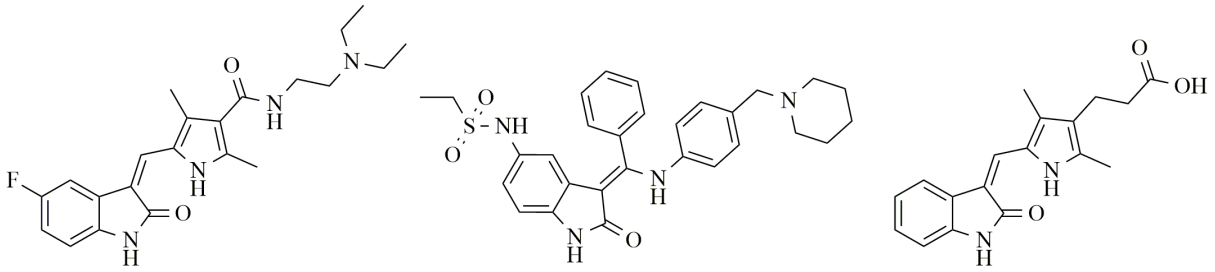

Sunitinibe **Hesperadina** **Orantinibe**

Fonte: do autor.

Pirrol-indolin-2-onas foram as primeiras estruturas identificadas como inibidores de quinases. O primeiro composto deste tipo a atingir a clínica foi o sunitinibe, aprovado para tratamento de carcinoma avançado de células renais e tumores gastrintestinais do estroma e comercializado por meio do Sutent®, Pfizer – detentora da patente até 2021. O composto precedente ao sunitinibe foi originalmente desenvolvido como um inibidor multi-quinases. Em estudos proteômicos, mostrou-se como inibidor de Aurora quinases (KRUG; HILGEROTH, 2008).

O sunitinibe inibe a proliferação e induz a apoptose de células tumorais, atuando sobre receptores de tirosina quinase, receptores de fatores de crescimento derivados de plaquetas (PDGFR), receptores de fatores de crescimento vascular endotelial (VEGFR), receptores de fatores de células-tronco (c-KIT), receptores TK-3 do tipo FMS (FLT3) e receptores de fatores neurotróficos, RET (BELLO et al., 2006).

Devido a seu largo espectro de ação, o sunitinibe é capaz de ser eficaz em diferentes tipos de câncer. No entanto, isto também aumenta as chances de efeitos adversos, sendo mais frequentemente observados fadiga, diarreia, hipertensão, além de hipotireoidismo e efeitos

cardiotóxicos, sendo que existem relatos de pacientes que interromperam o tratamento devido a quadros de insuficiência cardíaca congestiva (MOTZER et al., 2007; CHU et al., 2007).

Dentre uma segunda geração de inibidores de quinases, foi identificado o quizartinibe, um derivado indolinônico que mostrou-se como um potente e seletivo inibidor de FLT3, com boas propriedades farmacêuticas, perfil farmacocinético, atividade em modelos com ratos e tolerabilidade (CHAO et al., 2009). No entanto, uma limitação de seu uso deve-se a ocorrência de mutações que tornam o alvo resistente ao quizartinibe (OSTRONOFF; ESTEY, 2013), tornando importante o desenvolvimento de novos inibidores que contemplem estas questões.

Como exemplos da importância do padrão indoli-2-ona, podemos citar Lv e colaboradores (LV et al., 2011), que desenvolveram uma série de estudos com base em indolin-2-onas como candidatos a fármacos antitumorais. Seus estudos têm focado na introdução de grupos funcionais na posição N-1 do anel indolin-2-ona. Estes autores sintetizaram uma série de derivados 1-[(3-dimethyl-amino)propyl] indolin-2-ona pela introdução de grupos carbamoílas lineares e cíclicos na posição C-4 do anel pirrol do composto TMP-20 (FIGURA 8) previamente obtido em outros estudos. Com isso, descobriram o composto LK-B030 (FIGURA 8), o mais ativo da série, com atividade antitumoral *in vitro* maior que do sunitinibe contra todas as células testadas.

Figura 8 – Estrutura química dos compostos TMP-20 e LK-B030.

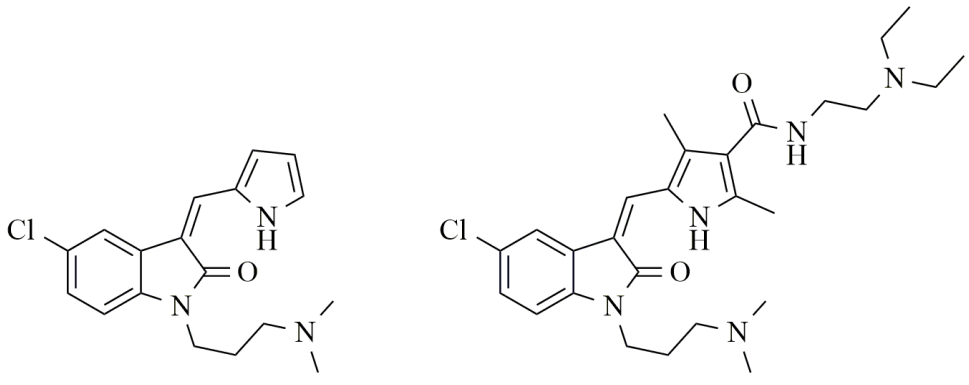

TMP-20 **LK-B030**

Fonte: Adaptado de LV et al. (2011).

Tendo em vista que tanto Aurora B quanto o FLT3 foram apresentados neste trabalho como possíveis alvos para o tratamento anticâncer, e considerando que estudos demonstraram que inibidores duais apresentam melhor eficácia contra mutações que inibidores seletivos (BAVETSIAS et al., 2012; MOORE et al., 2012), observa-se a relevância e significância da busca por compostos que sejam inibidores duais, possibilitando o uso de uma única molécula para atuar na inibição de ambos os alvos. Neste sentido, alguns estudos já foram desenvolvidos partindo do uso do padrão estrutural indolin-2-ona, com foco na inibição de Aurora e FLT3 (KHANWELKAR et al., 2010; JAGTAP et al., 2014).

2.6 Ancoramento molecular ou *docking* molecular

O processo que envolve o desenvolvimento de novos fármacos é considerado bastante complexo e dispendioso, necessitando de imenso aporte financeiro ao longo das etapas envolvidas até atingirem o mercado farmacêutico como autênticos fármacos. Atualmente, existem diferentes estratégias de planejamento, desenho e modificações moleculares que são empregadas na busca racional de novos potenciais ligantes (BARREIRO; FRAGA, 2008). Dentre estas estratégias podemos destacar o uso de técnicas computacionais que têm ganhado cada vez mais espaço e credibilidade ao longo dos anos, onde temos constantes evoluções na capacidade de processamento dos computadores, desenvolvimento de interfaces gráficas de visualização de estruturas geradas e na operacionalização dos *softwares* disponíveis. A utilização adequada de técnicas *in silico*, associadas a dados experimentais, podem ser capazes de predizer diferentes parâmetros, como propriedades de absorção, metabolismo, toxicidade, minimizando os riscos de falhas ao longo do processo de desenvolvimento, possibilitando probabilidades maiores de sucessos (NG, 2004; ENGEL, 2006).

O *docking* molecular ou ancoramento molecular, assim como outras técnicas computacionais, são considerados de grande interesse na área de planejamento de novos fármacos. Metodologia-chave descoberta na década de 1980 (KUNTZ et al., 1982), pode ser definida como uma predição da energia e especificidade na qual uma molécula se liga a uma biomacromolécula, mais comumente a uma enzima (LAZARIDIS, 2002). Seus algoritmos e

funções são capazes de gerar estruturas dos complexos receptor-ligante, ranquear compostos e até mesmo estimar as energias de ligação (YURIEV; HOLIEN; RAMSLAND, 2015).

Por meio do *docking* é possível determinar qual o melhor alinhamento entre duas moléculas, comumente uma pequena molécula e uma proteína, onde exige-se a presença de dados por homologia, RMN ou raio-X da proteína em estudo. A proteína deve possuir um ligante para que seu sítio ativo seja identificado pelas análises de raio-X, permitindo-se que outros compostos sejam ancorados neste sítio ativo através da substituição do ligante, possibilitando a identificação de novas entidades moleculares com afinidades de ligação ou interações mais fortes e adequadas (JENSEN, 2007).

O *docking* é idealizado como um processo onde cada etapa introduz um ou mais níveis de complexidade (BROOIJMANS; KUNTZ, 2003). O método inicia-se com a aplicação de algoritmos em poses ou orientações de moléculas orgânicas no interior do sítio de interação, sendo um grande desafio, uma vez que moléculas orgânicas, geralmente, apresentam elevado grau de liberdade conformacional. A identificação das diferentes conformações que melhor correspondem à estrutura do receptor deve ser realizada com eficiente acurácia e ser suficientemente rápida na avaliação de centenas de compostos em uma determinada série ou corrida. Os algoritmos são complementados por *Scoring Functions* que são empregadas para predizer a atividade biológica através da avaliação das interações entre os compostos e alvos em estudo (KITCHEN et al., 2004). Os confôrmeros pré-selecionados são sempre avaliados adicionalmente com relação às interações eletrostáticas e van der Waals, além da inclusão de algum solvente ou efeito entrópico (GOHLKE; KLEBE, 2002).

Segundo Kapetanovic (2008), a identificação das conformações de ligação mais prováveis envolve duas etapas:

- ✓ Exploração de um grande espaço conformacional representando diferentes potenciais modos de ligação;
- ✓ Previsão precisa da energia de interação associada às conformações das ligações previstas.

De acordo com Ferreira et al. (2015), na busca conformacional os parâmetros estruturais dos ligantes (graus de liberdade torsional, translacional e rotacional) são consideravelmente modificados. Para tal busca, os algoritmos aplicam métodos sistemáticos e estocásticos.

A Figura 9 ilustra esquematicamente o processo do *docking* molecular.

Figura 9 – Esquematização do processo de *docking* molecular.

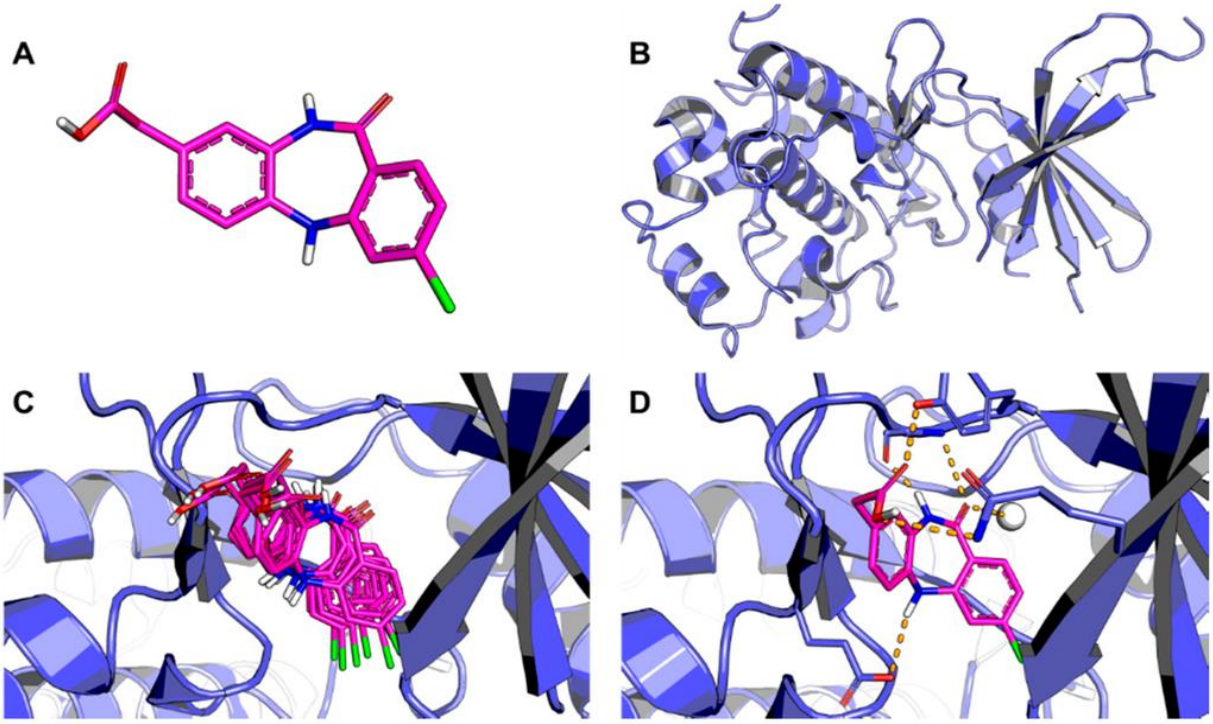

Legenda: A – Estrutura 3D do ligante; B – Estrutura 3D do receptor; C – Docking do ligante na cavidade de ligação do receptor; D – Identificação da conformação mais apropriada e suas interações intermoleculares.

Fonte: Adaptado de Ferreira et al. (2015).

O ancoramento molecular pode ser aplicado em diferentes alvos macromoleculares, como ancoramento proteína-proteína, proteína-DNA e proteína-ligante, sendo largamente utilizado para identificação de líderes promissores de um grande conjunto de dados de compostos (TANG; MARSHALL, 2011). Essa aplicação conduz a otimizações estruturais, predição de afinidades biológicas, identificação de sítios de interação, racionalização de

mecanismos de reações enzimáticas. O ancoramento proteína-ligante é o mais empregado e bastante útil na descoberta de novos agentes terapêuticos, sendo ainda um sistema mais simples quando comparado com os outros tipos de ancoramento (BALLANTE; MARSHALL, 2015).

O *docking* molecular proteína-ligante é capaz de predizer qual a conformação mais plausível de um ligante no sítio de ligação de um alvo terapêutico através da formação de um complexo estável por meio de métodos de busca ou amostragem, explorando possíveis orientações e conformações do ligante no interior de sítio de interação e estimando as interações usando-se *Scoring Functions* (BABINE; BENDER, 1997) ou campos de força empíricos e mecânica estatística (STEINBRECHER; CASE; LABAHN, 2006).

As interações receptor-ligante são governadas por meio da combinação de fatores entrópicos e entálpicos, podendo a entalpia e/ou entropia dominar interações específicas. Isto sempre expõe um problema para as *Scoring Functions*, onde a maioria destas funções são mais focadas na obtenção de valores energéticos do que nos efeitos entrópicos. Adicionalmente, outras complicações como resolução limitada de dados cristalográficos, flexibilidade inerente, ajuste induzido ou outras alterações conformacionais que ocorrem na interação e a participação de moléculas de água nas interações proteína-ligante fazem do ancoramento molecular um processo relativamente complexo (KITCHEN et al., 2004).

Para a avaliação dos diferentes métodos de ancoramento molecular é importante considerar como receptor e ligante são representados. Existem três formas básicas de representação do receptor, como atômica, superfície e grade (HALPERIN et al., 2002). A representação atômica é utilizada em combinação com uma função de energia potencial e durante procedimentos finais de ranqueamento devido à complexidade computacional de avaliação de interações atômica emparelhadas (BURNETT; TAYLOR, 2000). Representações baseadas na superfície são comumente utilizadas em *docking* proteína-proteína (NOREL et al., 1999), onde busca-se o alinhamento de pontos na superfície minimizando o ângulo entre as superfícies opostas das moléculas (NOREL; WOLFSON; NUSSINOV, 1999). No entanto, aproximações que mantêm rígidas as estruturas proteicas são ainda o padrão para muitas

técnicas deste tipo de ancoramento. Já representações em grade para cálculos de energia possuem como ideia básica o armazenamento das informações sobre as contribuições energéticas do receptor nos pontos de grade, onde os dois tipos de potenciais envolvidos são o eletrostático (Eq. 1) e o de van der Waals (Eq. 2) (KITCHEN et al., 2004).

$$E_{coul}(r) = \sum_{i=1}^{N_A} \sum_{j=1}^{N_B} \frac{q_i q_j}{4\pi\varepsilon_0 r_{ij}} \qquad \text{(Eq. 1)}$$

$$E_{vdW}(r) = \sum_{j=1}^{N} \sum_{i=1}^{N} 4\varepsilon \left[\left(\frac{\sigma_{ij}}{r_{ij}} \right)^{12} - \left(\frac{\sigma_{ij}}{r_{ij}} \right)^{6} \right] \qquad \text{(Eq. 2)}$$

A energia potencial eletrostática (Eq. 1) é representada pela soma das interações Coulombianas, onde N_A é o número de átomos na molécula A, N_B é o número de átomos na molécula B e q é a carga de cada átomo. Já a energia potencial de van der Waals para o tratamento de interações não ligadas são sempre moduladas por uma função 6-12 Lennard-Jones (Eq. 2), onde ε é a profundidade do potencial e σ é o diâmetro dos respectivos átomos *i* e *j* (KITCHEN et al., 2004).

O ancoramento molecular pode apresentar limitações relacionadas à interdependência entre amostragem e *Scoring* empregados, podendo comprometer assim a capacidade preditiva das poses no sítio de interação. Esta limitação determina comportamentos instáveis de um determinado protocolo de ancoramento para diferentes sistemas-alvo, necessitando a validação de sua habilidade de reproduzir as poses experimentais de interação dos ligantes para determinar sua capacidade preditiva (BALLANTE; MARSHALL, 2015).

O estudo e uso do docking tem sido essencial para identificar compostos promissores que possam representar futuras soluções para diferentes áreas que tratam da saúde humana (FERREIRA et al., 2015). Diferentes estudos teóricos de nosso grupo de pesquisa podem ser citados, busca por novos agentes antimaláricos (SANTOS-GARCIA et al., 2018), anti-Leishmania (GOODARZI et al., 2010), anticolinesterásicos (TERRA et al., 2018), inibidores de tirosina quinase (ASSIS et al., 2016), agentes antitumorais (GUIMARÃES et al., 2016).

3 OBJETIVOS

3.1 Objetivos gerais

O trabalho visou avaliar o nível de interação proteína-ligante de uma grande variedade de compostos indolinônicos e as enzimas Aurora B e FLT3 humanas através da técnica de *docking* molecular. Por meio desses estudos buscou-se propor novos potenciais ligantes que futuramente possam tornar-se promissores protótipos candidatos a fármacos para utilização no tratamento de diferentes patologias tumorais.

3.2 Objetivos específicos

- Compreender as interações envolvidas para as enzimas Aurora B e FLT3 humanas com a classe de compostos indolinônicos que foram avaliados;

- Reconhecer os resíduos de aminoácidos que foram de maior relevância nas interações para as duas enzimas estudadas;

- Propor novos derivados inibidores de Aurora B ou FLT3 humanas capazes de interagir de forma mais efetiva com os sítios estudados;

- Propor novos derivados com atividade *dual* relevante contra as enzimas Aurora B e FLT3 humanas, visando a busca de um novo promissor protótipo a fármaco anticâncer, destacando-se leucemia mieloide aguda;

- Contribuir para o desenvolvimento de um possível protótipo candidato a fármaco anticâncer no futuro.

4 CONCLUSÃO

Foram realizadas análises de docking para a compreensão das interações entre derivados indolin-2-ona com as enzimas humanas Aurora B e FLT3, ambas envolvidas em processos tumorais em mamíferos. Diferentes derivados foram explorados por meio dos compostos **1-45** e **IAF1-IAF100** evidenciados nos dois artigos presentes na segunda parte desse trabalho.

Os resultados de ancoramento molecular obtidos, juntamente com dados experimentais de inibição disponíveis, sugerem a presença de importantes vacâncias próximas às subunidades indolin-2-ona e subunidade terminal diretamente ligada ao anel pirrólico desses compostos para ambas as enzimas Aurora B e FLT3. Assim, subunidades ou grupos substituintes mais adequados para as vacâncias em questão, considerando compostos com padrão estrutural similiar, poderiam aumentar consideravelmente a afinidade para ambas enzimas, podendo refletir diretamente na atividade inibitória.

Para os novos compostos propostos, quatro deles puderam ser destacados com maior estabilidade energética para Aurora B quinase (**IAF61**, **IAF63**, **IAF66** e **IAF79**) e seis deles para a enzima FLT3 (**IAF70**, **IAF72**, **IAF75**, **IAF80**, **IAF84** e **IAF88**). Todos esses compostos preencheram de forma mais adequada a vacância próxima à subnidade indolin-2-ona mencionada e exibiram conjunto de parâmetros de interação mais adequados e satisfatórios, mostrando que os estudos de docking podem ser considerados como uma importante ferramenta da química medicinal empregada na busca de compostos mais efetivos e no planejamento racional de novos fármacos.

Assim, essa classe de compostos, tendo a subunidade indolin-2-ona central, pode ser considerada como promissora na busca de um possível inovador candidato à fármaco que possa ser empregado no tratamento de diferentes tipos de câncer, inclusive leucemia mieloide aguda. Alguns compostos propostos estudados, destacando-se **IAF79**, exibiram atividades duais promissoras contra Aurora B/FLT3, além de um interessante padrão molecular que deve ser melhor investigado sinteticamente e biologicamente na busca por novos candidatos a fármacos anticâncer, corroborando assim com os estudos de docking realizados.

REFERÊNCIAS

ADAMS, R. R.; CARMENA, M.; EARNSHAW, W. C. Chromosomal passengers and the (aurora) ABCs of mitosis. **Trends in Cell Biology**, Cambridge, Elsevier Science Publishers, v. 11, n. 2, p. 49-54, Fevereiro, 2001.

ALVES, F. R.; BARREIRO, E. J.; FRAGA, C. A. From Nature to Drug Discovery: The Indole Scaffold as a 'Privileged Structure'. **Mini Reviews in Medicinal Chemistry**, Sharjah, Bentham Science Publishers, v. 9, n. 7, p. 782-793, Junho, 2009.

ANDREWS, P. D. et al. Mitotic mechanics: the auroras come into view. **Current Opinion Cell Biology**, Philadelphia, Current Science, v. 15, n. 6, p. 672-683, Dezembro, 2003.

ANDRICOPULO, A. D.; SALUM, L. B.; ABRAHAM, D. J. Structure-Based Drug Design Strategies in Medicinal Chemistry. **Current Topics in Medicinal Chemistry**, Sharjah, Bentham Science Publishers, v. 9, n. 9, p. 771-790, 2009.

ASSIS, L. C. et al. Structure-based Drugs Design Studies on Spleen Tyrosine Kinase Inhibitors. **Letters in Drug Design & Discovery**, San Francisco, Bentham Science Publishers, v. 13, n. 9, p. 845-858, Novembro, 2016.

BABINE, R. E.; BENDER, S. L. Molecular Recognition of Protein-Ligand Complexes: Applications to Drug Design. **Chemical Reviews**, Washington, American Chemical Society, v. 97, n. 5, p. 1359−1472, Agosto, 1997.

BALLANTE, F.; MARSHALL, G. R. An Automated Strategy for Binding-Pose Selection and Docking Assessment in Structure-Based Drug Design. **Journal of Chemical Information and Modeling**, Washington, American Chemical Society, v. 56, n. 1, p. 54–72, Dezembro, 2015.

BARREIRO, E. J.; FRAGA, C. A. M. **Química Medicinal: as bases moleculares da ação dos fármacos**. 2ª ed. Porto Alegre: Artmed, 536 p., 2008.

BAVETSIAS, V. et al. Optimization of Imidazo[4,5-*b*]pyridine-Based Kinase Inhibitors: Identification of a Dual FLT3/Aurora Kinase Inhibitor as an Orally Bioavailable Preclinical Development Candidate for the Treatment of Acute Myeloid Leukemia. **Journal of Medicinal Chemistry**, Washington, American Chemical Society, v. 55, p. 8721-8734, Outubro, 2012.

BEBBINGTON, D. et al. The discovery of the potent aurora inhibitor MK-0457 (VX-680). **Bioorganic & Medicinal Chemistry Letters**, Oxford, Elsevier Science Ltd., v. 19, n. 13, p. 3586-3592, Julho, 2009.

BELLO, C. L. et al. Effect of food on the pharmacokinetics of sunitinib malate (SU11248), a multi-targeted receptor tyrosine kinase inhibitor: results from a phase I study in healthy subjects. **Anticancer Drugs**, London, Lippincott Williams & Wilkins, v. 17, n. 3, p. 353-358, Março, 2006.

BERENSTEIN, R. Class III Receptor Tyrosine Kinases in Acute Leukemia – Biological Functions and Modern Laboratory Analysis. **Biomarker Insights**, Auckland, Libertas Academica Ltd., v. 10, n. 3, p. 1-14, Julho, 2015.

BHEEMANAPALLI, L. N. et al. Synthesis, evaluation of 6,8-dibromo-2-aryl-2,3-dihydroquinolin-4(1H)-ones in MCF-7 (breast cancer) cell lines and their docking studies. **Medicinal Chemistry Research**, New York, Springer, v. 21, n. 8, p. 1741-1750, Agosto, 2012.

BOLANOS-GARCIA, V. M. Aurora kinases. **The Internationl Journal of Biochemistry & Cell Biology**, Amsterdam, Elsevier, v. *37*, n. 8, p. 1572-1577, Agosto, 2005.

BRASIL. Ministério da Saúde – Instituto Nacional de Câncer José Alencar Gomes da Silva (INCA). **Estimativa 2018**: Incidência de Câncer no Brasil. Rio de Janeiro: INCA, 2018.

BROOIJMANS, N.; KUNTZ, I. D. Molecular recognition and docking algorithms. **Annual Reviews Biophysics and Biolmolecular Structure**, Palo Alto, Annual Reviews, v. 32, p. 335–373, Janeiro, 2003.

BURNETT, R. M.; TAYLOR, J. S. Darwin: A program for docking flexible molecules. **Proteins: Structure, Function, and Bioinformatics**, New York, Wiley-Liss, v. 41, n. 2, p. 173-191, Novembro, 2000.

BYRNE, J. D.; YEH, J. J.; DESIMONE, J. M. Use of iontophoresis for the treatment of cancer. **Journal of Controlled Release**, Amsterdam, Elsevier, v. 284, p. 144-151, Junho, 2018.

CADET, J. et al. Oxidatively generated complex DNA damage: Tandem and clustered lesions. **Cancer Letters**, Limerick, Elsevier Science Ireland, v. 327, n. 1-2, p. 5-15, Dezembro, 2012.

CARMENA, M.; RUCHAUD, S.; EARNSHAW, W. C. Making the Auroras glow: regulation of Aurora A and B kinase function by interacting proteins. **Current Opinion in Cell Biology**, London, Current Biology, v. 21, n. 6, p. 796-805, Dezembro, 2009.

CARVAJAL, R. D.; TSE, A.; SCHWARTZ, G. K. Aurora Kinases: New Targets for Cancer Therapy. **Clinical Cancer Research**, Denville, The Association, v. 12, n. 23, p.6869-6875, Dezembro, 2006.

CHAO, Q. et al. Identification of *N*-(5-*tert*-Butyl-isoxazol-3-yl)-N'-{4-[7-(2-morpholin-4-yl-ethoxy)imidazo-[2,1-*b*][1,3]benzothiazol-2-yl]phenyl}urea Dihydrochloride (AC220), a Uniquely Potent, Selective, and Efficacious FMS-Like Tyrosine Kinase-3 (FLT3) Inhibitor. **Journal of Medicinal Chemistry**, Washington, American Chemical Society, v. 52, p. 7808-7816, Setembro, 2009.

CHOW, L. Q.; ECKHARDT, S. G. Sunitinib: From Rational Design to Clinical Efficacy. **Journal of Clinical Oncology**, Alexandria, American Society of Clinical Oncology, v. 25, n. 7, p. 884-896, Março, 2007.

CHU, T. F. et al. Cardiotoxicity associated with tyrosine kinase inhibitor sunitinib. **Lancet**, London, Elsevier, v. 370, n. 9604, p. 2011-2019, Dezembro, 2007.

DESCAMPS, S.; PRIGENT, C. Two Mammalian Mitotic Aurora Kinases: Who's Who? **Science Signaling**, Washington, Stanford University Libraries, v. 2001, n. 73, p. 1-5, Março, 2001.

DIPPLE, A. DNA adducts of chemical carcinogens. **Carcinogenesis**, Oxford, Irl Press at Oxford University Press, v. 16, n. 3, p. 437-441, Março, 1995.

DUBBS, S. B. The Latest Cancer Agents and Their Complications. **Emergency Medicine Clinics of North America**, Philadelphia, Elsevier Health Sciences Division, v. 36, n. 3, p. 485-492, Agosto, 2018.

DUCAT, D.; ZHENG, Y. Aurora kinases in spindle assembly and chromosome segregation. **Experimental Cell Research**, Orlando, Academic Press, v. 301, n. 1, p. 60-67, Novembro, 2004.

ELKINS, J. M. et al. Crystal Structure of Human Aurora B in Complex with INCENP and VX-680. **Journal of Medicinal Chemistry**, Washington, American Chemical Society, v. 55, n. 17, p. 7841-7848, Agosto, 2012.

ENGEL, T. Basic overview of chemoinformatics. **Journal of Chemical Information and Modeling**, Washington, American Chemical Society, v. 46, n. 6, p. 2267-2277, Novembro, 2006.

ERKIZAN, H. V. et al. A small molecule blocking oncogenic protein EWS-FLI1 interaction with RNA helicase A inhibits growth of Ewing's sarcoma. **Nature Medicine**, New York, Nature Publishing Company, v. 15, n. 7, p. 750–756, Julho, 2009.

FERREIRA, L. G.; DOS SANTOS, R. N.; OLIVA, G.; ANDRICOPULO, A. D. Molecular Docking and Structure-Based Drug Design Strategies. **Molecules**, Basel, MDPI, v. 20, p. 13384-13421, Julho, 2015.

GASSMANN, R. et al. Borealin: a novel chromosomal passenger required for stability of the bipolar mitotic spindle. **The Journal of Cell Biology**, New York, Rockefeller University Press, v. 166, n. 2, p. 179-191, Julho, 2004.

GAUTSCHI, O. et al. Aurora kinases as anticancer drug targets. **Clinical Cancer Research**, Denville, The Association, v. 14, n. 6, p. 1639-1648, Março, 2008.

GLOVER, D. M. et al. Mutations in aurora prevent centrosome separation leading to the formation of monopolar spindles. **Cell**, Cambridge, Cell Press, v. 81, n. 1, p. 95-105, Fevereiro, 1995.

GODL, K. et al. Proteomic Characterization of the Angiogenesis Inhibitor SU6668 Reveals Multiple Impacts on Cellular Kinase Signaling. **Cancer Research**, Baltimore, American Association for Cancer Research, v. 65, n. 15, p. 6919-6926, Agosto, 2005.

GOHLKE, H.; KLEBE, G. Approaches to the description and prediction of the binding affinity of small-molecule ligands to macromolecular receptors. **Angewandte Chemie**, Weinheim, Wiley-VCH, v. 41, n. 15, p. 2644–2676, Agosto, 2002.

GOLDENSON, B.; CRISPINO, J. D. The aurora kinases in cell cycle and leucemia. **Oncogene**, Basingstoke, Nature Publishing Group, v. 34, n. 5, p. 537-545, Janeiro, 2015.

GOODARZI, M. et al. QSAR and Docking Studies of Novel Antileishmanial Diaryl Sulfides and Sulfonamides. **European Journal of Medicinal Chemistry**, Paris, Editions Scientifiques Elsevier, v. 45, n. 11, p. 4879-4889, Novembro, 2010.

GORDON, D. J.; RESIO, B.; PELLMAN, D. Causes and consequences of aneuploidy in cancer. **Nature Reviews Genetics**, London, Nature Publishing Group, v. 13, n. 3, p. 189-203, Janeiro, 2012.

GUIDO, R. V.; OLIVA, G.; ANDRICOPULO, A. D. Virtual screening and its integration with modern drug design technologies. **Current Medicinal Chemistry**, Schiphol, Bentham Science Publishers, v. 15, n. 1, p. 37-46, Janeiro, 2008.

GUIMARÃES, K. G. et al. Synthesis, antiproliferative activities, and computational evaluation of novel isocoumarin and 3,4-dihydroisocoumarin derivatives. **European Journal of Medicinal Chemistry**, Paris, Editions Scientifiques Elsevier, v. 111, p. 103-113, Março, 2016.

GUPTA, L.; TALWAR, A.; CHAUHAN, P. M. Bis and Tris Indole Alkaloids from Marine Organisms: New Leads for Drug Discovery. **Current Medicinal Chemistry**, Schiphol, Bentham Science Publishers, v. 14, n. 16, p. 1789-1803, Julho, 2007.

HAUF, S. et al. The small molecule Hesperadin reveals a role for Aurora B in correcting kinetochore–microtubule attachment and in maintaining the spindle assembly checkpoint. **The Journal of Cell Biology**, New York, Rockefeller University Press, v. 161, n. 2, p. 281-294, Abril, 2003.

HALPERIN, I. et al. Principles of docking: an overview of search algorithms and a guide to scoring functions. **Proteins: Structure, Function, and Bioinformatics**, New York, Wiley-Liss, v. 47, n. 4, p. 409-443, Junho, 2002.

HU, Y.; FU, L. Targeting cancer stem cells: a new therapy to cure cancer patients. **American Journal of Cancer Research**, Madison, e-Century Publishing Corporation, v. 2, n. 3, p. 340-356, Abril, 2012.

JAGTAP, A. D. et al. Novel acylureidoindolin-2-one derivatives as dual Aurora B/FLT3 inhibitors for the treatment of acute myeloid leucemia. **European Journal of Medicinal Chemistry**, Paris, Editions Scientifiques Elsevier, v. 85, p. 268-288, Julho, 2014.

JENSEN, F. **Introduction to computacional chemistry**, 2ª ed. Chichester: John Wiley & Sons, 599 p., 2007.

KAMMASUD, N. et al. 5-Substituted pyrido[2,3-d]pyrimidine, an inhibitor against three receptor tyrosine kinases. **Bioorganic & Medicinal Chemistry Letters**, Oxford, Elsevier Science Ltd., v. 19, n. 3, p. 745-750, Fevereiro, 2009.

KAPETANOVIC, I. M. Computer-aided drug discovery and development (CADDD): In silico-chemico-biological approach. **Chemico-Biological Interactions**, Limerick, Elsevier, v. 171, p. 165-176, Dezembro, 2008.

KATAYAMA, H.; BRINKLEY, W. R.; SEN, S. The Aurora kinases: Role in cell transformation and tumorigenesis. **Cancer Metastasis Reviews**, Boston, Kluwer Academic, v. 22, n. 4, p. 451-464, Dezembro, 2003.

KAYSER, S. et al. Insertion of FLT3 internal tandem duplication in the tyrosine kinase domain-1 is associated with resistance to chemotherapy and inferior outcome. **Blood**, Washington, American Society of Hematology, v. 114, n. 12, p. 2386-2392, Julho, 2009.

KEEN, N.; TAYLOR, S. Aurora-kinase inhibitors as anticancer agents. **Nature Reviews Cancer**, London, Nature Publishing Group, v. 4, n. 12, p. 927-936, Dezembro, 2004.

KEREKES, A. D. et al. Aurora Kinase Inhibitors Based on the Imidazo[1,2-a]pyrazine Core: Fluorine and Deuterium Incorporation Improve Oral Absorption and Exposure. **Journal of Medicinal Chemistry**, Washington, American Chemical Society, v. 54, n. 1, p. 201-210, Janeiro, 2011.

KHANWELKAR, R. R. et al. Synthesis and structure–activity relationship of 6-arylureido-3-pyrrol-2-ylmethylideneindolin-2-one derivatives as potent receptor tyrosine kinase inhibitors. **Bioorganic & Medicinal Chemistry**, Oxford, Elsevier Science, v. 18, p. 4674-4686, Maio, 2010.

KIELBASSA, C.; ROZA, L.; EPE, B. Wavelength dependence of oxidative DNA damage induced by UV and visible light. **Carcinogenesis**, Oxford, Irl Press at Oxford University Press, v. 18, n. 4, p. 811-816, Abril, 1997.

KITCHEN, D. B. et al. Docking and scoring in virtual screening for drug discovery: methods and applications. **Nature Reviews Drug Discovery**, London, Nature Pub. Group, v. 3, n. 11, p. 935–949, Novembro, 2004.

KUNTZ, I. D. et al. A geometric approach to macromolecule-ligand interactions. **Journal of Molecular Biology**, Amsterdam, Elsevier, v. 161, n. 2, p. 269-288, Outubro, 1982.

KRUG, M.; HILGEROTH, A. Recent Advances in the Development of Multi-Kinase Inhibitors. **Mini Reviews in Medicinal Chemistry**, Hilversum, Bentham Science Publishers, v. 8, n. 13, p. 1312-1327, Novembro, 2008.

LADYGINA, N. G.; LATSIS, R. V.; YEN, T. Effect of the pharmacological agent hesperadin on breast and prostate tumor cultured cells. **Biomeditsinskaia Khimiia**, Moskva, Rossiĭskaia Akademiia Meditsinskikh Nauk, v. 51, n. 2, p. 170-176, Março-Abril, 2005.

LAYEK, M. et al. Transition metal mediated construction of pyrrole ring on 2,3-dihydroquinolin-4(1H)-one: synthesis and pharmacological evaluation of novel tricyclic heteroarenes. **Organic & Biomolecular Chemistry**, Cambridge, Royal Society of Chemistry, v. 9, n. 4, p. 1004-1007, Fevereiro, 2011.

LAZARIDIS, T. Binding Affinity and Specificity from Computational Studies. **Current Organic Chemistry**, Sharjah, Bentham Science Publishers, v. 6, n. 14, p. 1319-1332, Dezembro, 2002.

LV, K. et al. Synthesis and antitumor activity of 5-[1-(3-(dimethylamino)propyl)-5-halogenated-2-oxoindolin-(3Z)-ylidenemethyl]-2,4-dimethyl-1H-pyrrole-3-carboxamides. **Bioorganic & Medicinal Chemistry Letter**s, Oxford, Elsevier Science Ltd., v. 21, n. 10, p. 3062-3065, Maio, 2011.

MA, F. et al. Design, synthesis and biological evaluation of indolin-2-one-based derivatives as potent, selective and efficacious inhibitors of FMS-like tyrosine kinase3 (FLT3). **European Journal of Medicinal Chemistry**, Paris, Editions Scientifiques Elsevier, v. 127, p. 72-86, Janeiro, 2017.

MILLER, E. C.; MILLER, J. A. Searches for Ultimate Chemical Carcinogens and Their Reactions with Cellular Macromolecules. **Cancer**, Hoboken, Wiley, v. 47, n.10, p. 2327-2345, Maio, 1981.

MOORE, A. S. et al. Selective FLT3 inhibition of FLT3-ITD^{+} acute myeloid leukaemia resulting in secondary D835Y mutation: a model for emerging clinical resistance patterns. **Leukemia**, London, Nature Publishing Group, v. 26, n. 7, p. 1462-1470, Julho, 2012.

MOTZER, R. J. et al. Sunitinib versus Interferon Alfa in Metastatic Renal-Cell Carcinoma. **The New England Journal of Medicine**, Boston, Massachusetts Medical Society, v. 356, n. 2, p. 115-124, Janeiro, 2007.

MOUNTZIOS, G.; TERPOS, E.; DIMOPOULOS, M. A. Aurora kinases as targets for cancer therapy. **Cancer Treatment Reviews**, New York, Elsevier Scientific Publishers Co., v. 34, n. 2, p. 175-182, Abril, 2008.

NG, R. **Drugs: from discovery to approval**. 1ª ed. Hoboken: John Wiley & Sons Inc., 368 p., 2004.

NIKONOVA, A. S. et al. Aurora A kinase (AURKA) in normal and pathological cell division. **Cellular and Molecular Life Sciences**, Basel, mBirkhauser, v. 70, p. 661-687, Agosto, 2012.

NOREL, R.; WOLFSON, H.; NUSSINOV, R. Small molecular recognition: solid angles surface representation and shape complementarity. **Combinatorial Chemistry & High Throughput Screening**, Miami, Bentham Science Publishers, v. 2, n. 4, p. 223-237, Agosto, 1999.

NOREL, R. et al. Examination of shape complementarity in docking of unbound proteins. **Proteins: structure, function, and genetics**, Hoboken, Wiley, v. 36, n. 3, p. 307-317, Agosto, 1999.

OSTRONOFF, F.; ESTEY, E. The role of quizartinib in the treatment of acute myeloid leucemia. **Expert Opinion on Investigational Drugs**, London, Ashley Publications Ltd., v. 22, n. 12, p. 1659-1669, Dezembro, 2013.

OTTO, T.; SICINSKI, P. Cell cycle proteins as promising targets in cancer therapy. **Nature Reviews: Cancer**, London, Nature Publishing Group, v. 17, n. 2, p. 93-115, Julho, 2017.

PASTORE, D. FLT3 inhibitors in acute myeloid leucemia. **Drugs and cell therapies in hematology**, Pavia, EDIMES, v. 4, n. 1, p. 14-21, Janeiro, 2016.

PEJOVIC, A. et al. Antimicrobial ferrocene containing quinolinones: Synthesis, spectral, electrochemical and structural characterization of 2-ferrocenyl-2,3-dihydroquinolin-4(1H)-one and its 6-chloro and 6-bromo derivatives. **Polyhedron**, London, Elsevier, v. 31, n. 1, p. 789-795, Janeiro, 2012.

PENTHALA, N. R. et al. Synthesis and in vitro evaluation of N-alkyl-3-hydroxy-3-(2-imino-3-methyl-5-oxoimidazolidin-4-yl)indolin-2-one analogs as potential anticancer agents. **Bioorganic & Medicinal Chemistry Letters**, Oxford, Elsevier Science Ltd., v. 20, n. 15, p. 4468-4471, Agosto, 2010.

POLLARD, J. R.; MORTIMORE, M. Discovery and Development of Aurora Kinase Inhibitors as Anticancer Agents. **Journal of Medicinal Chemistry**, Washington, American Chemical Society, v. 52, n. 9, p. 2629-2651, Maio, 2009.

PORT, M. et al. Prognostic significance of FLT3 internal tandem duplication, nucleophosmin 1, and CEBPA gene mutations for acute myeloid leukemia patients with normal karyotype and younger than 60 years: a systematic review and meta-analysis. **Annals of Hematology**, Berlin, Springer Verlag, v. 93, p. 1279–1286, Maio, 2014.

PRAKASH, C. R.; RAJA, S. Indolinones as Promising Scaffold as Kinase Inhibitors: A Review. **Mini Reviews in Medicinal Chemistry**, Hilversum, Bentham Science Publishers, v. 12, n. 2, p. 98-119, Fevereiro, 2012.

PRIGENT, C.; DIMITROV, S. Phosphorylation of serine 10 in histone H3, what for? **Journal of Cell Science**, Cambridge, Company of Biologists, v. 116, n. 18, p. 3677-3685, Setembro, 2003.

PRIME, M. E. et al. Phthalazinone Pyrazoles as Potent, Selective, and Orally Bioavailable Inhibitors of Aurora-A Kinase. **Journal of Medicinal Chemistry**, Washington, American Chemical Society, v. 54, n. 1, p. 312-319, Janeiro, 2011.

QI, W. et al. Aurora inhibitor MLN8237 in combination with docetaxel enhances apoptosis and anti-tumor activity in mantle cell lymphoma. **Biochemical Pharmacology**, Oxford, Elsevier Science, v. 81, n. 7, p. 881-890, Abril, 2011.

ROOS, W. P.; KAINA, B. DNA damage-induced cell death: from specific DNA lesions to the DNA damage response and apoptosis. **Cancer Letters**, Limerick, Elsevier Science Ireland, v. 332, n. 2, p. 237-248, Maio, 2013.

RUCHAUD, S.; CARMENA, M.; EARNSHAW, W. C. Chromosomal passengers: conducting cell division. **Nature Reviews Molecular Cell Biology**, London, Nature Publushing Group, v. 8, n. 10, p. 798-812, Outubro, 2007.

SANTOS-GARCIA, L. et al. QSAR Study of N-Myristoyltransferase Inhibitors of Antimalarial Agents. **Molecules**, Basel, MDPI, v. 23, n. 9, p. 2348-2356, Setembro, 2018.

SATO, N. et al. Correlation between centrosome abnormalities and chromosomal instability in human pancreatic cancer cells. **Cancer Genetics and Cytogenetics**, New York, Elsevier Scientific Publishers Co., v. 126, n. 1, p. 13-19, Abril, 2001.

SESSA, F. et al. Mechanism of Aurora B Activation by INCENP and Inhibition by Hesperadin. **Molecular Cell**, Cambridge, Cell Press, v. 18, n. 3, p. 379-391, Abril, 2005.

SHANNON, K. B.; SALMON, E. D. Chromosome Dynamics: New Light on Aurora B Kinase Function. **Current Biology**, Cambridge, Cell Press, v. 12, n. 13, p. R458-R460, Julho, 2002.

SIEGEL, R.; NAISHADHAM, D.; JEMAL, A. Cancer Statistics for Hispanics/Latinos, 2012. **CA: Cancer Journal for Clinicians**, Hoboken, Wiley, v. 62, n. 5, p. 283-298, Setembro-Outubro, 2012.

SMITH, C. C. et al. Validation of ITD mutations in FLT3 as a therapeutic target in human acute myeloid leukaemia. **Nature**, London, Nature Publishing Group, v. 485, n. 7397, p. 260-263, Julho, 2012.

STEINBRECHER, T.; CASE, D. A.; LABAHN, A. A Multistep Approach to Structure-Based Drug Design: Studying Ligand Binding at the Human Neutrophil Elastase. **Journal of Medicinal Chemistry**, Washington, American Chemical Society, v. 49, n. 6, p. 1837-1844, Março, 2006.

STOLS, L. et al. New vectors for co-expression of proteins: Structure of Bacillus subtilis ScoAB obtained by high-throughput protocols. **Protein Expression and Purification**, Orlando, Academic Press, v. 53, n. 2, p. 396-403, Junho, 2007.

SUIT, H. et al. Secondary carcinogenesis in patients treated with radiation: a review of data on radiation induced cancers in human, non-human primate, canine and rodent subjects. **Radiation Research**, Washington, Radiation Research Society, v. 167, n. 1, p. 12-42, Janeiro, 2007.

TANNER, M. M. et al. Frequent Amplification of Chromosomal Region 20q12-q13 in Ovarian Cancer. **Clinical Cancer Research**, Denville, The Association, v. 6, n. 5, p. 1833-1839, Maio, 2000.

TANG, Y. T.; MARSHALL, G. R. Virtual Screening for Lead Discovery. **Methods in Molecular Biology**, Totowa, Humana Press, v. 716, p. 1-22, Janeiro, 2011.

TANG, A. et al. Aurora kinases: novel therapy targets in cancers. **Oncotarget**, Albany, Impact Journals, v. 8, p. 23937-23954, Janeiro, 2017.

TAKAHASHI, T. et al. Centrosomal Kinases, HsAIRK1 and HsAIRK3, are Overexpressed in Primary Colorectal Cancers. **Japanese Journal of Cancer Research**, Tokyo, Japanese Cancer Association, v. 91, n. 10, p. 1007-1014, Outubro, 2000.

TERRA, B. et al. Two Novel Donepezil-Lipoic Acid Hybrids: Synthesis, Anticholinesterase and Antioxidant Activities and Theoretical Studies. **Journal of the Brazilian Chemical Society**, São Paulo, Sociedade Brasileira de Química, v. 29, n. 4, p. 738-747, Abril, 2018.

VADER, G.; MEDEMA, R. H.; LENS, S. M. The chromosomal passenger complex: guiding Aurora-B through mitosis. **The Journal of Cell Biology**, New York, Rockefeller University Press, v. 173, n. 6, p. 833-837, Junho, 2006.

VADER, G. et al. The chromosomal passenger complex controls spindle checkpoint function independent from its role in correcting microtubule kinetochore interactions. **Molecular Biology of the Cell**, Bethesda, American Society for Cell Biology, v. 18, p. 4553-4564, Novembro, 2007.

VADER, G.; LENS, S. M. A. The Aurora kinase family in cell division and cancer. **Biochimica et Biophysica Acta**, Amsterdã, Elsevier Scientific Publishers Co., v. 1786, p. 60-72, Julho, 2008.

VINE, K. L. et al. Cytotoxic and Anticancer Activities of Isatin and Its Derivatives: A Comprehensive Review from 2000-2008. **Anti-cancer Agents in Medicinal Chemistry**, Amsterdam, Bentham Science Publishers, v. 9, n. 4, p. 397-414, Maio, 2009.

VOULGARIDOU, G. P. et al. DNA damage induced by endogenous aldehydes: current state of knowledge. **Mutation Research**, Amsterdam, Elsevier, v. 711, n. 1-2, p. 13-27, Junho, 2011.

WATANABE, T. et al. Differentially Regulated Genes as Putative Targets of Amplifications at 20q in Ovarian Cancers. **Japanese Journal of Cancer Research**, Tokyo, Japanese Cancer Association, v. 93, n. 10, p. 1114-1122, Outubro, 2002.

WEIDERHOLD, K. N. et al. Dynamic Phosphorylation of NudC by Aurora B in Cytokinesis. **PLoS One**, San Francisco, Public Library of Science, v. 11, n. 4, p. 1-22, Abril, 2016.

WHO, World Health Organization. **Cancer**. Disponível em: http://www.who.int/cancer/en/. Acesso em: 10 Janeiro 2016.

WHO, World Health Organization. **Cancer**. Disponível em: https://www.who.int/news-room/fact-sheets/detail/cancer. Acesso em: 11 Dezembro 2018.

XIE, H. et al. Discovery of the Novel mTOR Inhibitor and Its Antitumor Activities In Vitro and In Vivo. **Molecular Cancer Therapeutics**, Philadelphia, American Association for Cancer Research, v. 12, n. 6, p. 950-958, Junho, 2013.

YURIEV, E.; HOLIEN, J.; RAMSLAND, P. A. Improvements, trends, and new ideas in molecular docking: 2012–2013 in review. **Journal of Molecular Recognition**, Chichester, John Wiley & Sons, v. 28, p. 581-604, Março, 2015.

ZEKRI, A. et al. AZD1152-HQPA induces growth arrest and apoptosis in androgen-dependent prostate cancer cell line (LNCaP) via producing aneugenic micronuclei and polyploidy. **Tumour Biology**, Tokyo, Saikon Pub. Co., v. 36, n. 2, p. 623-632, Fevereiro, 2015.

ZIEMSKA, J.; SOLECKA, J. Tyrosine Kinase, Aurora Kinase And Leucine Aminopeptidase As Attractive Drug Targets In Anticancer Therapy - Characterisation Of Their Inhibitors. **Roczniki Państwowego Zakładu Higieny**, Warsaw, National Institute of Public Health, v. 67, n. 4, p. 329-342, Outubro, 2016.

ZIMMERMAN, E. I. et al. Crenolanib is active against models of drug-resistant FLT3-ITD-positive acute myeloid leukemia. **Blood**, Washington, American Society of Hematology, v. 122, n. 22, p. 3607-3615, 2013.

SEGUNDA PARTE

Artigo 1: Aprovado na "*Letters in Drug Design & Discovery*", aguardando publicação.

INDOLIN-2-ONE DERIVATIVES: THEORETICAL STUDIES AIMED AT FINDING MORE POTENT AURORA B KINASE INHIBITORS

Indolin-2-one Derivatives: Theoretical Studies Aimed at Finding More Potent Aurora B Kinase Inhibitors

Ítalo Antônio Fernandes[a,b], Tamiris Maria de Assis[a,b], Isael Aparecido Rosa[a,c], Elaine Fontes Ferreira da Cunha[*a,b]

[a]*Laboratório de Modelagem Molecular, LABGQC, Chemistry Department, Federal University of Lavras, Lavras, MG, Brazil;* [b]*Programa de Pós-Graduação em Agroquímica, Chemistry Department, Federal University of Lavras, Lavras, MG, Brazil;* [c]*Multicêntrico em Química de Minas Gerais (Rede Mineira de Química – RQ-MG), Federal University of Lavras, Lavras, MG, Brazil*

Abstract: Aurora kinases perform roles of importance in mammals, mainly in cell cycle. Overexpression of these enzymes is related to tumor processes and indicative of clinical worsening. Aurora kinases have been considered as promising targets in searching for new anticancer drugs, highlighting Aurora B. This work was designed to study and understand the interactions between human Aurora B and several indolin-2-one derivatives, structurally similar to sunitinib. MVD software was utilized in docking analyses of indolin-2-one derivatives. Human Aurora B kinase was obtained from the PDB (4AF3) and redocked with hesperadin, which was used as reference compound. The predicted model of the training group, considering 21 amino acid residues, performed in Chemoface, achieved an R^2 of 0.945, suggesting that the binding conformations of the ligands with human Aurora B are reasonable and the data can be used to predict the interaction energy of other Aurora B inhibitors indolin-2-one derivatives. MolDock Score energy for compound **1** showed more stable interaction energy (-225.90 kcal.mol^{-1}) than the other inhibitors studied, while sunitinib was the least stable (-135.63 kcal.mol^{-1}). Compounds **1**-**45**, hesperadin and sunitinib, interacted with Glu171 (*–NH* from indolinonic moiety), and the majority of them with Ala173 (C=O from indolinonic moiety) via hydrogen bonds, thus these two residues are relevant for potency. Docking studies and biological activity in literature show subunits likely for structural optimizations, leading to four new proposed derivatives (**IAF61**, **IAF63**, **IAF66**, **IAF79**) as promising compounds for synthesis and biological evaluation against human Aurora B, validating or ratifying the docking studies.

Keywords: Aurora B kinase. Aurora B kinase inhibitors. Indolin-2-one derivatives. Cancer. Medicinal Chemistry. Anticancer compounds. Computational Chemistry. Docking.

1. INTRODUCTION

Aurora kinases are represented by a small family of three homologous serine/threonine kinases (Aurora A, Aurora B, and Aurora C) that perform different roles of paramount importance in mammals, mainly in cell cycle regulation processes [1]. Overexpression of these enzymes is related to a variety of tumor processes, also being indicative of worsening of the clinical condition of diagnosed patients [2-4].

These three enzymes have been considered as promising targets in search for new anticancer compounds, highlighting Aurora B kinase, activated by phosphorylation of both itself and INCENP (Inner Centromere Protein). Human Aurora B is 80% identical to *Xenopus laevis* Aurora B over the kinase domain (55 – 344) and 72% identical to human Aurora A in the catalytic domain. The structure of Human Aurora B has previously been determined in complex with INCENP and VX-680 [5]. Aurora B inhibitors (Fig. **1**) such as barasertib (IC_{50} = 0.37nM) [6, 7], VX-680 (IC_{50} = 18nM) [8], ZM447439 (IC_{50} = 130nM) [9], hesperadin (IC_{50} = 250nM) [10], besides sunitinib (IC_{50} = 1.5µM) [11], a multikinase inhibitor, have been developed as anticancer agents. Hesperadin is an indolin-2-one derivative, presenting a kinase-privileged scaffold, with a sulfonamide substituent at the C-5 position. Molecular docking gives a prediction of the ligand-receptor complex structure using computation methods and has become an increasingly important tool for drug discovery. Looking forward to new potent inhibitors of human Aurora B, docking studies were performed in order to understand the binding mode of indolin-2-one derivatives, developed by Chern and coworkers [12], inside the enzyme active site.

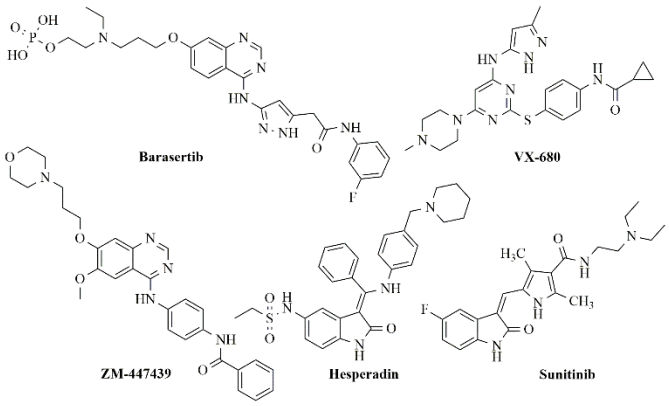

Fig. (1). Chemical structures of Barasertib, VX-680, ZM-447439, Hesperadin, and Sunitinib.

*Address correspondence to this author at the Department of Chemistry, Federal University of Lavras, P.O. Box: 3037, Lavras, Brasil; Tel/Fax: +55-35-38295129; E-mail: elaine_cunha@dqi.ufla.br

Table 1. Chemical structures, IC_{50} and pIC_{50} values of Aurora B Kinase inhibitors [12]. Test set compound numbers are marked with an asterisk.

Compound	Chemical Structure	IC_{50} (nM)	pIC_{50}
1	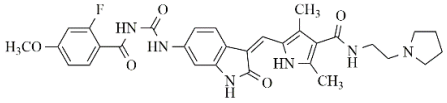	0.4	9.398
2	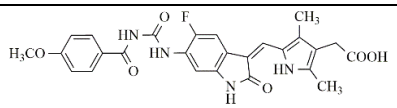	1.0	9.000
3	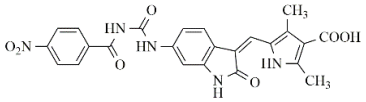	1.2	8.921
4	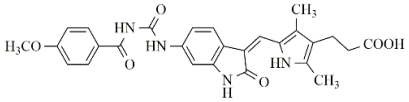	1.2	8.921
5	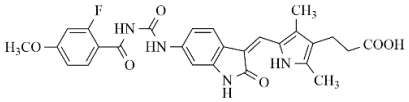	1.3	8.886
6	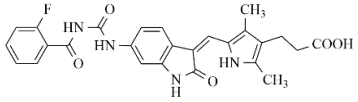	1.5	8.824
7	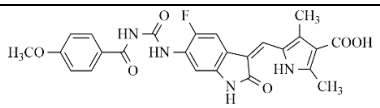	1.5	8.824
8	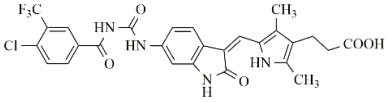	1.6	8.796
9	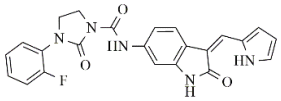	1.8	8.745
10	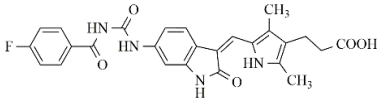	1.8	8.745
11	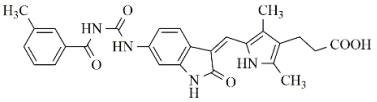	1.9	8.721
12	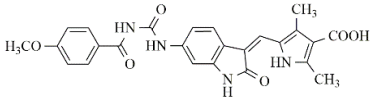	1.9	8.721
13	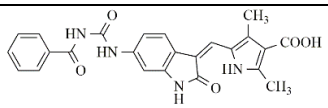	2.1	8.678
14*	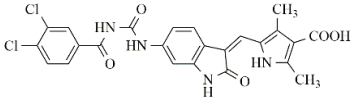	2.1	8.678
15	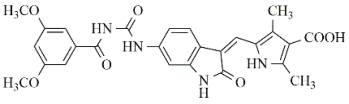	2.1	8.678

16*	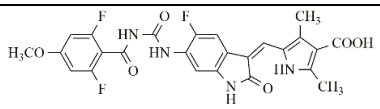	2.1	8.678
17	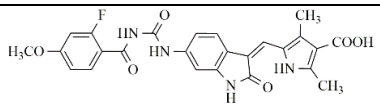	2.3	8.638
18	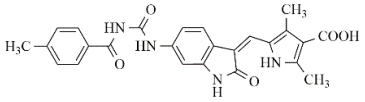	2.5	8.602
19	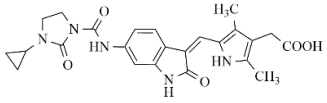	2.7	8.569
20	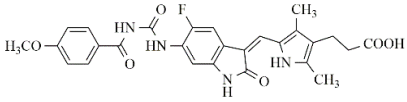	3.0	8.523
21	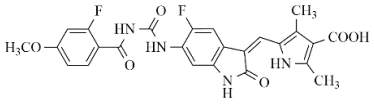	3.0	8.523
22*	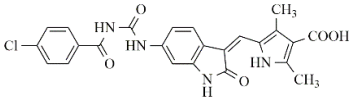	3.1	8.509
23	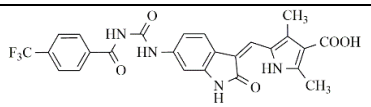	3.1	8.509
24	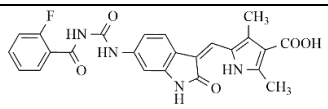	3.7	8.432
25	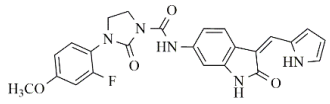	4.4	8.356
26	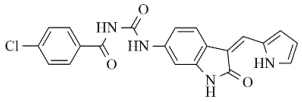	6.5	8.187
27	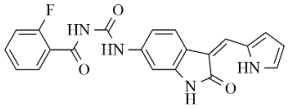	6.5	8.187
28	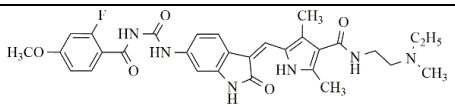	7.6	8.119
29	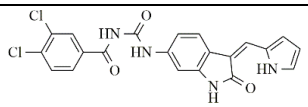	7.7	8.113
30	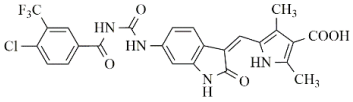	10.7	7.971
31	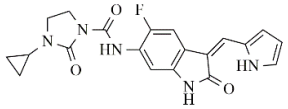	10.7	7.971
32*	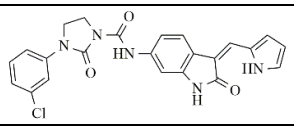	14.3	7.845

33	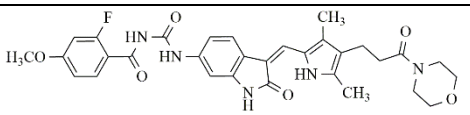	16.4	7.785
34	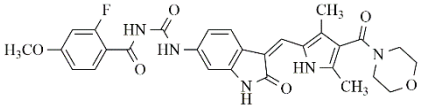	16.8	7.775
35	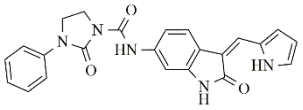	17.3	7.762
36*	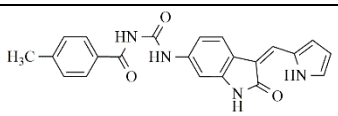	18.4	7.735
37	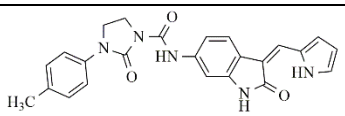	19.3	7.714
38	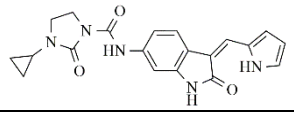	19.9	7.701
39	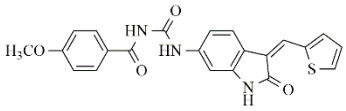	21.5	7.668
40	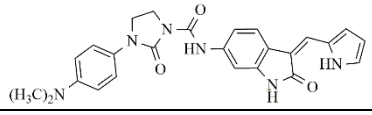	24.2	7.616
41	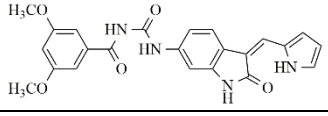	29.8	7.526
42*	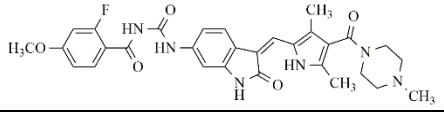	30.6	7.514
43	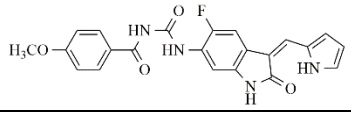	35.1	7.455
44	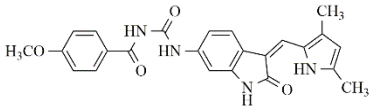	55.5	7.256
45	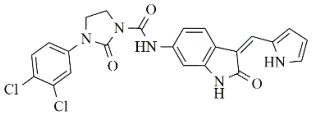	145.3	6.838
Hesperadin	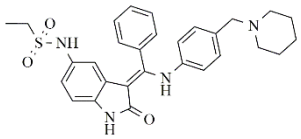	250.0 [a]	6.602
Sunitinib	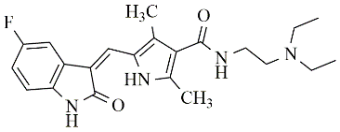	1500.0 [b]	7.232

[a] [10]
[b] [11]

2. MATERIALS AND METHOD

2.1. Data set

The enzyme crystal coordinates (organism: *Homo sapiens*) were downloaded from the Protein Data Bank (PDB code: 4AF3) [5]. The compounds [12] (Table **1**) were docked into the Aurora B binding sites using the Molegro Virtual Docker (MVD) [13, 14]. MVD is a program for predicting the most likely conformation of how a ligand will bind to a macromolecule. MolDock Scoring Function (MolDock Score) employed by the MVD program is regulated on a new hybrid search algorithm, called guided differential evolution. This algorithm combines the differential evolution optimization technique with a cavity prediction algorithm during the searching procedure, which allows fast and accurate recognition of potential binding modes, the poses. It is derived from the Piecewise Linear Potential (PLP), a simplified potential whose parameters are fit to protein-ligand structures and binding data scoring functions [13] and further extended in GEMDOCK program (Generic Evolutionary Method for molecular DOCK) with a new hydrogen bonding term and new charge schemes. The docking scoring function, Escore, is defined by the following energy terms:

$$E_{score} = E_{inter} + E_{intra} \quad \text{[Eq. 1]}$$

where the ligand-protein interaction energy, E_{inter}, is given by:

$$E_{inter} = \sum_{i \in ligand} \sum_{j \in protein} \left[E_{PLP}(r_{ij}) + 332.0 \frac{q_i q_j}{4r_{ij}^2} \right]$$

[Eq. 2]

The E_{PLP} term is a "piecewise linear potential" that uses two different sets of parameters: one set for approximating the steric term between atoms (van der Waals), and another stronger potential for hydrogen bonds. The second term describes the electrostatic interactions between charged atoms. It is a Coulomb potential with a distance-dependent dielectric constant, D(r) = 4r. The numerical value of 332.0 fixes the units of the electrostatic energy to kilocalories per mole (Molegro ApS).

The E_{intra} terms is the internal energy of the ligand:

$$E_{intra} = \sum_{i \in ligand} \sum_{j \in ligand} E_{PLP}(r_{ij}) + \sum_{flexiblebonds} A\,[1 - \cos(m.\theta - \theta_0)] + E_{clash}$$

[Eq. 3]

The first term, double summation, is the energy between all atom pairs in the ligand excluding atom pairs which are connected by two bonds. The second term is a torsional energy term, where θ is the torsional angle of the bond. The average of the torsional energy bond contribution is used if several torsions could be determined. The last term, E_{clash}, assigns a penalty of 1000 if the distance between two heavy atoms is less than 2.0Å, punishing infeasible ligand conformations (Molegro ApS). The docking search algorithm used in MVD is based on interaction optimization techniques conducted by Darwinian Evolution Theory (evolutionary algorithms, EA). A population of individuals is exposed to competitive selection that weeds out poor solutions. Recombination and mutation are used to create new solutions [13].

2.2. Predicted model

The prediction model was constructed considering the interaction energies from MVD for the most relevant amino acid residues located at a distance of 5Å from the interaction site. Subsequently, Chemoface software version 1.61 was used, where the training or calibration and test or validation groups were obtained from compounds **1**-**45**.

2.3. Novel proposed indolin-2-one derivatives

Considering the indolin-2-one subunit, new derivatives were also proposed and evaluated *in silico*. One hundred new derivatives were proposed and evaluated, being submitted to the docking studies using the MVD and subsequently the application of pre-established predictive model. The selected compounds for the predictive model were all those that presented adequate poses, comparing with the hesperadin redocked. Interactions in most relevant amino acid residues occurring at a distance of 5Å from the site of enzyme interaction were considered. Searching for potential promising inhibitors for human Aurora B kinase enzyme, besides the predictive model, it was considered the following energetic parameters of docking: MolDock Score, protein-ligand interaction and hydrogen bonding.

3. RESULTS AND DISCUSSION

Crystal coordinates of human Aurora B kinase enzyme, VX-680, and the crystallographic water molecules were taken from PDB [5]. However, this enzyme is not complete. The residues 53-69, 221-344 and 833-903 were not located. Then, the crystal structural coordinates of *X. laevis* (PDB code: 2BFY) Aurora B was used as a template structure to build the missing amino acid residues. Hesperadin was transferred from the 2BFY to the 4AF3 active site, once the studied compounds are similar to it (indolin-2-one subunit). Inside the 4AF3 interaction site, the hesperadin structure was redocked and the conformation (Fig. **2A**) with the most appropriate spatial arrangement and more favorable energy values was selected (RMSD = 0.94Å) as a reference for our docking study, similarly evidenced by Sessa and coworkers [15]. The active site analyzed in docking studies was defined as a subset region around the center of the hesperadin chemical structure in human Aurora B kinase and the amino acid residues are shown in Fig. **2B**.

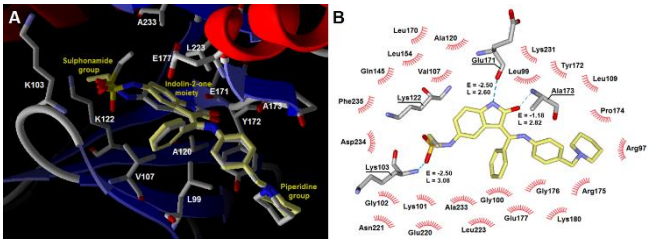

Fig. (2). Hesperadin into Aurora B active site. Structure with yellow carbon atoms is redocked hesperadin (**A**); H-bonds evidenced for hesperadin and amino acid residues located at a distance of 5Å (**B**).

The compounds **1**-**45** and sunitinib were docked into the human Aurora B kinase binding site using the MVD. The ligands and amino acids residues close to 5Å from the interaction site (Fig. **2B**) were considered flexible during the docking simulation. Thus, a candidate solution is encoded by

Table 2. Interaction energy values (kcal.mol^{-1}) and regression coefficients of each amino acid residue for each training group.

Compound/aa	*Ala120*	*Ala173*	*Ala233*	*Arg175*	*Asn221*	*Asp234*	*Glu171*	*Glu177*	*Glu220*	*Gly102*	*Gly176*	*Leu99*	*Leu154*	*Leu170*	*Leu223*	*Lys103*	*Lys122*	*Lys180*	*Pro174*	*Tyr172*	*Val107*
1	-2.05	-11.44	-7.19	-9.17	-11.32	-12.50	-6.44	-13.98	-2.90	-1.62	-11.95	-9.82	-7.53	5.78	-12.27	-6.28	-5.55	-5.43	-5.63	-17.87	-8.23
2	-2.05	-6.95	-4.78	-8.36	-10.87	-10.26	-6.63	-12.75	4.33	-1.35	-9.54	-7.96	-7.81	3.76	-12.09	-4.09	-9.42	-5.51	-4.60	-18.22	-7.61
3	-2.13	-10.27	-4.21	-5.79	-6.74	-10.14	-5.96	-8.92	4.69	-1.99	-9.75	-11.43	-5.28	-3.23	-10.84	-12.84	-4.21	3.96	-9.30	-20.18	-8.92
4	-2.73	-9.36	-3.99	-3.91	-0.70	-6.63	-6.63	-4.26	-2.42	-5.51	-8.14	-13.26	-5.72	-4.32	-11.36	-18.71	-3.22	-0.48	-6.05	-24.09	-7.77
5	-2.02	-7.40	-6.19	-7.96	-10.61	-14.69	-5.95	-10.96	-7.74	-1.28	-10.77	-12.27	-5.99	-2.86	-13.22	-6.43	-2.16	-6.01	-4.60	-19.90	-7.32
6	-2.05	-11.71	-7.23	-11.53	-9.56	-7.63	-6.17	-7.23	-3.80	-1.94	-10.78	-12.35	-1.76	-4.76	-12.81	-11.37	-1.33	-1.02	-7.61	-20.51	-6.07
7	-2.19	-11.37	-3.39	-6.36	-9.94	-6.30	-5.97	-9.09	-0.43	-2.73	-9.51	-10.80	-4.66	-2.52	-10.16	-13.40	-4.25	3.61	-9.91	-20.51	-9.93
8	-2.45	-10.07	-5.50	-2.41	-3.79	-11.02	-6.49	-5.65	-2.67	-6.76	-6.91	-12.90	-6.25	-4.77	-12.43	-24.20	-2.86	-2.08	-3.46	-19.96	-6.28
9	-1.96	-10.36	-6.52	-2.09	-2.91	-12.06	-6.19	-8.57	-2.07	-6.89	-6.74	-10.54	-5.89	-4.39	-13.73	-21.08	-1.28	-2.04	-3.64	-17.60	-5.68
10	-2.41	-4.98	-4.45	-8.94	-7.65	-8.03	-5.67	-7.24	-5.29	-3.09	-10.79	-12.72	-6.44	-4.60	-12.93	-18.78	-5.85	-5.86	-5.30	-19.45	-5.34
12	-2.68	-12.56	-4.24	-5.71	-8.80	-9.66	-6.57	-10.50	1.31	-2.69	-8.60	-11.09	-6.07	-0.48	-10.85	-12.36	-5.68	3.91	-8.63	-19.42	-8.93
15	-2.30	-6.89	-4.47	-4.12	-5.70	-12.01	-5.94	-6.41	-5.13	-8.46	-9.64	-11.63	-6.72	-7.26	-12.39	-17.99	-3.74	-0.37	-5.15	-20.84	-4.25
17	-1.96	-11.07	-6.37	-4.87	-5.28	-8.49	-6.39	-7.94	-4.16	-2.45	-9.79	-10.98	-6.36	-3.35	-12.99	-17.14	-2.41	3.72	-9.10	-19.17	-7.15
18	-1.95	-11.70	-4.21	-6.03	-7.59	-8.34	-5.96	-10.91	-1.25	-1.79	-9.45	-11.55	-5.70	-4.14	-11.97	-10.83	-2.48	4.10	-9.37	-19.35	-7.52
19	-1.92	-12.83	-5.54	-7.31	-5.77	-11.03	-6.65	-10.26	-3.29	-1.88	-11.26	-11.74	-6.49	-4.21	-13.98	-13.58	-3.40	3.96	-9.74	-18.91	-5.14
20	-1.66	-13.71	-7.14	-4.60	-10.47	-13.99	-5.82	-10.82	-6.51	-1.33	-7.63	-8.91	-7.14	-3.72	-13.64	-6.40	-3.19	-3.17	-8.96	-17.77	-7.65
21	-2.15	-9.74	-5.38	-6.96	-12.19	-9.53	-6.03	-8.12	-6.24	-3.11	-9.31	-10.47	-3.71	-2.58	-10.34	-11.21	-2.69	2.12	-7.92	-22.00	-9.31
23	-2.02	-11.90	-4.84	-5.99	-9.26	-8.57	-6.11	-11.94	-4.59	-2.00	-10.10	-11.98	-6.19	-3.87	-12.45	-10.09	-2.30	4.07	-6.52	-19.75	-6.82
24	-1.95	-12.07	-4.02	-6.20	-7.70	-5.60	-5.96	-12.96	-1.70	-1.96	-9.73	-11.84	-5.06	-4.29	-12.34	-7.00	-4.25	3.84	-9.67	-19.82	-7.78
25	-2.48	-11.28	-4.73	-2.86	-13.14	-12.57	-5.77	-11.28	-14.00	-1.80	-3.56	-7.75	-4.40	-3.20	-10.71	-8.76	-3.61	-1.41	-4.16	-18.39	-9.32
27	-1.99	-10.89	-5.45	-2.50	-7.32	-9.99	-6.13	-12.67	-0.60	-1.98	-6.69	-10.04	-6.21	-4.88	-12.94	-6.25	-1.61	-1.02	-3.67	-17.24	-6.40
28	-2.24	-12.01	-6.75	-16.87	-11.73	-13.95	-6.75	-11.47	-6.03	-1.64	-11.79	-9.33	-5.89	1.88	-12.98	-6.74	-3.95	2.79	-6.25	-19.19	-8.16
29	-2.41	-9.49	-3.79	-3.08	-7.70	-8.37	-5.93	-9.01	-5.71	-1.99	-6.59	-10.41	-4.89	-4.45	-11.10	-14.08	-2.50	-1.27	-3.37	-17.47	-8.45
30	-2.04	-9.50	-3.47	-7.76	-4.20	-6.46	-6.12	-5.70	-5.56	-5.82	-9.83	-11.60	-4.23	-4.28	-11.68	-22.86	-1.70	3.19	-11.04	-20.61	-7.56
31	-2.65	-11.01	-4.36	-3.17	-7.43	-12.09	-5.93	-8.82	-0.63	-2.52	-4.15	-8.28	-4.93	-0.85	-10.58	-8.71	-4.68	-1.45	-3.45	-17.72	-10.38
33	-1.87	-8.94	-8.37	-6.21	-8.85	-8.34	-6.45	-11.87	-3.81	-1.85	-13.94	-11.17	-3.74	2.05	-13.68	-13.05	-3.06	0.55	-6.72	-17.81	-7.19
34	-1.94	-11.29	-5.77	-4.96	-9.83	-10.85	-6.59	-13.75	-6.27	-3.37	-12.36	-11.75	-7.12	3.83	-12.75	-11.92	-6.42	3.19	-6.46	-17.12	-7.11
35	-2.49	-14.53	-6.14	-2.83	-0.31	-10.57	-6.19	-8.65	-1.09	-9.99	-6.75	-10.79	-6.01	-3.81	-13.22	-18.06	-1.44	-1.94	-2.80	-14.28	-5.54
37	-1.98	-10.82	-4.15	-2.92	-13.71	-14.23	-5.75	-12.30	-9.79	-1.59	-4.12	-9.71	-4.85	-5.23	-12.05	-5.22	-2.61	-1.50	-4.08	-18.32	-8.51
38	-2.37	-14.12	-5.31	-3.07	-7.31	-8.53	-5.78	-8.65	-3.56	-1.76	-7.21	-10.95	-5.61	-3.67	-13.09	-12.69	-3.15	-2.12	-2.90	-14.56	-5.81
39	-1.88	-10.51	-4.96	-2.41	-7.41	-8.06	-5.97	-9.32	-5.06	-1.68	-6.27	-10.20	-5.96	-4.88	-12.59	-11.45	-1.66	-1.57	-3.56	-17.38	-6.56
40	-1.97	-14.30	-6.42	-3.07	-0.68	-10.91	-5.75	-8.78	-1.02	-12.31	-7.39	-10.95	-5.81	-4.16	-13.39	-18.41	-1.48	-2.05	-2.92	-14.63	-5.30
41	-1.92	-11.41	-3.41	-3.29	-5.20	-7.30	-4.48	-4.73	-3.93	-8.37	-6.61	-9.97	-3.51	-4.61	-11.16	-19.88	-1.83	-1.48	-3.79	-17.39	-7.79
43	-2.22	-10.64	-2.79	-3.07	-2.52	-0.78	-5.99	-4.12	-2.54	-5.50	-4.84	-8.55	-4.37	-3.14	-9.88	-21.58	-4.18	-0.99	-3.97	-18.22	-10.25
45	-1.98	-6.43	-5.53	-2.91	-0.38	-9.48	-6.11	-8.90	-1.12	-12.25	-6.83	-9.41	-5.69	-4.33	-13.62	-19.21	-0.64	-1.58	-4.13	-16.31	-5.65
Regression Coeficients	-0.12	-0.12	-0.18	-0.03	0.05	-0.06	0.26	-0.23	0.05	0.13	-0.06	0.11	-0.07	-0.08	0.48	-0.10	-0.03	-0.13	-0.02	-0.28	0.20

an array of real-valued numbers representing ligand position, conformation, and orientation as cartesian coordinates for the ligand translation, whereas there are four variables specifying the ligand orientation, and one angle for each flexible torsion angle in the ligand. MolDock Score energy values were obtained from each of the selected pose for all these evaluated compounds, including hesperadin and sunitinib, and the values are expressed in kcal.mol^{-1} (supplementary material), where the energy values for pose-protein interaction and hydrogen bonds are also evidenced. The interaction modes of the ligand with the active site were determined as the highest energy scored protein–ligand complex used during docking and the conformers of each compound were mostly associated with conformations of hesperadin. Compound **1** showed more stable interaction energy (-225.90 kcal.mol^{-1}) than the other inhibitors studied, while sunitinib was the least stable (-135.63 kcal.mol^{-1}).

These compounds, including hesperadin and sunitinib, interacted with Glu171 (*–NH* from indolinonic moiety), and the majority of them with Ala173 (*C=O* from indolinonic moiety) via hydrogen bond formations. Thus, these two residues are of great relevance for potency of the compounds. In addition, hydrogen bond interactions were observed between:

i) Compounds **3**, **4**, **7**, **8**, **10**, **11**, **12**, **13**, **14**, **18**, **21**, **23**, **27**, **28**, **29**, **30**, **34**, **39**, **41**, **43** and Lys103 through the carbonyl group attached to terminal benzene ring; **9**, **19**, **25**, **31**, **32**, **35**, **37**, **38**, **40**, **45** and Lys103 through the carbonyl group on imidazolidinone subunit;

ii) **2**, **10**, **44** and Lys122 through the carbonyl group attached to indolin-2-one ring;

iii) **4**, **20** and Tyr172 through *–COOH* terminal group, where saturated carbons between the pyrrole ring and the carboxyl group increase the degree of freedom favoring conformations for this interaction;

iv) **3**, **7**, **12**, **16**, **17**, **18**, **19**, **24**, **30** and Pro174 through *–COOH* terminal group; **28** and Pro174 through *N*-amidic attached to the pyrrole ring. The presence of saturated alkyl substituents on the pyrrolic subunit showed better interaction energy values for the Pro174 apolar residue when compared to those not substituted, indicating that the presence of apolar groups attached to the pyrrolic moiety would be relevant for potency;

v) **1** and Arg175 through *N*-amidic attached to pyrrole group; Compounds **2**, **5**, **6**, **10** and Arg175 through *–COOH* terminal group. The presence of electronegative atoms or groups, such as *–COOH*, favor interaction through hydrogen bonds or electrostatic interactions with Arg175, a basic polar amino acid. In addition, the saturated alkyl chain of 1 or 2 carbons attached to this terminal carboxyl group has been shown to acquire different conformations in order to better interact with the amino acid residue in question;

vi) **2**, **5**, **10**, **11** and Lys180 through *–COOH* terminal group, similar to Arg175 interaction;

vii) **1**, **2**, **5**, **10**, **14**, **15**, **16**, **17**, **20**, **22**, **33**, **36**, **42** and Asp234 through *NH*-group located between two carbonyl groups, with energy values that varied from -14,69 kcal.mol^{-1}, compound **5**, to +3,67 kcal.mol^{-1} for compound **44**, showing importance of orientation and substitution of benzene ring inside binding site.

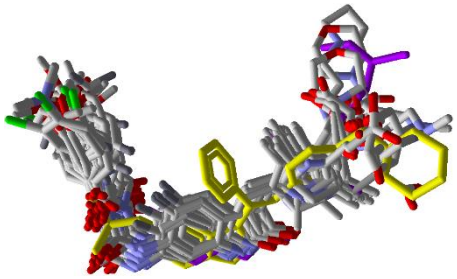

Fig. (3). Overlapped conformations of Aurora B Kinase inhibitors. Hesperadin is shown in yellow, and Sunitinib in purple.

The total energy between each selected ligand conformation and the amino acid residues present at a distance of 5Å (those that exhibited some type of interaction: bonding hydrogen, electrostatic or steric) for the training group was calculated and the results of the decomposition analysis of inhibitors and amino acid residues are shown in Table **2**. These data were used to derive a multiple regression linear fit to the experimental pIC_{50}. The model achieved a squared linear correlation coefficient (R^2) of 0.945. The R^2 values greater than 0.7 indicates that the model is correlated and may be considered to represent the training set in the same manner [16]. This good correlation suggests that the binding conformations of the ligands with human Aurora B are reasonable and data can be used to predict the interaction energy of other Aurora B inhibitors indolin-2-one derivatives.

The equation coefficients from regression analysis may provide useful information: the terms with positive coefficients signs decrease the predicted potency of a compound. The same concept can be applied to terms with negative coefficient signs, it increases the predicted potency. In both cases, the predicted potency values are directly proportional to the magnitude of each term coefficient of this equation. The predicted pIC_{50} values for the training were computed and are shown in the supplementary material. The standard deviation (SD) of the residual values is 0.133. To establish outlier compounds, we observed which residuals are more than twice the SD of the residual of fit. Analyses of the data showed one outlier, compound **17**.

Leu223 contributes to decrease the interaction potency of the compound and presents the largest positive regression coefficient (0.48). This amino acid is close to the indolin-2-one ring (Fig. **2A**) and these points to feasible predominance of the steric over the electrostatic contribution in the position of the active site. Tyr172 contributes to increase interaction potency of the compound and presents the most negative regression coefficient (-0.28). This amino acid is close to the benzene ring attached to the terminal piperidine group of hesperadin (Fig. **2A**). All the compounds **1**-**45** have a pyrrol ring, except for compound **39** with a thiophene ring,

substituted or not, that could induce hydrophobic interactions with Tyr172 residue.

The theoretical prediction of the biological potency (pIC_{50}) for Compounds **14**, **16**, **22**, **32**, **36**, **42**, which make up the test group, was performed. Experimental (pIC_{50exp}) and predicted (pIC_{50pred}) potency values are shown in Table **3**. The experimentally observed activity agrees with the predicted with an R^2_{test} equal to 0.717. Considering only the test set compounds, the standard deviation (SD) of the residuals computed is 0.327. Based in this information, outliers were not found.

Table 3. Experimental (pIC_{50exp}) and calculated (pIC_{50pred}) potencies and residual values (pIC_{50exp} - pIC_{50pred}) for test group.

Compound	pIC_{50exp}	pIC_{50pred}	Residue
14	8.68	8.36	0.32
16	8.68	9.23	-0.56
22	8.51	8.83	-0.32
32	7.84	8.00	-0.16
36	7.74	8.21	-0.47
42	7.51	7.49	0.03

When compounds **1** and hesperadin are compared using interaction energy values (kcal.mol^{-1}) of each amino acid residue from supplementary material, the widest energy variations are shown in Ala233, Arg175, Asn221, Asp234, Glu177, Glu220, Gly176, Lys103, and Lys122, of which amino acid residues Asn221 and Glu220 showed no interactions. When comparing compound **1** and sunitinib, since all compounds **1**-**45** can be considered structural optimizations of this one, the widest energy variations are shown in Ala233, Asn221, Asp234, Glu177, Glu220, Leu154, Lys103, Lys122, and Lys180 residues, of which amino acid residues Asn221, Asp234, Glu220, Lys103, and Lys122 showed no interactions.

Having observations from the docking studies, one hundred new indolinonic derivatives were proposed and evaluated applying our predictive model, besides the observation of other related parameters (MolDock Score, pose-protein interaction, and H bond energy). Among the 100 new proposed indolinonic derivatives, satisfactory poses were obtained in 79, and 54 showed interactions in the twenty-one defined amino acid residues. Decomposition analysis table, chemical structures, MolDock Score, Pose-Protein Interaction and H Bond energy values for the new proposed compounds are presented in the supplementary material. Four compounds (**IAF61**, **IAF63**, **IAF66** and **IAF79**) could be highlighted and considered to be more promising for future synthesis and biological evaluations. These four compounds present a benzyl moiety attached in a sp^2 carbon atom located between the indolin-2-one and the pyrrolic ring, suggesting the filling of an important verified vacancy, as in the case of Hesperadin, leading to additional interactions that would considerably contribute to inhibitory activity of these compounds. It is also noted that benzyl moiety presence would be more important than phenyl moiety for these compounds. Besides that, the **IAF79** compound presented the higher predictive activity (pIC_{50} = 11.39) and H bond energy value of -15.61kcal.mol^{-1} (Table **4**), with presence of seven interactions: Leu18, Lys22, Glu90, Tyr91, Ala92 (for two distinct groups, indolinonic oxygen and amidic nitrogen attached to the pyrrol ring), and Asn140, highlighting the interaction between phenolic hydroxyl group in para position and Leu18 (-2.50 kcal.mol^{-1}).

Table 4. Chemical structures, predicted pIC_{50}, MolDock Score (kcal.mol^{-1}), ligand-protein interaction (kcal.mol^{-1}) and H-bond interaction (kcal.mol^{-1}) for new more promising derivatives.

Compound	Chemical Structure	pIC_{50} pred Aurora B	MolDock Score	Lig-Prot. Interaction	H Bond Energy
IAF61	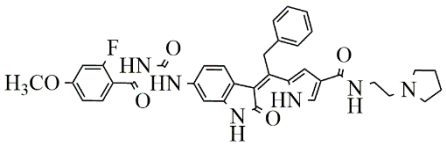	10.17	-238.40	-246.12	-9.55
IAF63	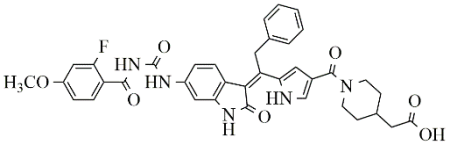	10.85	-221.89	-250.15	-7.37
IAF66	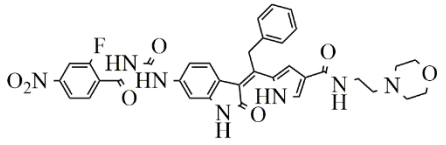	10.23	-211.78	-240.45	-11.01
IAF79	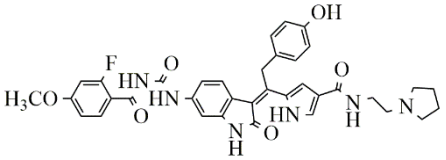	11.39	-236.71	-240.59	-15.61

CONCLUSION

We carried out molecular docking studies in order to understand the interactions of a variety of indolin-2-one derivatives with human Aurora B kinase. The different substituent groups were exploited at 3 and 6 positions of the indolinone ring and are shown in Table **1**. Docked structures were evaluated based on binding energy, electrostatic and hydrogen bonding interactions. Our molecular docking results, combined with experimental data for human Aurora B kinase inhibition, suggest the presence of empty spaces around the indolin-2-one moiety and especially around the terminal group attached to the pyrrolic ring. Thus, more favorable substituents attached at the 3-position of the pyrrolic ring and in the sp^2 carbon atom located between the indolin-2-one and pyrrolic ring groups may increase affinity for human Aurora B kinase. For new 100 proposed indolinone derivatives, four of them could be detached (**IAF61**, **IAF63**, **IAF66**, and **IAF79**), which have a benzyl group attached in the sp^2 carbon atom located between the indolin-2-one and pyrrolic ring groups, highlighting **IAF79**, which presented the best predicted inhibitory activity. The present study on this class of indolinone derivative compounds seems to be promising for future obtainment of a possible candidate for an innovative drug for treatment of different types of cancer, since some of them have already exhibited activity against different cancer cell lines.

CONFLICT OF INTEREST

The authors declare no conflict of interest, financial or otherwise.

ACKNOWLEDGEMENTS

The authors thank to the Brazilian agencies "Conselho Nacional de Desenvolvimento Científico e Tecnológico" (CNPq) and "Coordenação de Aperfeiçoamento de Pessoal de Nível Superior" (CAPES) for their financial supports.

SUPPLEMENTARY MATERIAL

1. MolDock Score, Pose-Protein Interaction and H Bond energy values from each of the selected pose for compounds **1**-**45**, Hesperadin, and Sunitinib.
2. Measured and predicted pIC_{50} and residual values for the training compounds.
3. Interaction energy values ($kcal.mol^{-1}$) of each amino acid residue for compounds **1**-**45**, Hesperadin, and Sunitinib.
4. Chemical structures for all new proposed compounds **IAF1**-**IAF100**.
5. MolDock Score, Pose-Protein Interaction and H Bond energy values from each of the selected pose for all new proposed compounds, **IAF1**-**IAF100**.
6. Interaction energy values ($kcal.mol^{-1}$) of each amino acid residue for all new proposed compounds.

REFERENCES

[1] Carmena, M.; Earnshaw, W.C. The Cellular Geography of Aurora Kinases. *Nat. Rev. Mol. Cell Biol.*, **2003**, *4*, 842-854.

[2] Lee, E.C.; Frolov, A.; Li, R.; Ayala, G.; Greenberg, N.M. Targeting Aurora Kinases for the Treatment of Prostate Cancer. *Cancer Res.*, **2006**, *66*, 4996-5002.

[3] Zeng, W.F.; Navaratne, K.; Prayson, R.A.; Weil, R.J. Aurora B Expression Correlates with Aggressive Behaviour in Glioblastoma Multiforme. *J. Clin. Pathol.*, **2007**, *60*, 218-221.

[4] Cheung, C.H.; Coumar, M.S.; Hsieh, H.P.; Chang, J.Y. Aurora Kinase Inhibitors in Preclinical and Clinical Testing. *Expert Opin. Investig. Drugs*, **2009**, *18*, 379-398.

[5] Elkins, J.M.; Santaguida, S.; Musacchio, A.; Knapp, S. Crystal Structure of Human Aurora B in Complex with INCENP and VX-680. *J. Med. Chem.*, **2012**, *55*, 7841-7848.

[6] Yang, J.; Ikezoe, T.; Nishioka, C.; Tasaka, T.; Taniguchi, A.; Kuwayama, Y.; Komatsu, N.; Bandobashi, K.; Togitani, K.; Koeffler, H.P.; Taguchi, H.; Yokoyama, A. AZD1152, a novel and selective Aurora B kinase inhibitor, induces growth arrest, apoptosis, and sensitization for tubulin depolymerizing agent or topoisomerase II inhibitor in human acute leukemia cells *in vitro* and *in vivo*. *Blood*, **2007**, *110*, 2034-2040.

[7] Ju, S.; Peng, X.; Yang, X.; Sozar, S.; Muneri, C.W.; Xu, Y.; Chen, C.; Cui, P.; Xu, W.; Rui, R. Aurora B inhibitor barasertib prevents meiotic maturation and subsequent embryo development in pig oocytes. *Theriogenology*, **2016**, *86*, 503-515.

[8] Tyler, R.K.; Shpiro, N.; Marquez, R.; Eyers, P.A. VX-680 inhibits Aurora A and Aurora B kinase activity in human cells. *Cell Cycle*, **2007**, *6*, 2846-2854.

[9] Ditchfield, C.; Johnson, V.L.; Tighe, A.; Ellston, R.; Haworth, C.; Johnson, T.; Mortlock, A.; Keen, N.; Taylor, S.S. Aurora B couples chromosome alignment with anaphase by targeting BubR1, Mad2, and Cenp-E to kinetochores. *J. Cell Biol.*, **2003**, *161*, 267-280.

[10] Hauf, S.; Cole, R.W.; Laterra, S.; Zimmer, C.; Schnapp, G.; Walter, R.; Heckel, A.; Van Meel, J.; Rieder, C.L.; Peters, J.M. The small molecule Hesperadin reveals a role for Aurora B in correcting kinetochore-microtubule attachment and in maintaining the spindle assembly checkpoint. *J. Cell Biol.*, **2003**, *161*, 281-294.

[11] Determann, R.; Dreher, J.; Baumann, K.; Preu, L.; Jones, P.G.; Totzke, F.; Schächtele, C.; Kubbutat, M.H.G.; Kunick, C. 2-Anilino-4-(benzimidazol-2-yl)pyrimidines – A multikinase inhibitor scaffold with antiproliferative activity toward cancer cell lines. *Eur. J. Med. Chem.*, **2012**, *53*, 254-263.

[12] Chern, J.W.; Jagtap, A.D.; Wang, H.C.; Chen, G.S. Indolin-2-one Derivatives as Protein Kinase Inhibitors. U.S. Patent 2013/158373 A1, October 24, **2013**.

[13] Gehlhaar, D.K.; Verkhivker, G.M.; Rejto, P.A.; Sherman, C.J.; Fogel, D.R.; Fogel, L.J.; Freer, S.T. Molecular Recognition of the Inhibitor AG-1343 by HIV-1 Protease: Conformationally Flexible Docking by Evolutionary Programming. *Chem. Biol.*, **1995**, *2*, 317-324.

[14] Thomsen, R.; Christensen, M.H. MolDock: A New Technique for High-Accuracy Molecular Docking. *J. Med. Chem.*, **2006**, *49*, 3315-3321.

[15] Sessa, F.; Mapelli, M.; Ciferri, C.; Tarricone, C.; Areces, L.B.; Schneider, T.R.; Stukenberg, P.T.; Musacchio, A. Mechanism of Aurora B Activation by INCENP and Inhibition by Hesperadin. *Mol. Cell*, **2005**, *18*, 379-391.

[16] Hopfinger, A.J.; Wang, S.; Tokarski, J.S.; Jin, B.; Albuquerque, M.; Madhav, P.J.; Duraiswami, C. Construction of 3D-QSAR Models Using the 4D-QSAR Analysis Formalism. *J. Am. Chem. Soc.*, **1997**, *119*, 10509-10524.

SUPPLEMENTARY MATERIAL

Ítalo Antônio Fernandes[a,b], Tamiris Maria de Assis[a,b], Isael Aparecido Rosa[a,c], Elaine Fontes Ferreira da Cunha[*a,b]

[a]Laboratório de Modelagem Molecular, LABGQC, Chemistry Department, Federal University of Lavras, Lavras, MG, Brazil; [b]Programa de Pós-Graduação em Agroquímica, Chemistry Department, Federal University of Lavras, Lavras, MG, Brazil; [c]Multicêntrico em Química de Minas Gerais (Rede Mineira de Química – RQ-MG), Federal University of Lavras, Lavras, MG, Brazil

SUPPLEMENTARY MATERIAL 1

MolDock Score, Pose-Protein Interaction and H Bond energy values from each of the selected pose for compounds **1**-**45**, Hesperadin, and Sunitinib.

Compound	MolDock Score	Pose-Protein Interaction	H Bond
1	-225.90	-219.66	-7.54
2	-180.40	-174.19	-11.78
3	-165.41	-166.44	-11.05
4	-176.98	-170.77	-11.88
5	-194.61	-186.03	-10.29
6	-179.84	-182.82	-8.12
7	-180.17	-174.74	-11.04
8	-180.42	-186.11	-12.35
9	-168.95	-166.46	-7.50
10	-189.51	-187.26	-14.34
11	-182.89	-179.34	-10.45
12	-181.54	-183.16	-11.01
13	-175.70	-174.74	-10.88
14	-175.90	-176.46	-9.98
15	-185.97	-183.20	-10.17
16	-180.78	-174.14	-6.34
17	-179.60	-176.65	-6.30
18	-167.71	-162.42	-8.50
19	-195.13	-184.43	-12.97
20	-188.13	-186.14	-7.59
21	-184.78	-182.12	-7.91
22	-165.53	-162.62	-5.06
23	-174.68	-176.73	-7.64
24	-161.07	-163.96	-8.13
25	-181.86	-170.58	-7.88
26	-148.93	-157.02	-6.19
27	-146.55	-150.57	-6.21
28	-215.04	-199.57	-7.35
29	-152.53	-155.12	-8.55
30	-177.61	-180.30	-10.00
31	-160.12	-147.30	-5.78
32	-158.37	-156.78	-7.40
33	-201.76	-201.73	-5.20
34	-186.66	-197.41	-9.67
35	-169.62	-164.88	-9.43
36	-145.62	-148.62	-5.16
37	-172.59	-168.50	-4.17
38	-162.79	-157.95	-9.31
39	-148.17	-151.04	-5.72
40	-181.80	-174.41	-9.20
41	-166.24	-166.40	-10.89
42	-180.46	-175.52	-5.52
43	-154.10	-152.73	-8.01
44	-154.50	-159.08	-6.95

45	-169.70	-163.67	-7.42
Hesperadin	-152.50	-162.53	-6.18
Sunitinib	-135.63	-137.04	-4.33

SUPPLEMENTARY MATERIAL 2

Ítalo Antônio Fernandes[a,b], Tamiris Maria de Assis[a,b], Isael Aparecido Rosa[a,c], Elaine Fontes Ferreira da Cunha[*a,b]

[a]*Laboratório de Modelagem Molecular, LABGQC, Chemistry Department, Federal University of Lavras, Lavras, MG, Brazil;* [b]*Programa de Pós-Graduação em Agroquímica, Chemistry Department, Federal University of Lavras, Lavras, MG, Brazil;* [c]*Multicêntrico em Química de Minas Gerais (Rede Mineira de Química – RQ-MG), Federal University of Lavras, Lavras, MG, Brazil*

Measured and predicted pIC_{50} and residual values for the training compounds.

Compound	Measured	Predicted	Residue
1	9.40	9.44	-0.04
2	9.00	8.82	0.18
3	8.92	9.08	-0.16
4	8.92	8.96	-0.04
5	8.89	8.67	0.22
6	8.82	8.70	0.12
7	8.82	8.64	0.18
8	8.80	8.88	-0.08
9	8.74	8.55	0.20
10	8.74	8.90	-0.15
12	8.72	8.78	-0.06
15	8.68	8.66	0.02
17	8.64	8.23	0.41
18	8.60	8.55	0.05
19	8.57	8.64	-0.07
20	8.52	8.70	-0.17
21	8.52	8.61	-0.09
23	8.51	8.50	0.01
24	8.43	8.37	0.06
25	8.36	8.29	0.06
27	8.19	8.34	-0.15
28	8.12	8.20	-0.08
29	8.11	8.01	0.11
30	7.97	8.08	-0.11
31	7.97	7.99	-0.02
33	7.79	7.97	-0.18
34	7.77	7.76	0.01
35	7.76	7.70	0.06
37	7.71	7.75	-0.04
38	7.70	7.65	0.05
39	7.67	7.88	-0.21
40	7.62	7.66	-0.04
41	7.53	7.48	0.05
43	7.45	7.51	-0.06
45	6.84	6.86	-0.02

SUPPLEMENTARY MATERIAL 3

Ítalo Antônio Fernandes[a,b], Tamiris Maria de Assis[a,b], Isael Aparecido Rosa[a,c], Elaine Fontes Ferreira da Cunha[*a,b]

[a]*Laboratório de Modelagem Molecular, LABGQC, Chemistry Department, Federal University of Lavras, Lavras, MG, Brazil;* [b]*Programa de Pós-Graduação em Agroquímica, Chemistry Department, Federal University of Lavras, Lavras, MG, Brazil;* [c]*Multicêntrico em Química de Minas Gerais (Rede Mineira de Química – RQ-MG), Federal University of Lavras, Lavras, MG, Brazil*

Interaction energy values (kcal.mol^{-1}) of each amino acid residue for compounds **1-45**, Hesperadin, and Sunitinib.

Cpd/aa	*Ala120*	*Ala173*	*Ala233*	*Arg175*	*Asn221*	*Asp234*	*Glu171*	*Glu177*	*Glu220*	*Gly102*	*Gly176*	*Leu99*	*Leu154*	*Leu170*	*Leu223*	*Lys103*	*Lys122*	*Lys180*	*Pro174*	*Tyr172*	*Val107*
1	-2.05	-11.44	-7.19	-9.17	-11.32	-12.50	-6.44	-13.98	-2.90	-1.62	-11.95	-9.82	-7.53	5.78	-12.27	-6.28	-5.55	-5.43	-5.63	-17.87	-8.23
2	-2.05	-6.95	-4.78	-8.36	-10.87	-10.26	-6.63	-12.75	4.33	-1.35	-9.54	-7.96	-7.81	3.76	-12.09	-4.09	-9.42	-5.51	-4.60	-18.22	-7.61
3	-2.13	-10.27	-4.21	-5.79	-6.74	-10.14	-5.96	-8.92	4.69	-1.99	-9.75	-11.43	-5.28	-3.23	-10.84	-12.84	-4.21	3.96	-9.30	-20.18	-8.92
4	-2.73	-9.36	-3.99	-3.91	-0.70	-6.63	-6.63	-4.26	-2.42	-5.51	-8.14	-13.26	-5.72	-4.32	-11.36	-18.71	-3.22	-0.48	-6.05	-24.09	-7.77
5	-2.02	-7.40	-6.19	-7.96	-10.61	-14.69	-5.95	-10.96	-7.74	-1.28	-10.77	-12.27	-5.99	-2.86	-13.22	-6.43	-2.16	-6.01	-4.60	-19.90	-7.32
6	-2.05	-11.71	-7.23	-11.53	-9.56	-7.63	-6.17	-7.23	-3.80	-1.94	-10.78	-12.35	-1.76	-4.76	-12.81	-11.37	-1.33	-1.02	-7.61	-20.51	-6.07
7	-2.19	-11.37	-3.39	-6.36	-9.94	-6.30	-5.97	-9.09	-0.43	-2.73	-9.51	-10.80	-4.66	-2.52	-10.16	-13.40	-4.25	3.61	-9.91	-20.51	-9.93
8	-2.45	-10.07	-5.50	-2.41	-3.79	-11.02	-6.49	-5.65	-2.67	-6.76	-6.91	-12.90	-6.25	-4.77	-12.43	-24.20	-2.86	-2.08	-3.46	-19.96	-6.28
9	-1.96	-10.36	-6.52	-2.09	-2.91	-12.06	-6.19	-8.57	-2.07	-6.89	-6.74	-10.54	-5.89	-4.39	-13.73	-21.08	-1.28	-2.04	-3.64	-17.60	-5.68
10	-2.41	-4.98	-4.45	-8.94	-7.65	-8.03	-5.67	-7.24	-5.29	-3.09	-10.79	-12.72	-6.44	-4.60	-12.93	-18.78	-5.85	-5.86	-5.30	-19.45	-5.34
11	-1.98	-8.34	-5.19	-5.59	-5.84	-9.45	-6.10	-9.17	-5.78	-1.82	-10.84	-12.05	-6.59	-4.33	-12.54	-12.87	-2.11	-6.70	-5.36	-21.30	-6.51
12	-2.68	-12.56	-4.24	-5.71	-8.80	-9.66	-6.57	-10.50	1.31	-2.69	-8.60	-11.09	-6.07	-0.48	-10.85	-12.36	-5.68	3.91	-8.63	-19.42	-8.93
13	-2.04	-11.89	-4.58	-5.56	-0.64	-7.34	-6.68	-5.90	-1.03	-5.51	-10.12	-11.85	-6.78	-3.93	-12.74	-18.01	-3.64	3.70	-6.26	-19.24	-6.53
14	-2.52	-6.73	-2.72	-4.01	-10.30	-11.26	-5.85	-7.64	-3.89	-2.83	-8.86	-13.32	-6.32	-4.07	-12.36	-19.77	-4.33	-0.87	-4.68	-20.26	-6.27
15	-2.30	-6.89	-4.47	-4.12	-5.70	-12.01	-5.94	-6.41	-5.13	-8.46	-9.64	-11.63	-6.72	-7.26	-12.39	-17.99	-3.74	-0.37	-5.15	-20.84	-4.25
16	-1.85	-9.77	-7.14	-7.29	-5.11	-14.17	-5.63	-10.72	-9.14	-2.02	-9.51	-11.23	-3.37	-5.04	-12.59	-9.99	-0.47	1.22	-11.62	-20.99	-8.20
17	-1.96	-11.07	-6.37	-4.87	-5.28	-8.49	-6.39	-7.94	-4.16	-2.45	-9.79	-10.98	-6.36	-3.35	-12.99	-17.14	-2.41	3.72	-9.10	-19.17	-7.15
18	-1.95	-11.70	-4.21	-6.03	-7.59	-8.34	-5.96	-10.91	-1.25	-1.79	-9.45	-11.55	-5.70	-4.14	-11.97	-10.83	-2.48	4.10	-9.37	-19.35	-7.52
19	-1.92	-12.83	-5.54	-7.31	-5.77	-11.03	-6.65	-10.26	-3.29	-1.88	-11.26	-11.74	-6.49	-4.21	-13.98	-13.58	-3.40	3.96	-9.74	-18.91	-5.14
20	-1.66	-13.71	-7.14	-4.60	-10.47	-13.99	-5.82	-10.82	-6.51	-1.33	-7.63	-8.91	-7.14	-3.72	-13.64	-6.40	-3.19	-3.17	-8.96	-17.77	-7.65
21	-2.15	-9.74	-5.38	-6.96	-12.19	-9.53	-6.03	-8.12	-6.24	-3.11	-9.31	-10.47	-3.71	-2.58	-10.34	-11.21	-2.69	2.12	-7.92	-22.00	-9.31
22	-2.47	-7.08	-6.58	-6.10	-3.28	-9.82	-5.62	-7.45	-6.83	-0.52	-9.32	-11.35	-4.85	-5.41	-11.58	-10.32	-3.08	1.29	-7.26	-21.44	-9.02
23	-2.02	-11.90	-4.84	-5.99	-9.26	-8.57	-6.11	-11.94	-4.59	-2.00	-10.10	-11.98	-6.19	-3.87	-12.45	-10.09	-2.30	4.07	-6.52	-19.75	-6.82
24	-1.95	-12.07	-4.02	-6.20	-7.70	-5.60	-5.96	-12.96	-1.70	-1.96	-9.73	-11.84	-5.06	-4.29	-12.34	-7.00	-4.25	3.84	-9.67	-19.82	-7.78
25	-2.48	-11.28	-4.73	-2.86	-13.14	-12.57	-5.77	-11.28	-14.00	-1.80	-3.56	-7.75	-4.40	-3.20	-10.71	-8.76	-3.61	-1.41	-4.16	-18.39	-9.32
26	-2.51	-13.33	-5.41	-1.22	-13.98	3.64	-6.37	-9.33	-3.03	-0.68	-4.03	-7.60	-6.77	-5.95	-13.23	-9.84	-3.69	-1.27	-2.64	-16.36	-5.24
27	-1.99	-10.89	-5.45	-2.50	-7.32	-9.99	-6.13	-12.67	-0.60	-1.98	-6.69	-10.04	-6.21	-4.88	-12.94	-6.25	-1.61	-1.02	-3.67	-17.24	-6.40
28	-2.24	-12.01	-6.75	-16.87	-11.73	-13.95	-6.75	-11.47	-6.03	-1.64	-11.79	-9.33	-5.89	1.88	-12.98	-6.74	-3.95	2.79	-6.25	-19.19	-8.16
29	-2.41	-9.49	-3.79	-3.08	-7.70	-8.37	-5.93	-9.01	-5.71	-1.99	-6.59	-10.41	-4.89	-4.45	-11.10	-14.08	-2.50	-1.27	-3.37	-17.47	-8.45
30	-2.04	-9.50	-3.47	-7.76	-4.20	-6.46	-6.12	-5.70	-5.56	-5.82	-9.83	-11.60	-4.23	-4.28	-11.68	-22.86	-1.70	3.19	-11.04	-20.61	-7.56
31	-2.65	-11.01	-4.36	-3.17	-7.43	-12.09	-5.93	-8.82	-0.63	-2.52	-4.15	-8.28	-4.93	-0.85	-10.58	-8.71	-4.68	-1.45	-3.45	-17.72	-10.38
32	-2.70	-10.11	-4.92	-2.00	-0.76	-11.32	-7.32	-9.66	-6.43	-1.82	-6.49	-10.91	-6.29	-1.50	-12.64	-12.57	-4.14	-2.43	-3.12	-17.49	-7.03
33	-1.87	-8.94	-8.37	-6.21	-8.85	-8.34	-6.45	-11.87	-3.81	-1.85	-13.94	-11.17	-3.74	2.05	-13.68	-13.05	-3.06	0.55	-6.72	-17.81	-7.19
34	-1.94	-11.29	-5.77	-4.96	-9.83	-10.85	-6.59	-13.75	-6.27	-3.37	-12.36	-11.75	-7.12	3.83	-12.75	-11.92	-6.42	3.19	-6.46	-17.12	-7.11
35	-2.49	-14.53	-6.14	-2.83	-0.31	-10.57	-6.19	-8.65	-1.09	-9.99	-6.75	-10.79	-6.01	-3.81	-13.22	-18.06	-1.44	-1.94	-2.80	-14.28	-5.54
36	-2.42	-10.84	-6.97	-2.17	-2.62	-10.39	-5.80	-7.20	-6.60	-0.32	-5.78	-9.46	-4.20	-5.77	-12.51	-11.38	-1.61	-0.99	-3.43	-17.87	-8.09

37	-1.98	-10.82	-4.15	-2.92	-13.71	-14.23	-5.75	-12.30	-9.79	-1.59	-4.12	-9.71	-4.85	-5.23	-12.05	-5.22	-2.61	-1.50	-4.08	-18.32	-8.51
38	-2.37	-14.12	-5.31	-3.07	-7.31	-8.53	-5.78	-8.65	-3.56	-1.76	-7.21	-10.95	-5.61	-3.67	-13.09	-12.69	-3.15	-2.12	-2.90	-14.56	-5.81
39	-1.88	-10.51	-4.96	-2.41	-7.41	-8.06	-5.97	-9.32	-5.06	-1.68	-6.27	-10.20	-5.96	-4.88	-12.59	-11.45	-1.66	-1.57	-3.56	-17.38	-6.56
40	-1.97	-14.30	-6.42	-3.07	-0.68	-10.91	-5.75	-8.78	-1.02	-12.31	-7.39	-10.95	-5.81	-4.16	-13.39	-18.41	-1.48	-2.05	-2.92	-14.63	-5.30
41	-1.92	-11.41	-3.41	-3.29	-5.20	-7.30	-4.48	-4.73	-3.93	-8.37	-6.61	-9.97	-3.51	-4.61	-11.16	-19.88	-1.83	-1.48	-3.79	-17.39	-7.79
42	-1.82	-3.59	-6.90	-4.77	-10.58	-14.29	-5.31	-9.73	-5.88	-1.42	-9.00	-10.15	-7.24	-2.98	-13.41	-6.81	-2.91	1.38	-8.32	-19.87	-7.25
43	-2.22	-10.64	-2.79	-3.07	-2.52	-0.78	-5.99	-4.12	-2.54	-5.50	-4.84	-8.55	-4.37	-3.14	-9.88	-21.58	-4.18	-0.99	-3.97	-18.22	-10.25
44	-2.37	-9.69	-5.28	-2.77	-14.12	3.67	-7.13	-10.96	3.38	–	-7.79	-11.69	-7.05	-1.77	-13.18	-7.06	-6.30	–	-3.50	-18.60	-6.11
45	-1.98	-6.43	-5.53	-2.91	-0.38	-9.48	-6.11	-8.90	-1.12	-12.25	-6.83	-9.41	-5.69	-4.33	-13.62	-19.21	-0.64	-1.58	-4.13	-16.31	-5.65
Hesperadin	-2.67	-11.01	-1.26	-2.94	–	-3.61	-7.81	-7.97	–	-4.07	-5.99	-8.94	-5.47	-6.92	-13.28	-10.64	-0.63	-4.98	-3.14	-18.27	-9.01
Sunitinib	-2.98	-12.37	-0.37	-9.61	–	–	-7.77	-6.63	–	-0.33	-11.83	-11.84	-4.54	-3.79	-11.15	–	–	-0.75	-7.87	-18.08	-7.14

SUPPLEMENTARY MATERIAL 4

Ítalo Antônio Fernandes[a,b], Tamiris Maria de Assis[a,b], Isael Aparecido Rosa[a,c], Elaine Fontes Ferreira da Cunha[*a,b]

[a]Laboratório de Modelagem Molecular, LABGQC, Chemistry Department, Federal University of Lavras, Lavras, MG, Brazil; [b]Programa de Pós-Graduação em Agroquímica, Chemistry Department, Federal University of Lavras, Lavras, MG, Brazil; [c]Multicêntrico em Química de Minas Gerais (Rede Mineira de Química – RQ-MG), Federal University of Lavras, Lavras, MG, Brazil

Chemical structures for all new proposed compounds **IAF1-IAF100**.

IAF1 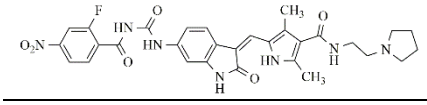	**IAF2** 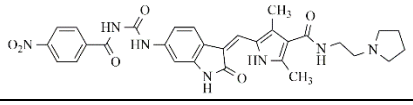	**IAF3** 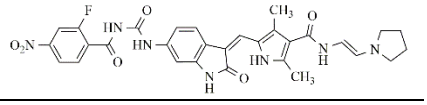
IAF4 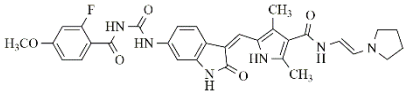	**IAF5** 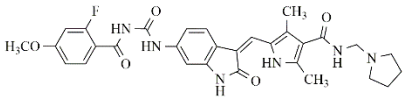	**IAF6** 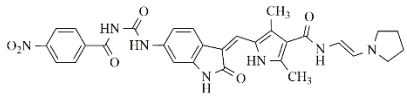
IAF7 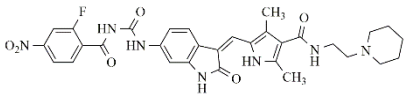	**IAF8** 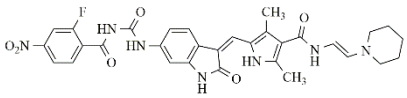	**IAF9** 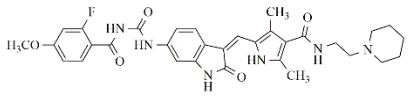
IAF10 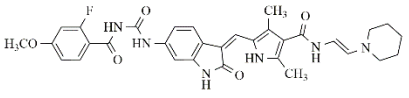	**IAF11** 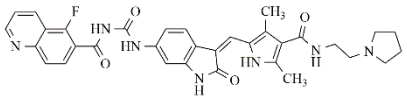	**IAF12** 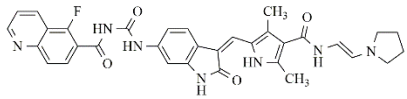
IAF13 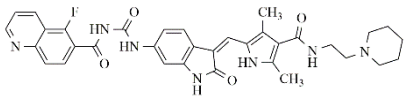	**IAF14** 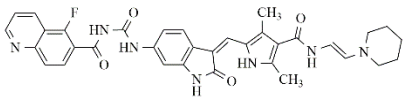	**IAF15** 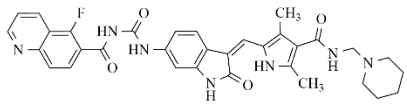
IAF16 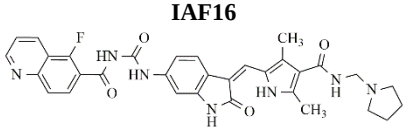	**IAF17** 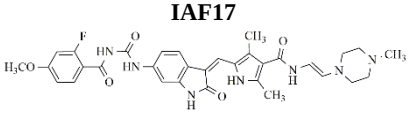	**IAF18** 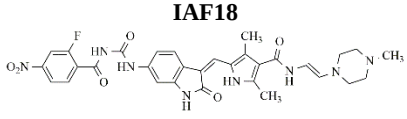
IAF19 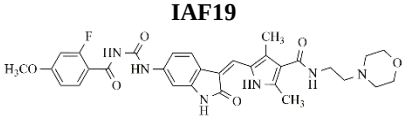	**IAF20** 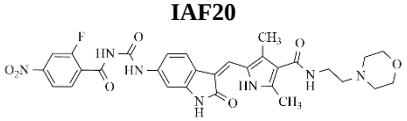	**IAF21** 
IAF22 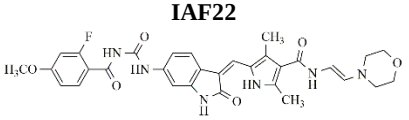	**IAF23** 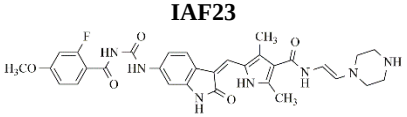	**IAF24** 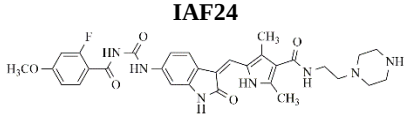
IAF25 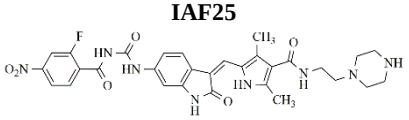	**IAF26** 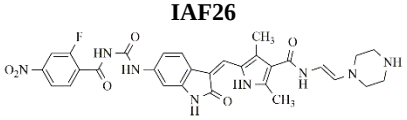	**IAF27** 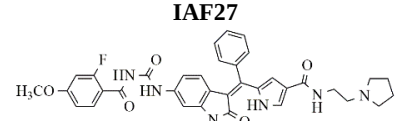
IAF28 	**IAF29** 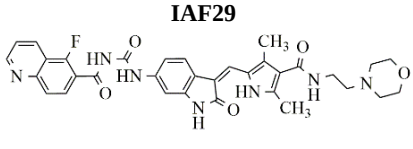	**IAF30** 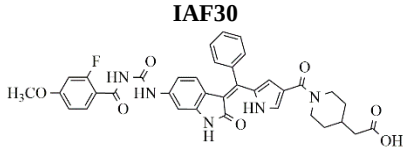

IAF31 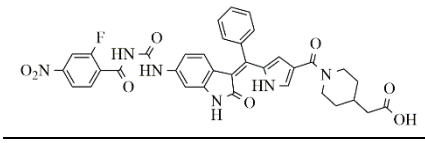	**IAF32** 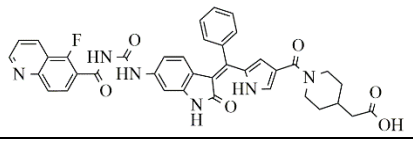	**IAF33** 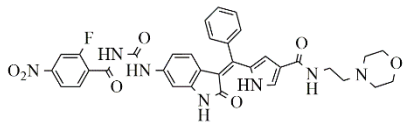
IAF34 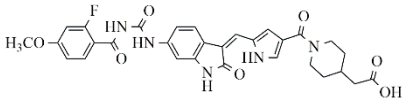	**IAF35** 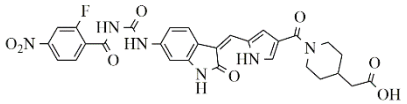	**IAF36** 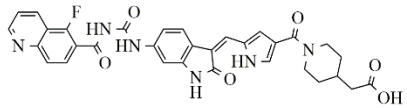
IAF37 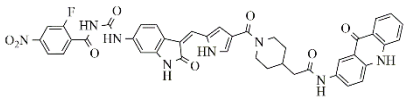	**IAF38** 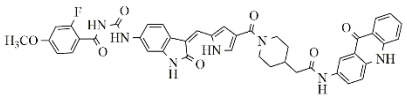	**IAF39** 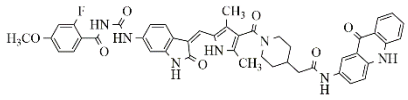
IAF40 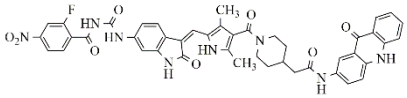	**IAF41** 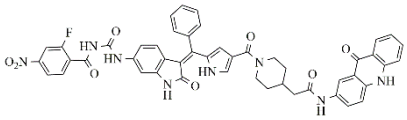	**IAF42** 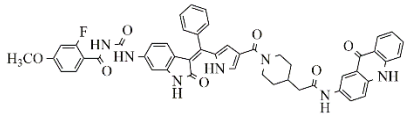
IAF43 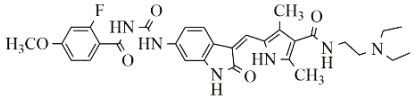	**IAF44** 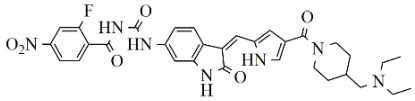	**IAF45** 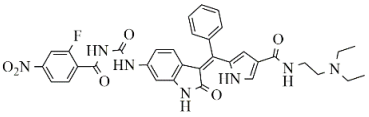
IAF46 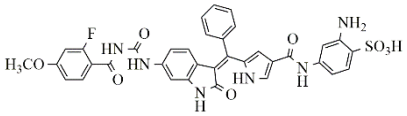	**IAF47** 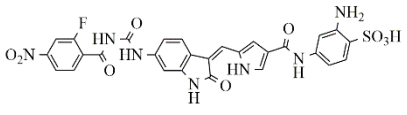	**IAF48** 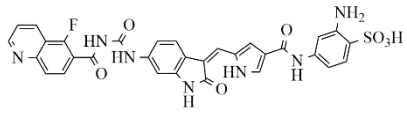
IAF49 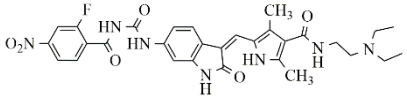	**IAF50** 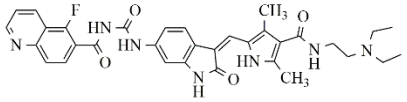	**IAF51** 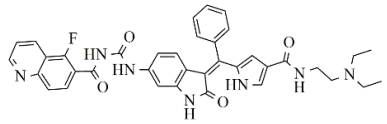
IAF52 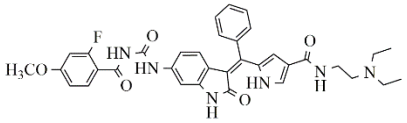	**IAF53** 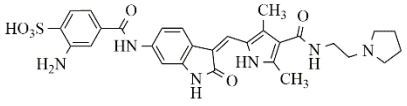	**IAF54** 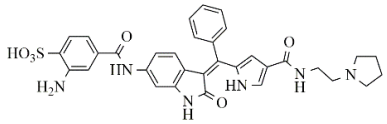
IAF55 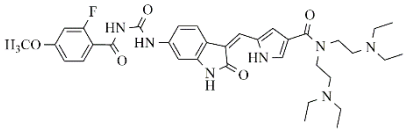	**IAF56** 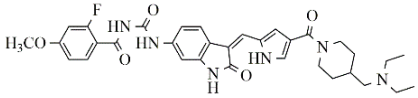	**IAF57** 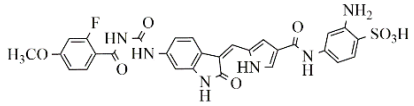
IAF58 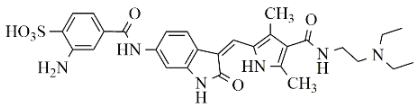	**IAF59** 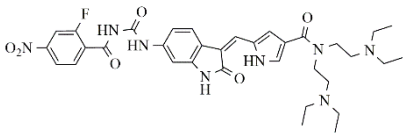	**IAF60** 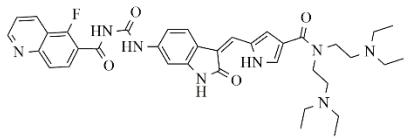
IAF61 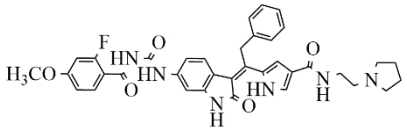	**IAF62** 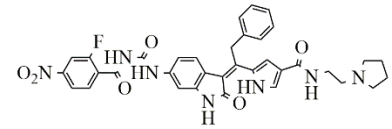	**IAF63** 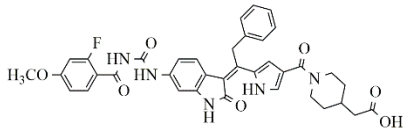
IAF64 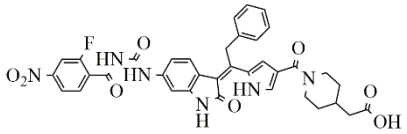	**IAF65** 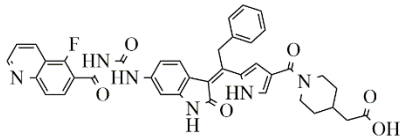	**IAF66** 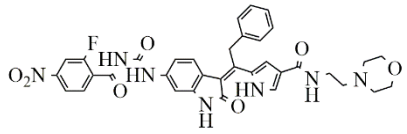

IAF67 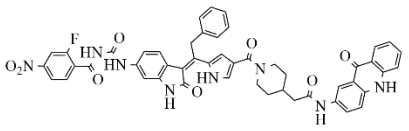	**IAF68** 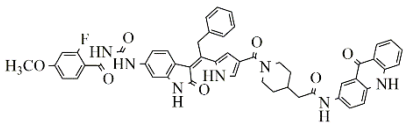	**IAF69** 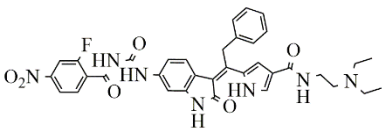
IAF70 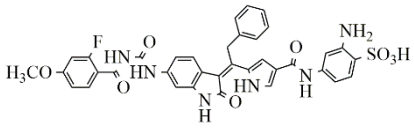	**IAF71** 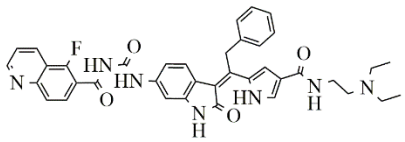	**IAF72** 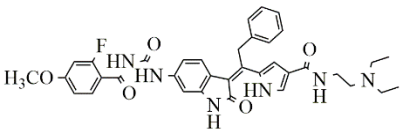
IAF73 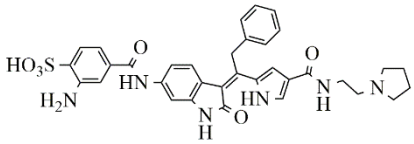	**IAF74** 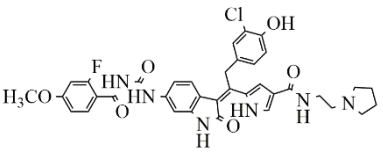	**IAF75** 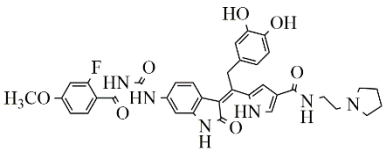
IAF76 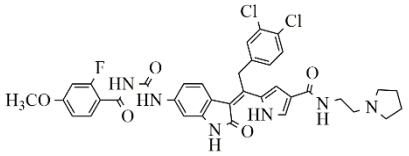	**IAF77** 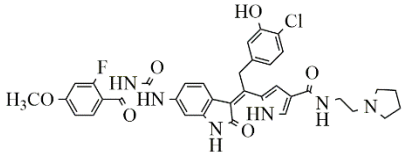	**IAF78** 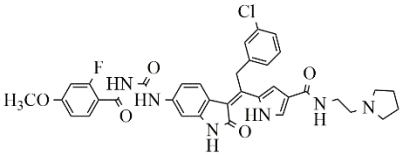
IAF79 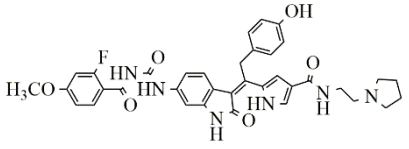	**IAF80** 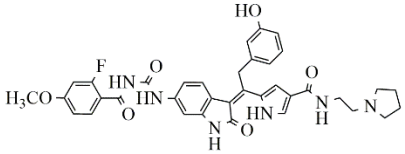	**IAF81** 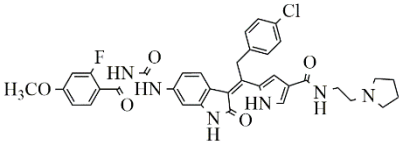
IAF82 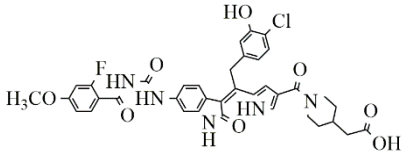	**IAF83** 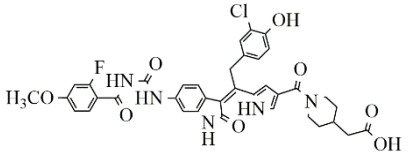	**IAF84** 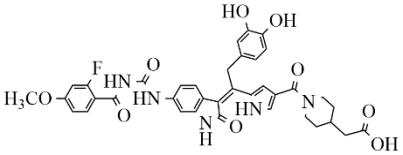
IAF85 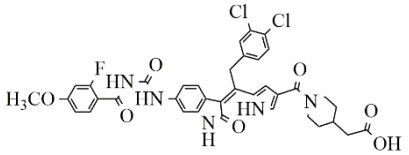	**IAF86** 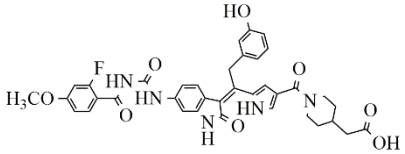	**IAF87** 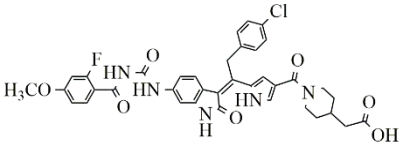
IAF88 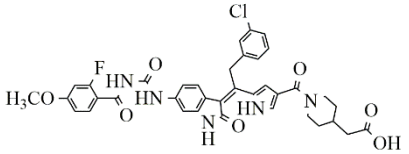	**IAF89** 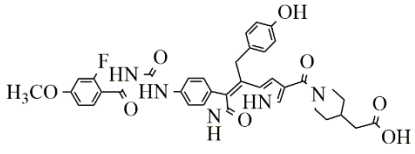	**IAF90** 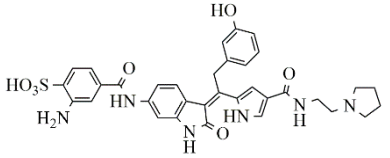
IAF91 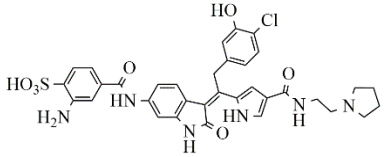	**IAF92** 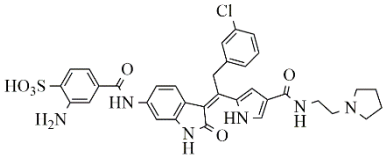	**IAF93** 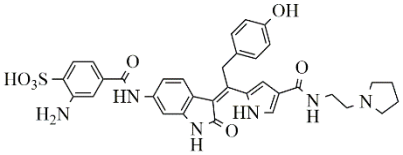
IAF94 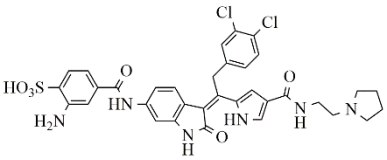	**IAF95** 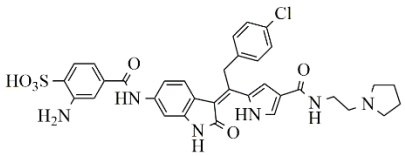	**IAF96** 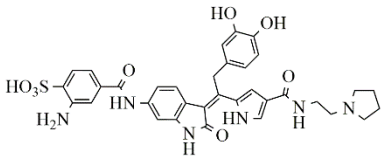

IAF97	IAF98	IAF99
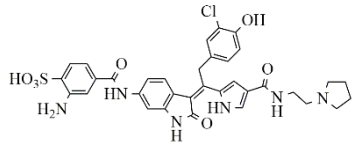	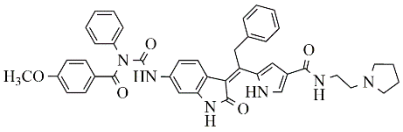	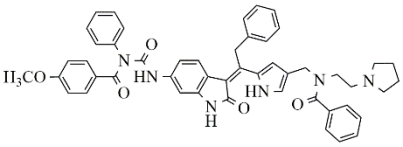

IAF100

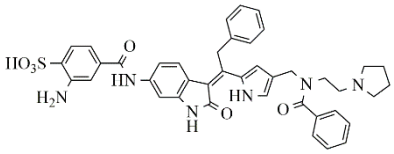

SUPPLEMENTARY MATERIAL 5

Ítalo Antônio Fernandes[a,b], Tamiris Maria de Assis[a,b], Isael Aparecido Rosa[a,c], Elaine Fontes Ferreira da Cunha[*a,b]

[a]Laboratório de Modelagem Molecular, LABGQC, Chemistry Department, Federal University of Lavras, Lavras, MG, Brazil; [b]Programa de Pós-Graduação em Agroquímica, Chemistry Department, Federal University of Lavras, Lavras, MG, Brazil; [c]Multicêntrico em Química de Minas Gerais (Rede Mineira de Química – RQ-MG), Federal University of Lavras, Lavras, MG, Brazil

MolDock Score, Pose-Protein Interaction and H Bond energy values from each of the selected pose for all new proposed compounds, **IAF1-IAF100**.

Compound	MolDock Score	Pose-Protein Interaction	H Bond Energy	Compound	MolDock Score	Pose-Protein Interaction	H Bond Energy
IAF1	-210.78	-219.68	-10.58	**IAF51**	-228.78	-240.73	-7.37
IAF2	-196.27	-195.50	-13.75	**IAF52**	-220.75	-217.71	-8.45
IAF3	-205.19	-203.35	-6.15	**IAF53**	-178.67	-189.61	-12.37
IAF4	-217.21	-213.53	-4.78	**IAF54**		Pose not found	
IAF5	-203.31	-204.63	-7.12	**IAF55**	-204.14	-197.75	-4.06
IAF6	-217.63	-212.59	-7.74	**IAF56**	-186.03	-196.14	-7.80
IAF7	-193.84	-210.42	-6.64	**IAF57**	-184.39	-182.19	-8.06
IAF8		Pose not found		**IAF58**	-164.89	-164.97	-12.31
IAF9	-205.99	-213.46	-7.19	**IAF59**	-195.92	-204.81	-6.28
IAF10		Pose not found		**IAF60**	-195.24	-204.67	-9.22
IAF11	-215.19	-217.10	-7.24	**IAF61**	-238.40	-246.12	-9.55
IAF12	-204.40	-204.92	-11.98	**IAF62**	-246.68	-251.46	-14.15
IAF13	-194.96	-214.47	-8.94	**IAF63**	-221.89	-250.15	-7.37
IAF14	-206.61	-216.46	-11.39	**IAF64**	-221.75	-246.27	-9.17
IAF15	-196.61	-213.46	-6.77	**IAF65**	-213.28	-236.57	-5.00
IAF16	-193.44	-207.87	-9.32	**IAF66**	-211.78	-240.45	-11.01
IAF17		Pose not found		**IAF67**		Pose not found	
IAF18		Pose not found		**IAF68**		Pose not found	
IAF19	-214.37	-226.09	-8.38	**IAF69**	-212.35	-235.16	-4.89
IAF20	-205.05	-215.39	-13.10	**IAF70**	-214.65	-239.05	-9.94
IAF21	-199.91	-204.18	-5.92	**IAF71**	-222.69	-240.77	-9.04
IAF22	-201.71	-206.99	-5.26	**IAF72**	-211.12	-224.84	-10.49
IAF23	-185.90	-203.09	-7.36	**IAF73**	-166.06	-178.47	-3.96
IAF24	-201.30	-211.83	-9.39	**IAF74**	-231.70	-235.50	-8.15
IAF25	-191.82	-198.33	-14.73	**IAF75**	-235.03	-237.19	-14.16
IAF26	-201.63	-206.39	-13.19	**IAF76**	-225.26	-242.40	-8.17
IAF27	-224.43	-224.28	-4.85	**IAF77**	-238.66	-240.04	-11.74
IAF28	-223.03	-230.18	-10.59	**IAF78**	-234.60	-243.31	-11.39
IAF29	-199.40	-212.92	-15.65	**IAF79**	-236.71	-240.59	-15.61
IAF30	-216.60	-226.53	-13.77	**IAF80**	-222.08	-237.75	-11.77
IAF31	-217.78	-222.78	-4.56	**IAF81**	-226.70	-234.87	-12.14
IAF32	-201.11	-208.47	-9.44	**IAF82**	-220.15	-233.58	-3.19
IAF33	-202.21	-212.70	-10.36	**IAF83**	-212.63	-221.79	-10.91
IAF34	-185.74	-199.21	-7.87	**IAF84**	-233.36	-250.31	-10.73
IAF35	-189.60	-204.12	-15.62	**IAF85**	-219.72	-238.43	-7.41
IAF36	-180.25	-195.16	-7.94	**IAF86**	-232.92	-245.90	-7.62
IAF37		Pose not found		**IAF87**	-212.75	-223.89	-14.56
IAF38		Pose not found		**IAF88**	-232.32	-238.03	-4.78
IAF39		Pose not found		**IAF89**	-223.18	-241.31	-5.57
IAF40		Pose not found		**IAF90**	-185.72	-193.12	-4.80
IAF41		Pose not found		**IAF91**		Pose not found	
IAF42		Pose not found		**IAF92**		Pose not found	
IAF43	-208.83	-204.78	-5.04	**IAF93**	-189.66	-198.35	-8.73
IAF44		Pose not found		**IAF94**		Pose not found	
IAF45	-191.50	-211.93	-12.85	**IAF95**		Pose not found	
IAF46	-209.41	-200.30	-2.69	**IAF96**		Pose not found	
IAF47	-180.08	-199.08	-15.28	**IAF97**		Pose not found	
IAF48	-195.93	-202.49	-10.52	**IAF98**	-221.26	-227.20	-2.50
IAF49	-201.99	-205.79	-9.97	**IAF99**	-259.42	-254.31	-2.78
IAF50	-215.74	-219.37	-9.85	**IAF100**		Pose not found	

SUPPLEMENTARY MATERIAL 6

Ítalo Antônio Fernandes[a,b], Tamiris Maria de Assis[a,b], Isael Aparecido Rosa[a,c], Elaine Fontes Ferreira da Cunha[*a,b]

[a]*Laboratório de Modelagem Molecular, LABGQC, Chemistry Department, Federal University of Lavras, Lavras, MG, Brazil;* [b]*Programa de Pós-Graduação em Agroquímica, Chemistry Department, Federal University of Lavras, Lavras, MG, Brazil;* [c]*Multicêntrico em Química de Minas Gerais (Rede Mineira de Química – RQ-MG), Federal University of Lavras, Lavras, MG, Brazil*

Interaction energy values (kcal.mol^{-1}) of each amino acid residue for all new proposed compounds.

Cpd/aa	Ala120	Ala173	Ala233	Arg175	Asn221	Asp234	Glu171	Glu177	Glu220	Gly102	Gly176	Leu99	Leu154	Leu170	Leu223	Lys103	Lys122	Lys180	Pro174	Tyr172	Val107
IAF1	-2.21	-10.59	-7.22	-5.76	-11.33	-13.03	-5.96	-11.80	-7.56	-1.12	-12.45	-8.82	-5.29	2.93	-11.34	-9.16	-4.77	-6.00	-5.89	-19.35	-7.94
IAF2	-1.69	-8.19	-7.45	-9.21	-6.18	-9.90	-5.59	-11.12	-5.91	–	-14.49	-11.16	-1.12	-5.47	-13.78	-16.19	–	-2.58	-12.78	-20.73	-6.99
IAF3	-2.21	-10.76	-8.51	-5.53	-10.16	-15.32	-6.61	-10.18	-6.87	-0.92	-11.45	-6.87	-7.66	3.95	-13.17	-8.65	-4.99	–	-8.30	-18.15	-7.37
IAF4	-1.79	-9.28	-8.41	-7.34	-10.58	-12.89	-6.31	-15.95	-5.36	-1.26	-11.96	-10.01	-6.07	5.80	-13.46	-10.61	-4.71	-5.48	-3.71	-13.75	-7.52
IAF5	-2.71	-11.51	-8.67	-12.37	-10.73	-13.93	-6.65	-11.11	-5.51	-0.75	-9.99	-10.57	-1.53	-1.89	-13.21	-8.09	-1.09	3.71	-10.63	-19.98	-7.95
IAF6	-1.80	-10.43	-6.17	-5.16	-11.94	-15.07	-6.30	-20.45	2.18	-0.39	-10.57	-8.01	-8.32	5.50	-13.70	-2.89	-4.83	-7.98	-3.34	-14.51	-6.98
IAF7	-2.51	-7.16	-6.47	-11.52	-10.26	-2.18	-5.92	-14.23	-6.98	-1.03	-12.38	-12.18	-6.98	-5.66	-13.99	-8.50	-5.17	-8.59	-6.15	-19.19	-4.59
IAF9	-2.04	-12.32	-7.30	-12.13	-9.92	-14.49	-5.97	-12.44	-7.51	-1.05	-12.43	-11.81	-3.00	-4.88	-13.59	-7.42	-0.54	-4.47	-11.43	-19.84	-7.52
IAF11	-1.86	-10.49	-6.67	-4.81	-9.34	-13.47	-6.54	-16.31	-5.81	-2.62	-12.02	-9.73	-8.13	5.27	-13.54	-8.59	-5.15	-10.71	-3.30	-13.82	-7.70
IAF12	-1.69	-9.77	-2.89	-7.19	-8.43	-3.30	-5.80	-21.43	-1.90	-3.14	-11.57	-10.54	-6.38	3.28	-11.45	-13.07	-7.14	-5.95	-3.53	-12.99	-8.54
IAF13	-2.03	-10.91	-4.26	-12.29	-9.52	-5.22	-5.92	-13.88	-8.31	-2.18	-11.35	-10.17	-5.43	-4.81	-11.10	-11.64	-2.92	-5.21	-9.40	-20.18	-8.56
IAF14	-1.89	-10.08	-3.49	-7.69	-11.18	2.29	-6.38	-14.96	-6.11	-2.25	-11.36	-8.77	-6.66	1.21	-11.38	-16.40	-6.16	-11.89	-4.68	-16.76	-8.14
IAF15	-2.45	-11.58	-6.92	-8.92	-8.57	-12.24	-6.06	-11.68	-6.26	-2.68	-14.02	-12.00	-2.45	-4.76	-13.83	-16.00	-0.30	-4.08	-9.64	-19.43	-6.99
IAF16	-2.82	-12.52	-5.95	-10.70	-10.71	-8.42	-7.48	-10.71	-3.27	-3.96	-11.35	-11.93	-6.62	-4.01	-12.70	-10.94	-2.81	–	-9.48	-17.83	-6.50
IAF19	-2.01	-10.27	-6.82	-9.18	-8.38	-10.51	-6.32	-15.14	-5.81	-1.79	-12.62	-11.31	-7.31	9.19	-12.44	-9.72	-6.08	-6.19	-3.28	-13.00	-8.59
IAF20	-1.93	-10.21	-3.99	-10.40	-4.93	-7.95	-6.61	-14.42	-4.39	-4.61	-12.25	-11.38	-6.81	-1.39	-12.29	-12.39	-4.68	-4.41	-5.78	-17.93	-7.78
IAF21	-2.30	-10.64	-7.64	-6.84	-11.97	-12.47	-6.57	-11.30	-3.37	-1.63	-11.71	-6.26	-5.35	6.94	-11.47	-7.08	-4.97	-4.29	-8.18	-19.92	-7.21
IAF22	-1.90	-11.06	-6.53	-9.13	-10.98	-14.42	-6.35	-17.41	-1.09	-1.62	-11.91	-8.20	-7.15	1.99	-13.23	-4.77	-4.54	-5.96	-5.45	-16.93	-7.83
IAF23	-1.61	-13.16	-6.13	-2.92	–	-13.56	-6.07	-5.29	–	–	-7.37	-9.57	-8.27	-6.46	-10.20	-0.35	-6.24	-2.80	-2.13	-19.88	-3.03
IAF24	-1.92	-11.00	-3.23	-8.34	-9.35	-1.53	-5.95	-18.05	-6.97	-1.92	-15.34	-11.89	-4.81	-4.38	-12.36	-11.35	-3.52	-6.42	-10.60	-19.98	-7.19
IAF25	-2.76	-6.29	-7.81	-3.01	-14.77	-13.50	-6.50	-9.22	-5.67	-1.04	-7.56	-12.48	-5.12	-6.69	-12.55	-11.52	-2.78	-1.71	-4.71	-21.54	-4.60
IAF26	-2.48	-12.29	-2.11	-16.37	-2.19	-5.75	-6.33	-9.41	-3.86	-5.68	-10.82	-1.23	-7.21	9.39	-10.62	-16.43	-10.10	-4.02	-6.68	-17.41	-5.72
IAF27	-2.10	-10.93	-7.39	-9.15	-10.34	-16.23	-6.68	-15.56	-4.96	-1.27	-10.14	-7.43	-7.85	4.62	-12.37	-5.18	-6.21	-14.29	-6.19	-19.13	-10.59
IAF28	-1.34	-10.80	-6.54	-5.50	-11.69	-10.54	-4.06	-16.71	-6.46	-2.41	-2.00	-16.85	-6.01	0.78	-12.99	-9.78	-4.29	-2.39	-18.95	-13.81	-8.05
IAF29	-1.98	-7.68	-6.18	-4.25	-9.53	-11.55	-6.47	-9.88	-8.32	-1.61	-9.81	-12.05	-8.31	–	-14.07	-9.31	-3.90	-1.20	-4.35	-22.00	-6.70
IAF30	-1.52	-13.07	-7.07	-15.01	–	-8.39	-6.14	-17.20	-0.77	-10.13	-13.16	-14.48	-3.91	-6.95	-9.29	-15.85	-3.68	-3.51	-5.41	-17.95	-5.92
IAF31	-1.74	-11.55	-6.52	-7.58	-12.08	-14.86	-6.13	-18.19	-1.62	-1.99	-9.17	-11.81	-8.02	1.74	-13.75	-5.57	-4.34	-11.73	-7.34	-19.80	-9.15
IAF32	-2.16	-9.09	-2.71	-3.52	-2.43	-6.13	-5.64	-11.11	-6.99	-6.13	-5.96	2.12	-6.08	5.60	-10.09	-16.29	-10.58	-2.27	-4.96	-22.87	-13.71
IAF33	-1.67	-8.66	-4.25	-11.76	-4.74	-8.55	-6.36	-19.21	-4.02	-3.16	-12.16	-13.44	-6.71	-2.30	-12.79	-11.36	-3.80	-3.96	-7.77	-20.12	-8.08
IAF34	-1.90	-10.37	-1.96	-4.75	-9.34	-12.28	-5.66	-12.52	-3.71	-5.37	-10.61	-7.65	-3.91	-4.49	-10.49	-17.30	-5.07	-7.49	-7.21	-18.94	-10.02
IAF35	-1.99	-10.36	-1.71	-8.58	-9.08	-13.03	-2.18	-7.11	-7.42	-5.19	-6.45	-5.63	-5.57	-5.56	-10.95	-20.87	-4.71	-8.55	-8.19	-24.05	-8.61
IAF36	-2.55	-11.87	-4.76	-4.54	-12.23	0.87	-5.71	-12.75	-0.82	-1.51	-9.91	-11.35	-6.65	-4.97	-13.18	-17.42	-3.57	-11.57	-4.77	-16.00	-5.05
IAF43	-1.83	-10.14	-6.74	-10.47	-9.61	-12.55	-5.70	-14.40	-6.66	-1.63	-12.54	-11.55	-6.07	-1.76	-12.53	-8.76	-4.45	-3.27	-5.36	-16.00	-8.51
IAF45	-1.20	-9.20	-3.93	-10.45	-4.00	-7.61	-4.18	-10.40	-7.24	-3.00	-9.30	-13.63	-5.41	-2.11	-11.95	-14.91	-3.38	-6.28	-5.93	-13.46	-9.99
IAF46	-0.34	-6.48	-4.77	-4.59	-7.80	-6.51	-0.41	-16.26	-7.91	-4.48	-8.90	-15.19	-1.96	-3.79	-7.28	-10.87	-6.30	0.76	-14.84	-14.58	-9.09
IAF47	-1.97	-13.63	-2.14	-8.23	-3.31	-13.79	-4.51	-9.51	-3.38	-4.11	-8.85	-4.01	-5.82	-3.60	-11.71	-18.47	-4.79	-6.20	-7.30	-17.69	-8.35
IAF48	-1.97	-11.46	-4.72	-5.74	-10.09	-9.94	-4.83	-19.96	-1.54	-2.77	-7.51	-4.55	-5.03	-1.34	-9.67	-5.58	-6.96	-12.11	-3.69	-13.56	-7.37
IAF49	-2.32	-10.55	-3.46	-12.00	-5.07	-8.92	-5.80	-11.47	-7.43	-2.69	-12.47	-11.72	-5.03	-4.16	-12.76	-16.63	-3.96	–	-8.76	-17.11	-6.75
IAF50	-2.18	-8.80	-6.99	-11.80	-10.69	-12.86	-6.00	-12.19	-5.48	-2.00	-11.28	-8.67	-6.68	1.84	-11.35	-7.20	-5.55	–	-8.65	-19.63	-8.03
IAF51	-1.73	-14.02	-6.85	-4.98	-10.75	-14.15	-5.32	-13.91	-6.03	-3.22	-8.02	-15.26	-5.16	4.82	-13.18	-8.67	-3.80	-4.03	-12.16	-22.71	-10.19
IAF52	-2.21	-10.29	-4.28	-4.27	-5.19	6.02	-3.20	-9.61	-5.90	-2.92	-6.53	0.85	-6.24	3.98	-9.50	-15.30	-11.32	-1.62	-10.22	-29.81	-12.88

IAF53	-2.45	-11.20	-8.25	-8.85	–	-10.13	-4.87	-7.31	–	–	-11.37	-12.18	-7.85	17.48	-12.12	–	5.36	-0.90	-4.29	-16.63	-5.56
IAF55	-1.19	-9.09	-6.81	-10.67	4.91	-4.81	-5.12	-10.70	-2.32	-1.36	-11.21	-20.36	-6.94	-2.42	-11.87	-13.88	-5.83	-9.59	-5.93	-16.97	-7.03
IAF56	-2.06	-9.07	-4.19	-6.25	-0.89	-8.85	-5.22	-13.81	-6.87	-3.84	-10.22	-11.74	-7.36	-3.65	-11.56	-14.02	-4.41	-15.56	-5.71	-20.04	-6.73
IAF57	0.83	-3.81	-4.02	-9.35	-4.85	-11.72	-4.34	-8.10	-5.62	-3.13	-9.54	-11.09	-6.35	0.44	-9.09	-18.55	-5.51	-2.41	-7.18	-21.67	-8.60
IAF58	-1.48	-10.82	-4.07	-1.27	–	-15.11	-5.53	-4.81	–	–	-7.71	-18.26	-6.49	10.55	-5.67	–	-8.24	-3.31	-3.77	-19.92	-2.91
IAF59	-2.29	-14.04	-6.14	-9.40	-11.43	-4.01	-6.56	-13.48	-4.34	-1.39	-8.27	-15.09	-6.19	-4.74	-13.50	-7.91	-5.87	-10.67	-1.97	-14.95	-5.29
IAF60	-1.86	-12.07	-4.85	-3.55	-9.90	14.32	-2.13	-10.66	-3.53	-0.67	-8.10	-15.94	-7.34	5.70	-12.22	-13.20	-8.08	-4.55	-11.85	-21.44	-7.87
IAF61	-2.11	-12.48	-6.47	-7.35	-10.24	-13.10	-6.67	-17.59	-1.79	-3.12	-12.17	-24.23	-6.95	-1.01	-13.08	-10.68	-4.74	-15.78	-5.90	-17.76	-9.60
IAF62	-1.77	-11.13	-4.81	-12.22	-13.29	-13.42	-6.00	-14.48	-6.17	-2.61	-12.67	-23.45	-5.49	-2.24	-13.58	-11.70	-3.51	-10.54	-10.94	-16.48	-8.31
IAF63	-2.62	-14.32	-8.32	-12.47	-8.07	-13.93	-7.31	-21.35	-3.23	-3.21	-11.44	-21.84	-5.83	-4.98	-14.07	-7.92	-2.94	-9.57	-6.02	-17.75	-8.20
IAF64	-2.68	-12.88	-5.73	-8.75	-7.96	-13.38	-6.96	-16.58	-6.77	-4.04	-9.57	-23.01	-5.92	-4.21	-13.79	-13.27	-5.34	-13.22	-7.46	-19.29	-9.21
IAF65	-2.56	-14.88	-7.40	-8.45	–	-9.75	-7.70	-15.57	-1.05	-10.90	-9.36	-21.40	-4.59	-5.75	-14.40	-9.65	-2.12	-11.67	-8.12	-16.50	-8.96
IAF66	-2.36	-12.41	-8.04	-5.22	-8.98	-14.47	-7.28	-20.47	-1.68	-3.02	-12.46	-23.50	-5.03	-4.44	-14.14	-7.88	-3.45	-11.82	-8.72	-17.48	-8.26
IAF69	-2.64	-12.86	-5.37	-10.04	-8.30	-13.66	-7.33	-21.21	-5.80	-0.97	-9.19	-24.04	-7.12	1.81	-14.13	-2.94	-4.36	-12.33	-7.37	-17.27	-7.89
IAF70	-1.78	-12.69	-5.05	-5.44	-0.70	1.90	-6.61	-14.45	-0.82	-8.83	-2.84	-21.88	-6.34	2.49	-14.02	-18.60	-5.93	-14.83	-4.54	-13.27	-8.34
IAF71	-2.56	-15.32	-4.15	-3.91	–	-6.12	-5.57	-10.14	-0.52	-11.35	-9.23	-24.16	-5.84	-4.18	-12.50	-13.00	-2.68	-4.00	-14.69	-24.26	-8.20
IAF72	-2.39	-10.74	-5.89	-7.84	-4.37	-9.40	-6.87	-12.67	-1.69	-2.50	-11.31	-24.17	-6.03	-3.24	-14.02	-14.92	-6.03	-9.86	-8.29	-18.96	-10.37
IAF73	-1.64	-11.20	2.51	-5.95	–	-9.98	-4.20	-6.97	–	-0.36	-8.17	-18.76	-7.36	-7.30	-12.35	–	-1.13	-3.53	-0.94	-24.27	-6.80
IAF74	-2.73	-14.64	-6.02	-12.35	–	-8.79	-7.15	-12.86	–	-13.12	-10.01	-18.81	-4.11	-5.45	-14.02	-12.18	-4.71	-3.48	-6.51	-16.13	-9.71
IAF75	-1.79	-12.00	-5.07	-12.82	–	-5.75	-5.23	-14.43	–	-12.51	-10.56	-20.51	-3.89	-5.05	-12.41	-11.45	-2.99	-9.33	-11.06	-17.26	-6.15
IAF76	-1.73	-15.15	-6.66	-4.20	-14.08	-4.22	-6.21	-12.82	0.68	-1.39	-9.00	-18.99	-5.11	–	-14.35	-11.67	-7.31	-7.98	-15.21	1.92	-6.35
IAF77	-2.73	-11.68	-6.24	-9.49	–	-9.74	-7.21	-11.65	–	-12.31	-11.45	-20.10	-3.11	-4.49	-14.31	-12.74	-5.46	-7.84	-8.11	-17.48	-9.48
IAF78	-1.87	-12.71	-4.13	-10.72	–	-4.78	-6.32	-14.15	-0.50	-11.21	-11.36	-24.12	-5.33	-5.31	-13.17	-12.60	-3.04	-10.31	-8.63	-18.12	-5.40
IAF79	-1.97	-17.16	-2.30	-4.81	-9.68	-8.15	-5.72	-10.59	-2.75	-3.92	-3.10	-28.75	-4.23	-1.87	-11.73	-14.72	-4.76	-4.98	-16.20	-34.00	-9.97
IAF80	-2.59	-13.15	-6.39	-11.27	-6.47	-14.08	-6.93	-14.40	-5.16	-4.96	-10.01	-23.42	-5.06	-3.01	-13.95	-14.08	-7.24	-4.04	-7.28	-18.39	-9.34
IAF81	-1.82	-12.96	-2.97	-6.38	–	-2.53	-4.80	-14.65	-0.92	-8.57	-8.24	-20.52	-5.43	-3.80	-12.82	-11.50	-2.78	-1.32	-22.53	-31.87	-6.38
IAF82	-2.48	-15.48	-7.99	-7.81	-1.47	-3.44	-7.19	-13.33	-1.33	-8.03	-11.04	-21.35	-5.67	-4.68	-14.51	-17.76	-1.93	-16.60	-6.45	-17.44	-5.06
IAF83	-2.73	-6.90	-5.44	-11.05	–	-8.83	-6.39	-13.17	-1.07	-9.14	-10.51	-18.32	-6.85	-4.34	-13.38	-16.00	-3.96	-5.48	-11.46	-20.32	-8.75
IAF84	-2.20	-13.17	-6.44	-4.75	-7.44	-13.36	-7.50	-18.23	-5.60	-3.93	-10.86	-26.40	-5.35	–	-13.63	-9.98	-5.26	-12.82	-5.07	-17.71	-6.56
IAF85	-2.72	-13.54	-3.90	-4.69	-10.26	-13.80	-7.07	-18.36	–	-2.60	-10.25	-23.21	-6.89	1.92	-13.09	-12.69	-8.31	-10.99	-6.47	-17.94	-8.58
IAF86	-2.55	-14.16	-6.55	-6.49	–	-9.53	-7.04	-13.97	-0.90	-10.15	-10.74	-24.15	-5.80	-3.12	-13.86	-14.00	-2.14	-12.38	-5.46	-17.17	-10.41
IAF87	-1.51	-11.21	-4.99	-3.68	-11.11	-12.02	-6.08	-14.36	-5.13	-2.53	0.84	-22.63	-6.69	2.50	-14.64	-13.54	-7.97	-6.13	-5.13	-19.26	-7.71
IAF88	-2.24	-14.20	-5.87	-3.78	-0.40	-8.39	-7.27	-9.31	-1.01	-8.66	-3.38	-25.03	-4.55	3.69	-13.89	-13.32	-3.63	-5.52	-17.65	-27.25	-8.12
IAF89	-2.67	-13.43	-6.90	-12.16	-0.36	-10.42	-6.00	-15.16	-1.18	-9.45	-11.37	-19.36	-6.83	-4.14	-14.62	-16.17	-1.52	-12.74	-7.41	-16.71	-6.18
IAF90	-2.03	-9.51	-6.30	-10.28	–	-10.90	-7.28	-10.25	–	-1.14	-7.61	-23.64	-5.74	14.32	-13.74	–	-2.44	-16.57	-4.65	-16.99	-6.24
IAF93	-1.58	-6.85	-4.12	-9.66	–	-9.27	-5.83	-8.02	–	–	-11.72	-26.88	-6.13	7.92	-6.95	–	-7.73	-10.95	-8.54	-21.18	-3.22
IAF98	-1.85	-8.75	-8.32	-11.58	-0.51	-11.05	-7.35	-17.43	-2.76	10.00	-9.70	-23.20	-3.65	-6.83	-14.25	-6.93	-5.19	-4.50	-8.26	-21.81	-0.31
IAF99	-2.64	-13.68	-8.84	-5.19	-0.46	-11.78	-7.51	-22.06	-2.58	-10.23	-11.88	-28.59	-3.99	-8.78	-14.32	-4.18	-5.01	-10.95	-4.74	-17.10	-2.92

Artigo 2: Elaborado conforme as normas da "*Computational and Theoretical Chemistry*" e em processo de submissão.

THEORETICAL STUDIES AIMED AT FINDING FLT3 INHIBITORS AND A PROMISING COMPOUND AND MOLECULAR PATTERN WITH DUAL AURORA B/FLT3 ACTIVITY

Theoretical studies aimed at finding FLT3 inhibitors and a promising compound and molecular pattern with dual Aurora B/FLT3 activity

Ítalo Antônio Fernandes[a]; Déborah Braga Resende[b]; Teodorico de Castro Ramalho[a]; Elaine Fontes Ferreira da Cunha[a*]

[a]Federal University of Lavras, Department of Chemistry, P.O. Box 3037, ZIP code 37200-000, Lavras-MG. italofernad@hotmail.com; teo@dqi.ufla.br; elaineffdacunha@gmail.com

[b]Federal University of Lavras, Department of Veterinary Medicine, P.O. Box 3037, ZIP code 37200-000, Lavras-MG. deborahbrr@gmail.com

*Corresponding author

elaineffdacunha@gmail.com

Elaine Fontes Ferreira da Cunha

Dept. of Chemistry (DQI)

UFLA - Federal University of Lavras

Campus Universitário, Caixa Postal 3037

Lavras – MG. 37200-000

Phone: + 55 35 38295129

Abstract: The FLT3 enzyme is expressed in membranes of precursor hematopoietic cells and have an important role in cellular differentiation, proliferation and multiplication. In AML disease, normally, there occurs hyperstimulation or mutations of this enzyme, leading to exacerbated cellular proliferation and lower response to standard cytotoxic agents. FLT3 and dual Aurora B/FLT3 inhibitors have shown relevance in searching for promising new anticancer compounds, mainly for AML. This work was designed to study and understand the interactions between human FLT3 in kinase domain with several indolin-2-one derivatives, structurally similar to sunitinib. MVD software was utilized in docking analyses. The FLT3 enzyme was obtained from the PDB (4XUF) and quizartinib was redocked and used as a reference compound. The predicted model of the training group, considering nineteen amino acid residues, performed in Chemoface, achieved an R2 of 0.82, suggesting that the binding conformations of the ligands with FLT3 are reasonable and the data can be used to predict the interaction energy of other FLT3 inhibitors with similar molecular pattern. MolDock Score energy for compound **1** showed more stable interaction energy (-233.25 kcal.mol^{-1}) than the other inhibitors studied, while sunitinib presented as one of the least stable (-160.94 kcal.mol^{-1}). **IAF70**, **IAF72**, **IAF75**, **IAF80**, **IAF84** and **IAF88** compounds can be highlighted as promising derivatives for synthesis and biological evaluation against FLT3. Furthermore, **IAF79** can be considered a promising dual Aurora B/FLT3 inhibitor and the molecular pattern evidenced exploited synthetically in searching for new indolin-2-one derivatives that may become a drug used in cancer treatment, including AML.

Keywords: Indolin-2-one derivatives; FLT3 inhibitors; Dual Aurora B/FLT3 inhibitors; Anticancer compounds; Computational Chemistry; Docking.

1. Introduction

Feline McDonough Sarcoma (FMS)-like tyrosine kinase 3 (FLT3, EC: 2.7.10.1) belongs to class III receptor protein tyrosine kinases, wherein five immunoglobulin-like domains are present in the extracellular region [1]. Under normal conditions this enzyme is expressed in membranes of precursor hematopoietic cells, being important for cellular differentiation, proliferation and multiplication. Blasts in acute myeloid leukemia (AML) express FLT3 and deregulation of its signaling pathway leads to exacerbated cellular proliferation, either by hyperstimulation or mutations, in which both processes contribute to AML onset [2,3].

Mutations in the FLT3 gene are observed in about 40% of AML cases, being highly affected in this disease [2]. Justamembranar domain mutations lead to a FLT3/ITD (internal tandem duplication) mutant allele, which has been associated to a decrease in leukemia remission of patients under chemotherapy with low response to standard cytotoxic agents [4]. Evidence shows that mutations in a justamembranar region interfere in the self-inhibitory mechanism, leading to a conformational modification and constitutive activation of this enzyme [1]. Bavetsias and Moore [5,6] showed that dual Aurora/FLT3 inhibitors might be more effective than selective FLT3 inhibitors in cases of AML mutations.

Searching for more efficient chemotherapic agents, FLT3/ITD inhibitors [7], as sunitinib (IC_{50} = 34.0 nM), quizartinib (IC_{50} = 1.1 nM) [8], midostaurin (IC_{50} = 9.3 nM), lestaurtinib (IC_{50} = 8.6 nM) and sorafenib (IC_{50} = 18.5 nM) [9] have been discovered (Fig. 1), and although presenting tolerability and toxicity problems, also inspire new studies in search of new promising anticancer agents.

We have reported a study between indolin-2-one derivatives and human Aurora B kinase through molecular docking [10]. Now, in this work we apply the same methodology looking forward to new potent FLT3 and Dual Aurora B/FLT3 inhibitors. Docking studies were performed in order to understand the binding mode of indolin-2-one derivatives, developed by Chern et al. [11], inside kinase domain FLT3, searching for new sunitinib analogues that may be more efficient and promising in the treatment of different cancer types, including AML.

Table 1
Chemical structures, IC_{50} and pIC_{50} values of **1**-**45** [11], Quizartinib and Sunitinib FLT3 inhibitor compounds. Test set compound numbers are marked with an asterisk.

Compound	Chemical Structure	IC_{50} (nM) FLT3	pIC_{50} FLT3
1	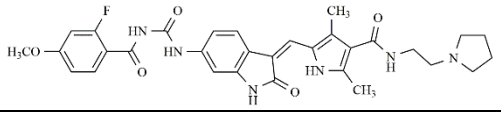	0.5	9.3010
2	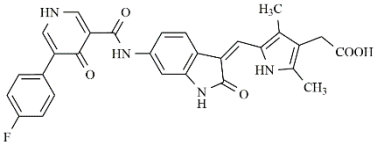	1.3	8.8861

3*	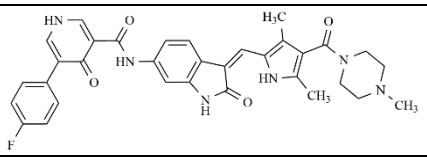	1.4	8.8539
4	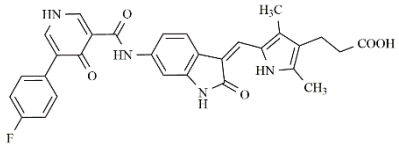	1.6	8.7959
5	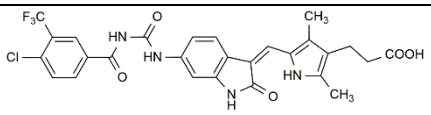	2.4	8.6198
6	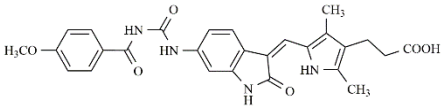	2.7	8.5686
7	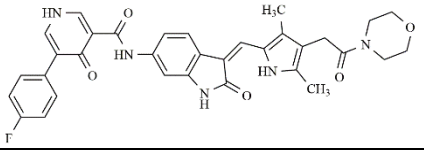	2.7	8.5686
8	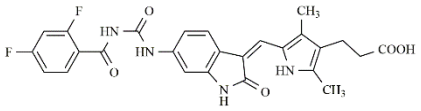	2.7	8.5686
9	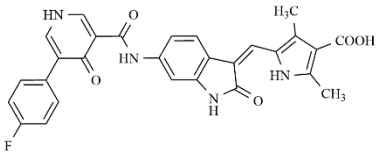	2.9	8.5376
10	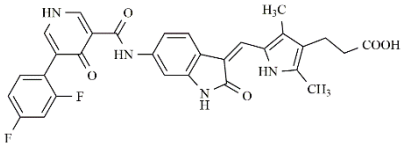	2.9	8.5376
11	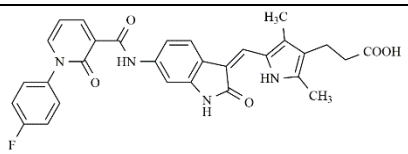	3.5	8.4559
12	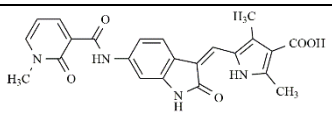	4.2	8.3768
13	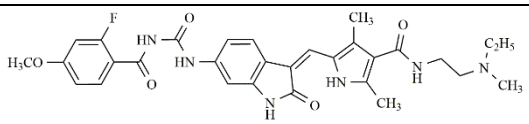	4.4	8.3565
14*	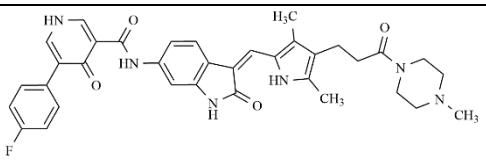	4.8	8.3188

15	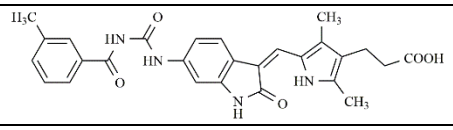	6.1	8.2147
16	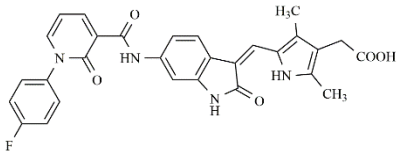	7.3	8.1367
17	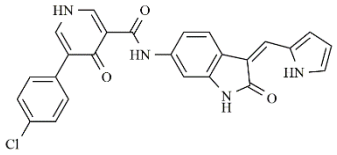	7.6	8.1192
18	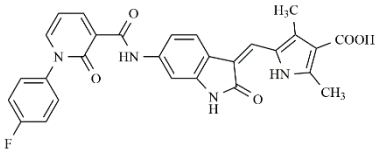	8.1	8.0915
19	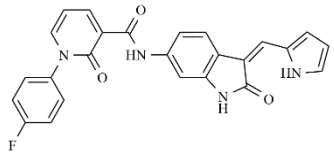	8.6	8.0655
20	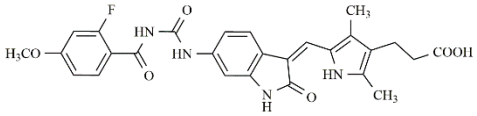	10.0	8.0000
21	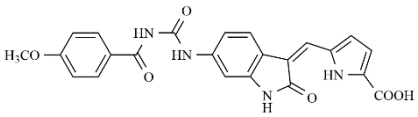	10.0	8.0000
22*	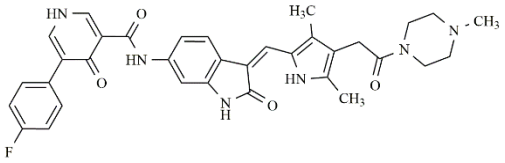	10.3	7.9872
23	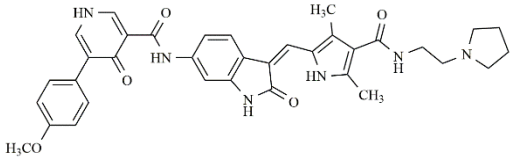	11.6	7.9355
24	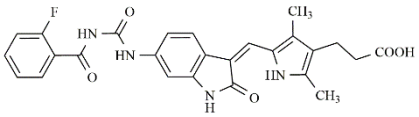	12.4	7.9066
25	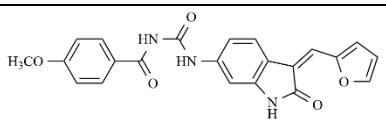	15.4	7.8125
26	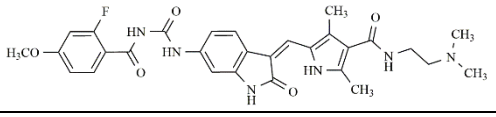	16.2	7.7905

27	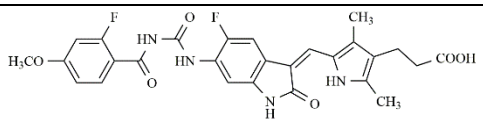	16.3	7.7878
28	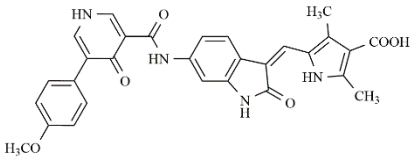	24.6	7.6091
29	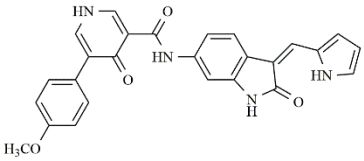	24.9	7.6038
30	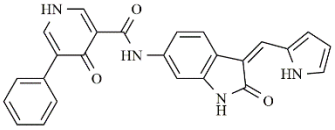	27.7	7.5575
31	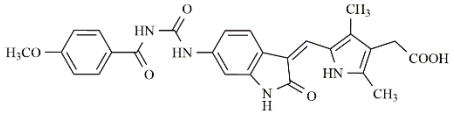	31.7	7.4989
32	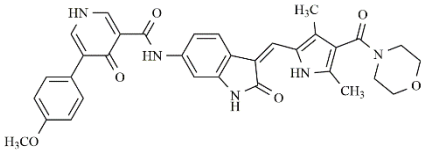	34.9	7.4572
33	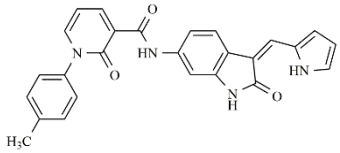	37.5	7.4260
34	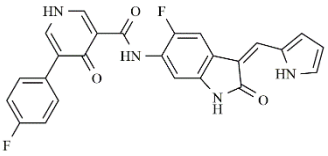	37.9	7.4214
35	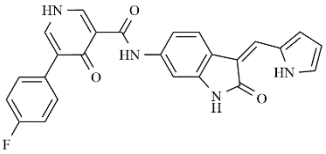	38.1	7.4191
36*	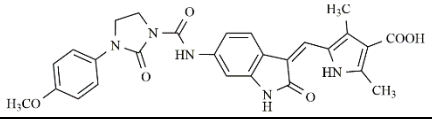	39.4	7.4045
37	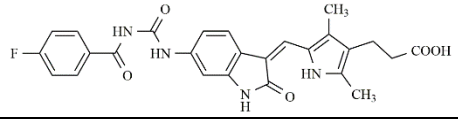	45.7	7.3401

38	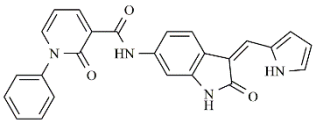	48.4	7.3152
39	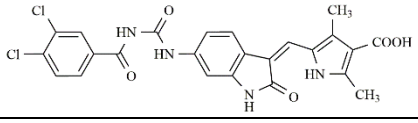	54.2	7.2660
40*	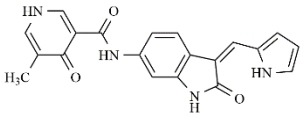	64.2	7.1925
41	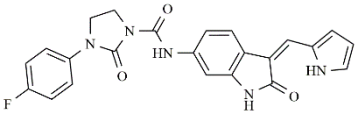	74.1	7.1302
42	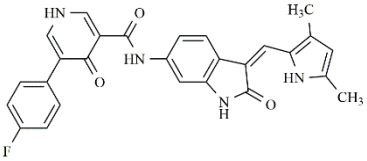	86.6	7.0625
43	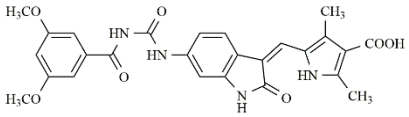	115.3	6.9382
44	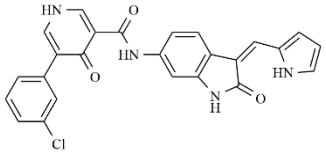	148.4	6.8286
45	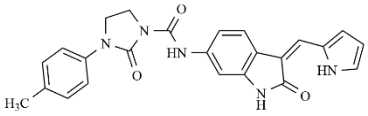	223.3	6.6511
Quizartinib	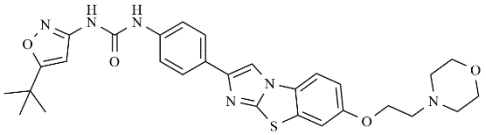	4.2 a1 1.1 a2	8.3768 8.9586
Sunitinib	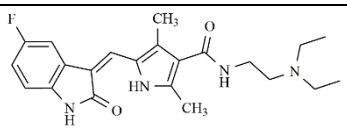	9.9 a1 34.0 a2	8.0044 7.4685

a1: FLT3/Wild [8]; a2: FLT3/ITD [8]

2. Materials and Methods

2.1. Data set

The enzyme crystal coordinates (organism: *Homo sapiens*) were downloaded from the Protein Data Bank (PDB code: 4XUF) [12]. The **1**-**45** [11], quizartinib and sunitinib FLT3 inhibitor compounds (Table 1) were docked into the FLT3 kinase domain using the Molegro Virtual Docker (MVD) [13, 14]. MVD is a program for predicting the most likely conformation of how a ligand will bind to a macromolecule. MolDock

Scoring Function (MolDock Score) employed by the MVD program is regulated on a new hybrid search algorithm, called guided differential evolution. This algorithm combines the differential evolution optimization technique with a cavity prediction algorithm during the searching procedure, which allows fast and accurate recognition of potential binding modes, the poses. It is derived from the Piecewise Linear Potential (PLP), a simplified potential whose parameters are fit to protein-ligand structures and binding data scoring functions [13] and further extended in the GEMDOCK program (Generic Evolutionary Method for molecular DOCK) [15] with a new hydrogen bonding term and new charge schemes. The docking scoring function, E_{score}, is defined by the following energy terms:

$$E_{score} = E_{inter} + E_{intra} \text{ (Eq. 1)}$$

where the ligand-protein interaction energy, E_{inter}, is given by:

$$E_{inter} = \sum_{i \in ligand} \sum_{j \in protein} \left[E_{PLP}(r_{ij}) + 332.0 \frac{q_i q_j}{4r_{ij}^2} \right] \quad \text{(Eq. 2)}$$

The E_{PLP} term is a "piecewise linear potential" that uses two different set of parameters: one set for approximating the steric term between atoms (van der Waals), and another stronger potential for hydrogen bonds. The second term describes the electrostatic interactions between charged atoms. It is a Coulomb potential with a distance-dependent dielectric constant, D(r) = 4r. The numerical value of 332.0 fixes the units of the electrostatic energy to kilocalories per mole (Molegro ApS).

The E_{intra} terms are the internal energy of the ligand:

$$E_{intra} = \sum_{i \in ligand} \sum_{j \in ligand} E_{PLP}(r_{ij}) + \sum_{flexiblebonds} A\,[1 - \cos(m.\theta - \theta_0)] + E_{clash}$$

(Eq. 3)

The first term, double summation, is the energy between all atom pairs in the ligand excluding atom pairs which are connected by two bonds. The second term is a torsional energy term, where θ is the torsional angle of the bond. The average of the torsional energy bond contribution is used if several torsions could be determined. The last term, E_{clash}, assigns a penalty of 1000 if the distance between two heavy atoms is less than 2.0Å, punishing infeasible ligand conformations (Molegro ApS). The docking search algorithm used in MVD is based on interaction optimization techniques conducted by Darwinian Evolution Theory (evolutionary algorithms, EA). A population of individuals is exposed to competitive selection that weeds out poor solutions. Recombination and mutation are used to create new solutions [13].

2.2. Predicted model

The prediction model was constructed considering the interaction energies from MVD for the nineteen most relevant amino acid residues located at a distance of 5Å from the evaluated interaction site and the biological activity against FLT3 according to Chern et al. [11]. Subsequently, Chemoface software [16] version 1.61 was used, wherein the

training or calibration and test or validation groups were obtained from compounds **1**-**45** (Table 1).

2.3. Searching for More Potent indolin-2-one FLT3 Inhibitors

In our previous study we performed the search for new promising inhibitors of human Aurora B kinase [10]. Using the same methodology and the same one hundred compounds we are looking for promising inhibitors for human FLT3, considering the orientations of compounds inside the interaction site compared to the co-crystallized compound quizartinib. These derivatives were evaluated *in silico*, being submitted to docking studies in MVD and subsequently to application of a pre-established predictive model. The selected compounds for the predictive model were all those that presented adequate poses, comparing with redocked quizartinib. Interactions in most relevant amino acid residues occurring at a distance of 5Å from the site of enzyme interaction were considered. Searching for potential promising inhibitors for human FLT3 enzyme, besides the predictive model, the following energetic parameters of docking were considered: MolDock Score, protein-ligand interaction and hydrogen bonding.

3. Results and Discussion

Crystal coordinates of the FLT3 enzyme, quizartinib, and the crystallographic water molecules were taken from the PDB [12]. In the interaction site, quizartinib was redocked and the conformation (Fig. 2A) with the most appropriate spatial arrangement and more favorable energy parameters was selected (RMSD = 0.99Å) and applied as a reference compound for our docking studies. The analyzed site in docking studies was defined as a subset region around the center of quizartinib chemical structure in human FLT3 enzyme and the amino acid residues are shown in Fig. 2B.

The **1**-**45** and sunitinib compounds (Table 1) were docked into the FLT3 binding site using the MVD. The ligands and amino acid residues close to 5Å from the interaction site (Fig. 2B) were considered flexible during the docking simulations. Thus, a candidate solution is encoded by an array of real-valued numbers representing ligand position, conformation, and orientation as cartesian coordinates for the ligand translation, whereas there are four variables specifying the ligand orientation, and one angle for each flexible torsion angle in the ligand. MolDock Score energy values were obtained from each of the

Table 2

Interaction energy values (kcal.mol^{-1}) and regression coefficients of each amino acid residue for training group.

Comp/ aa	*Ala 642*	*Asp 698*	*Asp 829*	*Cys 694*	*Cys 695*	*Cys 828*	*Glu 661*	*Glu 692*	*Gly 697*	*Leu 616*	*Leu 818*	*Lys 644*	*Met 665*	*Phe 691*	*Phe 830*	*Tyr 693*	*Tyr 696*	*Val 624*	*Val 675*
1	-1.90	-1.91	-28.29	-12.11	-3.75	-18.82	-10.10	-4.10	-10.57	-23.07	-11.32	-1.91	4.22	-14.37	-8.25	-14.65	-4.19	-3.53	-10.21
2	-3.47	-2.52	-8.60	-11.61	-3.78	-8.46	11.60	-4.30	-9.89	-23.55	-12.07	-9.62	70.68	-12.02	-8.44	-12.14	-3.83	-5.74	-7.10
4	-2.06	-1.81	-12.19	-11.28	-8.05	-9.41	-15.47	-1.70	-9.61	-16.22	-14.06	-3.23	1.95	-4.00	-12.28	-13.12	-6.78	-5.76	-8.14
5	-3.93	-4.79	-28.56	-10.96	-3.05	-24.34	-7.84	-4.92	-11.72	-14.22	-12.61	-2.69	2.79	-14.80	-9.70	-10.11	-5.02	-5.04	-8.56
6	-3.72	-3.25	-19.77	-12.07	-2.87	-21.27	-4.86	-4.94	-9.70	-24.01	-11.81	-2.57	7.50	-12.93	-8.96	-10.96	-2.66	-5.69	-10.26
7	-3.58	-5.82	-9.43	-12.55	-3.54	-10.52	0.52	-2.20	-10.90	-17.27	-11.75	-7.18	77.63	-8.56	-7.08	-10.75	-6.27	-5.58	-4.75
8	-4.03	-5.13	-15.80	-12.87	-2.02	-23.44	-2.34	-5.47	-8.53	-20.14	-12.68	-1.61	9.50	-14.83	-8.84	-9.66	-2.13	-5.05	-7.23
9	-5.14	-2.17	-11.28	-8.87	-3.82	-6.94	3.47	-3.14	-10.13	-18.14	-9.58	-6.53	65.61	-12.54	-7.25	-11.71	-4.78	-8.17	-5.69
10	-2.30	-1.62	-12.27	-11.99	-3.68	-12.31	-9.30	-5.20	-9.17	-21.41	-11.99	-4.35	38.66	-3.53	-7.94	-12.27	-3.17	-3.58	-8.62
11	-2.39	-1.70	-13.05	-12.58	-9.24	-10.14	-16.87	-2.00	-9.45	-11.96	-14.02	-2.97	3.85	-2.70	-11.56	-15.15	-7.67	-5.44	-8.52
12	-4.28	-2.09	-12.71	-9.35	-3.91	-6.00	27.67	-3.86	-10.59	-18.13	-10.75	-6.04	9.85	-14.90	-7.70	-11.99	-4.87	-6.52	-6.58
13	-3.22	-9.77	-17.90	-10.84	-4.04	-11.92	-25.33	-3.83	-15.35	-15.56	-12.73	-4.41	15.24	-14.71	-9.85	-10.81	-7.82	-5.72	-6.56
15	-2.15	-1.80	-25.45	-12.12	-3.52	-19.77	-8.72	-5.03	-9.32	-21.43	-11.89	-1.71	3.03	-16.56	-8.81	-12.82	-3.25	-3.42	-7.48
16	-2.66	-2.27	-10.52	-12.48	-4.21	-10.40	-1.77	-3.69	-10.22	-24.67	-12.05	-6.20	54.98	-1.02	-7.62	-11.22	-4.02	-3.64	-8.03
17	-2.77	-1.01	-16.21	-14.74	-2.24	-11.91	4.70	-5.36	-5.99	-11.54	-12.08	-7.04	28.74	-8.51	-6.83	-11.67	-1.20	-5.00	-8.43
18	-2.23	-1.92	-13.13	-13.07	-3.91	-10.60	-1.06	-4.51	-10.82	-17.85	-11.47	-5.12	39.50	-7.34	-7.64	-11.77	-4.50	-3.50	-9.17
19	-3.33	-0.91	-15.54	-14.26	-2.48	-12.12	8.11	-4.44	-6.15	-12.24	-11.87	-7.22	34.52	-3.82	-6.98	-12.19	-1.25	-5.27	-7.94
20	-3.48	-5.04	-20.27	-11.13	-2.16	-12.32	44.19	-1.95	-9.89	-22.54	-10.40	-2.13	-2.50	-18.51	-11.80	-7.48	-2.21	-4.43	-7.12
21	-2.15	-1.32	-25.70	-14.60	-2.07	-18.54	-9.08	-6.09	-6.94	-17.34	-11.95	-2.47	2.22	-16.83	-7.05	-12.42	-1.64	-4.73	-9.06
23	-1.80	-1.48	-10.81	-11.82	-7.05	-11.32	-12.80	-1.94	-6.00	-19.99	-13.32	-4.11	-0.97	-3.64	-11.52	-6.08	-3.90	-6.15	-7.82
24	-3.61	-3.62	-25.94	-10.41	-3.73	-18.31	3.73	-5.12	-11.62	-15.53	-13.52	-6.86	-0.74	-17.03	-10.83	-12.29	-5.90	-3.21	-9.34
25	-1.70	-1.31	-12.20	-14.35	-1.81	-23.16	-2.52	-6.30	-4.04	-10.48	-11.75	-2.02	8.27	-13.68	-6.37	-10.84	-1.64	-5.55	-6.99
26	-2.59	-1.66	-18.36	-11.64	-3.54	-12.63	32.16	-3.09	-9.04	-13.48	-12.99	-7.69	-2.75	-19.03	-8.37	-14.20	-3.84	-3.67	-8.31
27	-3.79	-2.92	-13.91	-10.77	-4.62	-11.30	-19.02	-4.05	-12.08	-14.31	-12.35	-4.78	12.84	-14.90	-13.07	-11.54	-6.93	-6.75	-6.40
28	-4.49	-2.12	-13.80	-9.24	-3.64	-11.07	7.10	-3.21	-10.41	-18.62	-11.74	-9.56	27.49	-10.24	-8.61	-11.81	-4.27	-6.65	-7.45
29	-4.44	-1.16	-23.81	-11.81	-3.31	-11.65	2.30	-2.16	-4.03	-10.48	-12.26	-8.10	-1.23	11.81	-8.98	-11.76	-2.85	-6.58	-8.21
30	-3.46	-1.01	-17.06	-12.26	-2.70	-15.76	5.74	-1.79	-5.98	-10.60	-12.48	-3.40	50.76	-13.89	-7.20	-10.54	-2.08	-6.03	-1.60
31	-3.04	-1.25	-21.42	-10.60	-3.94	-11.96	-21.37	-4.68	-8.62	-15.67	-11.82	-4.61	-1.05	-14.40	-9.63	-16.59	-3.29	-6.16	-7.27
32	-1.88	-1.12	-16.49	-8.57	-6.61	-10.78	-7.95	-0.93	-7.19	-21.41	-10.72	-6.68	4.37	0.54	-9.77	-12.12	-4.89	-8.58	-7.27

33	-2.58	-0.85	-19.75	-12.76	-3.21	-10.32	12.68	-1.89	-6.22	-13.12	-11.82	-4.08	29.51	-12.09	-6.24	-12.57	-2.05	-6.41	-4.56
34	-1.89	-0.79	-14.09	-13.14	-2.10	-11.77	-6.60	-5.49	-5.51	-5.58	-12.82	-4.48	-4.64	-8.71	-11.04	-11.76	-1.12	-4.29	-7.49
35	-3.00	-0.67	-20.12	-13.76	-2.70	-11.78	-4.00	-4.92	-5.82	-10.84	-11.69	-6.47	-2.56	5.56	-7.77	-12.88	-1.14	-5.24	-8.90
37	-2.96	-2.01	-14.00	-11.59	-3.68	-12.27	-21.55	-3.87	-10.00	-19.56	-12.71	-3.81	21.37	-16.47	-8.23	-12.49	-4.03	-4.28	-5.11
38	-2.04	-1.24	-14.85	-14.31	-2.46	-12.11	6.84	-5.96	-5.13	-8.97	-12.32	-5.81	27.07	-12.89	-6.44	-11.51	-1.79	-4.35	-8.87
39	-2.42	-1.55	-25.07	-11.15	-9.38	-18.03	-8.01	-2.73	-0.36	-13.27	-12.19	-1.68	-2.38	-15.94	-7.62	-16.61	-6.66	-4.76	-4.90
41	-2.23	-1.22	-17.23	-14.97	-1.41	-20.78	-5.56	-6.80	-5.08	-10.34	-12.09	-2.18	4.18	-17.93	-6.69	-10.49	-1.07	-4.24	-0.69
42	-2.24	-1.51	-14.39	-10.47	-3.64	-11.66	-8.32	-5.08	-8.20	-11.91	-12.40	-4.53	-4.61	-5.64	-9.53	-11.34	-2.65	-3.94	-7.51
43	-3.53	-2.64	-19.41	-8.51	-2.35	-17.95	-11.74	-1.44	-9.49	-17.55	-10.16	-1.61	8.11	-16.42	-13.80	-6.79	-3.21	-8.19	2.66
44	-2.77	-0.98	-22.08	-12.72	-3.36	-7.88	4.48	-1.86	-6.34	-12.98	-12.08	-4.22	-1.32	-10.22	-5.81	-12.47	-2.26	-6.27	-7.50
45	-2.49	-0.95	-20.72	-11.88	-2.64	-16.45	-4.52	-3.07	-5.30	-8.81	-10.73	-1.48	-4.84	-15.70	-8.74	-10.91	-1.32	-7.52	1.07
RCs	0.045	-0.019	-0.015	-0.068	-0.033	-0.024	0.025	-0.176	-0.071	-0.036	-0.146	0.132	0.017	0.030	-0.079	-0.064	-0.071	-0.204	-0.073

RCs: Regression Coeficients

selected pose for all these evaluated compounds, including quizartinib and sunitinib, and the values are expressed in kcal.mol^{-1} (supplementary material), wherein energy values for pose-protein interaction and hydrogen bonds are also evidenced. The interaction modes of the ligand with the interaction site were determined as the highest energy scored protein–ligand complex used during docking and the conformers of each compound were mostly associated with conformations of quizartinib. Analyzing the overlapping of **1**-**45** and sunitinib compounds (Fig. 3), the distribution pattern of the selected poses for these compounds can be verified, all following the alignment for the co-crystallized quizartinib compound. Compound **1** showed more stable interaction energy (-233.25 kcal.mol^{-1}) than the other inhibitors studied, while sunitinib presented as one of the least stable (-160.94 kcal.mol^{-1}). The overlapping conformations for compounds **1** and sunitinib, compared to co-crystallized quizartinib, can be visualized in Fig. 4, both exhibiting good alignment with the reference compound, highlighting compound **1** that fills, similarly, most of the position occupied by quizartinib.

Considering **1**-**45** and sunitinib, the great majority interacted, via H bond, with Glu692 and Cys694 (-NH and carbonyl indolinone moieties, respectively), wherein the following situations were observed: thirty-eight compounds with Cys694; thirty compounds plus sunitinib with Glu692; and twenty-six compounds with both. Besides those, thirty-four compounds plus sunitinib interacted with Cys694 or Leu616 residues through an NH-pyrrolic ring. Thus, Glu692 and Cys694 residues have an important contribution for potency of these compounds, wherein indolin-2-one and pyrrolic ring groups are important subunits. In addition, H bond interactions were observed between:

i) Compounds **3**, **10**, **14**, **16**, **17**, **18**, **19**, **22**, **23**, **28**, **29**, **32**, **34**, **35**, **38**, **40**, **42**, **44** and Asp829 through pyridinone carbonyl;
ii) Other compounds also interacted with Asp829 residue through different groups: *N*-imidazolidinone (**41**, **45**); amidic carbonyl (**9**, **12**, **22**); *NH* between pyridinone and indolinone groups (**30**, **33**); and amidic carbonyl located next to the terminal benzene (**13**, **20**, **27**, **31**);
iii) Compounds **4**, **10**, **14**, **23**, **30**, **34**, **42** and Glu661 through *NH*-pyridinone;
iv) Compounds **2**, **6**, **8**, **16**, **20** with Leu616 and **4**, **11**, **31**, **39** with Tyr693 and Cys695 through *–COOH* terminal group;
v) Other compounds also interacted with Tyr693 residue through different groups: carbonyl group (**3** and sunitinib) attached to pyrrol ring; *N*-pyrrolidine (**23**); *N*-morpholine (**32**);
vi) Compounds **9**, **12** and Cys828 through amidic carbonyl between pyridinone and indolinone groups;
vii) Compounds **1**, **5**, **6**, **15**, **21**, **24**, **25**, **39**, **44** with Asp829 and **13**, **20**, **26**, **27**, **31**, **37** with Glu661 through *–NH* group located between two acyclic carbonyls.

Regarding redocked quizartinib, H bond interactions were identified through *NH*-diaryl urea (Fig. 2B), similarly observed by Zorn et al. [12], being two interactions with Glu661 (-1.65; -0.67) and another with Asp829 (-0.93) residues.

Analyzing the amino acid residues that presented the greatest energy ranges (Table 2) for the **1**-**45**, quizartinib and sunitinib compounds, Met665 and Glu661 can be

highlighted. Sunitinib showed no interaction for both residues. For Met665, the most unfavorable energy values were observed for compounds **2** (70.68) and **7** (77.63), while for Glu661 the compounds **20** (44.19) and **26** (32.16), being explained by high structural proximity of one of the terminal moieties of these compounds that generated high steric impairment levels, as well unfavorable electrostatic interactions. Observing the level of steric impairment, it can be verified that these are the two amino acid residues that generate the greatest steric impairment, of which Met665 is the largest, followed by Glu661. In contrast, by analyzing the most favorable values, **34** (-4.64) and **45** (-4.84) compounds for Met665, **13** (-25.33) and **37** (-21.55) compounds for Glu661 were registered, orienting more appropriately and reflecting directly in interaction energy values, being considerably better for Glu661 due to much less steric impairment and being a charged amino acid, thus achieving a greater number of favorable electrostatic interactions, compared to Met665, an uncharged amino acid.

Another highlighted residue was Asp829, which showed a range of energy values between -8.60 (**2**) and -28.56 (**5**), but if sunitinib were also considered, it would show the least favorable value (-2.84) among all the compounds present in Table 1. This lower value for sunitinib, but still negative and favorable, can be explained by repulsion of charges between this negatively charged amino acid and the fluorine atom, despite the low steric impairment. For compounds **2** and **5** it can be seen that compound **2** showed a considerably more unfavorable orientation than compound **5**, which generated high steric impairment and H bond absence, found for **5**.

For Phe691, the range of values varied from -20.81 (**22**) and 5.56 (**35**), which can be explained by the better overlap of the pyridinone subunit in **22**, present in both compounds, with the benzenic subunit of this aromatic amino acid, thereby generating a more favorable energy value for **22**, in contrast to compound **35**, which has been shown to be sterically hindered by this amino acid due to a torsion in the pyridinone subunit.

The total energy between each selected ligand conformation and the amino acid residues present at a distance of 5Å (those that exhibited some type of interaction: hydrogen bond, electrostatic or steric) for the training group was calculated and the results of the decomposition analysis of inhibitors and amino acid residues are shown in Table 2. These data were used to derive a multiple linear regression (MLR) fit to the experimental pIC_{50}. The model achieved a squared linear correlation coefficient (R2) of 0.82. The R2 values greater than 0.70 indicates that the model is correlated and may be considered to represent the training set in the same manner [17]. This good correlation suggests that the binding conformations of the ligands with human FLT3 are reasonable and data can be used to predict the interaction energy of other FLT3 inhibitors with similar structural pattern.

The equation coefficients from regression analysis may provide useful information: the terms with positive coefficient signs decrease the predicted potency of a compound. The same concept can be applied to terms with negative coefficient signs that increase the predicted potency. In both cases, the predicted potency values are directly proportional to the magnitude of each term coefficient of this equation. The predicted pIC_{50} values for the training were computed and are shown in the supplementary material. The standard deviation (SD) of the residual values is 0.26. To establish outlier compounds, we observed which residuals are more than twice the SD of the residual of

fit. Analyses of the data showed one outlier, compound **1**, but due to its better activity beyond all the compounds and use as a molecular pattern for searching of new promising analogues, it was considered for the predictive model.

Lys644 contributes to decrease the interaction potency of compounds and presents the highest positive regression coefficient (0.132). This positively charged amino acid is located near the terminal subunit wherein the most of the **1**-**45** compounds have a substituted benzene or pyridinone, in the case of quizartinib is next to isoxazole group, and sunitinib has no interaction. It is verified that repulsive electrostatic interactions occur with positively charged atoms in the molecules and also steric impairment. Its distance is higher when compared to other residues in interaction site and can be observed in Fig. 2A, thus generating a lower influence on interactions for the evaluated compounds. Residues that can also be pointed to with positive regression coefficient values were Phe691 (0.030), Glu661 (0.025) and Met665 (0.017), all with interaction energy values in a wide range (Table 2).

Val624 contributes to increase the interaction potency of the compounds and presents the most negative regression coefficient (-0.204). This amino acid is close to the indolin-2-one and pyrrol, except for compound **25** which has a furane, groups (**1**-**45** and sunitinib compounds) and central phenyl-benzoimidazothiazole subunit for the quizartinib compound (Fig. 2A). All these compounds exhibited favorable hydrophobic interactions with this uncharged non-polar amino acid residue and absence of highly unfavorable steric or electrostatic interactions. Two other residues that can be pointed to with negative regression coefficient values were Glu692 (-0.176) and Leu818 (-0.146).

Structurally analyzing pyridinone, imidazolidinone, and acyclic diamide of different compounds **1**-**45**, it can be verified that the pyridinone generates a greater steric impairment between the three groups, therefore being a group that can be structurally optimized, but maintaining an acyclic subunit, as in the case of the diaryl urea group in quizartinib. Furthermore the imidazolidinone was not as sterically unfavorable as the pyridinone, but the acyclic diamide or diaryl urea still seem to be the most favorable, possibly due to greater conformational freedom.

The theoretical prediction of the biological potency (pIC_{50}) for compounds **3**, **14**, **22**, **36**, **40**, which set the test group, was performed. Experimental (pIC_{50exp}) and predicted (pIC_{50pred}) potency values are shown in Table 3. The experimentally observed activity agrees with the predicted with an R2 test equal to 0.83. Considering only the test set compounds, the standard deviation (SD) of the residuals computed is 0.38. Based on this information, outliers were not found.

When compounds **1** and quizartinib are compared using interaction energy values ($kcal.mol^{-1}$) of each amino acid residue from supplementary material, the widest energy variations are shown in Asp829, Cys694, Cys695, Leu616, Phe691, Phe830, Tyr693, Tyr696, Val624 and Val675. All nineteen important amino acid residues appeared in both compounds **1** and quizartinib. When comparing compound **1** and sunitinib, since all **1**-**45** compounds can be considered structural optimizations of this one, the widest energy variations are shown in Asp829, Cys695, Cys828, Glu661, Leu616, Lys644, Met665, Phe691, Tyr696, and Val675 residues, of which amino acid residues Glu661, Lys644, and Met665 showed no interactions.

Table 3
Experimental (pIC_{50exp}) and calculated (pIC_{50pred}) potencies and residual values (pIC_{50exp} - pIC_{50pred}) for test group.

Compound	pIC_{50exp}	pIC_{50pred}	Residue
3	8.85	8.28	0.57
14	8.32	8.20	0.12
22	7.99	7.87	0.12
36	7.40	6.81	0.59
40	7.19	7.18	0.01

Through observations from docking studies, the same one hundred new indolinonic derivatives proposed by Fernandes et al. [10] were evaluated applying our current predictive model, besides the observation of related parameters (MolDock Score, Pose-Protein Interaction, and H Bond Energy). Among the one hundred indolinonic derivatives, satisfactory poses were obtained in eighty-one derivatives, and all of them showed interactions in the nineteen defined amino acid residues. Decomposition analysis, chemical structures, MolDock Score, Pose-Protein Interaction and H Bond energy values for the new proposed compounds are presented in the supplementary material. Six compounds (**IAF70**, **IAF72**, **IAF75**, **IAF80**, **IAF84** and **IAF88**) could be highlighted and considered to be more promising for future synthesis and biological evaluations against human FLT3 enzyme. These six compounds present a benzyle moiety attached in a *sp2* carbon atom located between the indolin-2-one and the pyrrolic ring, suggesting the filling of an important verified vacancy, leading to additional interactions that would considerably contribute to inhibitory activity of these compounds. It is also noted that benzyle moiety presence would be more important than phenyl moiety for these compounds, as verified for Aurora B target [10]. Furthermore, the **IAF75** compound presented the most satisfactory set of parameters among the six most promising, predictive activity (pIC_{50} = 10.24), MolDock Score (-257.27 $kcal.mol^{-1}$), Lig-Prot. (-254.38 $kcal.mol^{-1}$) and H bond (-13.95 $kcal.mol^{-1}$) which can be evidenced in Table 4. Seven H bond interactions were observed for **IAF75**: Asn701, Asp698, Asp829, Cys694, Glu692, Gly697, and Tyr693 residues. **IAF84** can also be highlighted, as it presented the highest MolDock Score values (-261.42 $kcal.mol^{-1}$) and Pose-Protein interaction (-258.18 $kcal.mol^{-1}$), in addition to considerable H bond energy (-11.16 $kcal.mol^{-1}$) for seven amino acid residues Asn701, Asp698, Asp829, Cys694, Glu692, Leu616, and Tyr693, although it did not show the highest predicted activity.

Table 4
Chemical structures, predicted pIC_{50}, MolDock Score ($kcal.mol^{-1}$), ligand-protein interaction ($kcal.mol^{-1}$) and H bond interaction ($kcal.mol^{-1}$) for more promising derivatives against FLT3.

Compound	Chemical Structure	pIC_{50} pred	MolDock Score	Pose-Prot. Interaction	H Bond Energy
IAF70	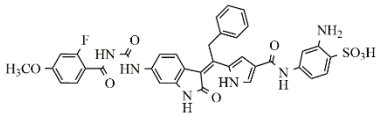	10.06	-236.96	-249.26	-9.37
IAF72	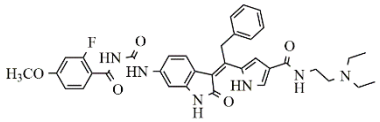	10.25	-238.17	-251.73	-6.74
IAF75	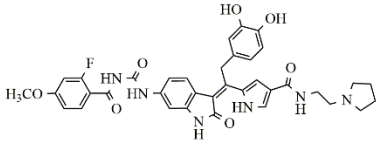	10.24	-257.27	-254.38	-13.95
IAF80	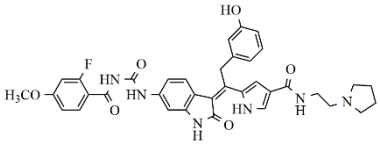	10.22	-255.22	-252.98	-11.75
IAF84	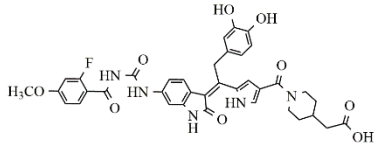	10.13	-261.42	-258.18	-11.16
IAF88	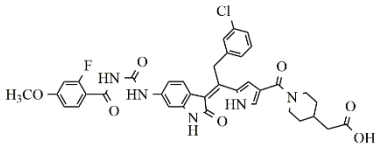	10.12	-254.29	-250.82	-8.30

Table 5
Chemical structure, predicted pIC_{50}, MolDock Score ($kcal.mol^{-1}$), ligand-protein interaction ($kcal.mol^{-1}$) and H bond interaction ($kcal.mol^{-1}$) for a promising dual Aurora B/FLT3 inhibitor.

Compound	Chemical Structure	Enzyme	pIC_{50} pred	MolDock Score	Lig-Prot. Interaction	H Bond Energy
IAF79	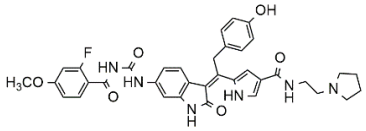	**Aurora B**	11.39 b	-236.71 b	-240.59 b	-15.61 b
		FLT3	9.83	-248.06	-246.77	-8.35

b [10]

Considering studies conducted by our research group in searching for new promising inhibitors of Aurora B kinase [10] and the current results, the **IAF79** compound (Table 5) can be considered a promising dual Aurora B/FLT3 inhibitor aiming at the treatment of different cancer types, including myeloid leukemia, presenting considerable

predicted activity and energy values for both targets studied. As shown by its chemical structure, this compound, an analogous structural variation of compound **1** (Table 1), shows an insertion of 4-ethylphenol or *p*-cresol moiety attached in the *sp2* carbon atom located between the indolin-2-one and pyrrolic groups, leading to additional and favorable interactions in both Aurora B and FLT3 therapeutic targets, being an important vacancy filled in both enzymes. Another structural difference observed was the absence of two methyl groups attached to the pyrrole ring that generate steric hindrances to the 4-ethylphenol group inserted, which could limit its conformational freedom during the interaction with the targets in question. Thus, its molecular pattern evidenced in Fig. 5 can be exploited synthetically at different positions, especially in X, Y, W and Z, and may aid in searching for new indolin-2-one derivatives with dual Aurora B/FLT3 activity that may become a drug used in the treatment of different types of cancer in the future.

4. Conclusion

We carried out molecular docking studies in order to understand the interactions of a variety of indolin-2-one derivatives with the human FLT3 enzyme. The different substituent groups were exploited at 3 and 6 positions of the indolinone ring and are shown in Table 1. Docked structures were evaluated based on binding energy, electrostatic and hydrogen bonding interactions. Our molecular docking results, combined with experimental data for the human FLT3 enzyme inhibition, suggest the presence of important empty space around the indolin-2-one moiety. Thus, more favorable substituents attached at the 3-position of the pyrrolic ring and in the *sp2* carbon atom located between the indolin-2-one and pyrrolic ring groups may increase affinity for the human FLT3 enzyme, that was verified to be of similar form to the Aurora B kinase by Fernandes et al. [10], using the same benzyle moiety. For new **IAF1**-**IAF100**, six of them could be detached (**IAF70**, **IAF72**, **IAF75**, **IAF80**, **IAF84** and **IAF88**), which have a benzyle group attached in the *sp2* carbon atom located between the indolin-2-one and pyrrolic ring groups, highlighting **IAF75** compound presenting the most satisfactory set of parameters, and **IAF84** that presented the highest values of MolDock Score and Pose-Protein interaction. Moreover there is the addition of considerable H bond energy to seven different amino acid residues.

The present study together with studies by Fernandes et al. [10] on this class of indolinone compounds seem to be promising for future obtainment of a possible candidate for an innovative drug for treatment of different cancer types, including myeloid leukemia, since some compounds, highlighting **IAF79**, exhibited possible promising dual predicted activity against Aurora B/FLT3 and a promising molecular pattern that can be further investigated synthetically in the search for new anticancer drug candidates, corroborating with these studies carried out.

Acknowledgements

The authors thank the Brazilian agencies “Conselho Nacional de Desenvolvimento Científico e Tecnológico” (CNPq) and “Coordenação de Aperfeiçoamento de Pessoal de Nível Superior” (CAPES) for their financial supports.

Conflict of Interest

The authors declare no conflict of interest, financial or otherwise.

References

[1] R. Berenstein, Class III Receptor Tyrosine Kinases in Acute Leukemia – Biological Functions and Modern Laboratory Analysis, Biomarker Insights 10 (2015) 1-14, https://doi.org/10.4137/BMI.S22433.

[2] S. Kayser, R.F. Schlenk, M.C. Londono, F. Breitenbuecher, K. Wittke, J. Du, S. Groner, D. Späth, J. Krauter, A. Ganser, H. Döhner, T. Fischer, K. Döhner, Insertion of FLT3 internal tandem duplication in the tyrosine kinase domain-1 is associated with resistance to chemotherapy and inferior outcome, Blood 114 (2009) 2386-2392, https://doi.org/10.1182/blood-2009-03-209999.

[3] M. Port, M. Böttcher, F. Thol, A. Ganser, R. Schlenk, J. Wasem, A. Neumann, L. Pouryamout, Prognostic significance of FLT3 internal tandem duplication, nucleophosmin 1, and CEBPA gene mutations for acute myeloid leukemia patients with normal karyotype and younger than 60 years: a systematic review and meta-analysis, Ann. Hematol. 93 (2014) 1279-1286, https://doi.org/10.1007/s00277-014-2072-6.

[4] D. Pastore, FLT3 inhibitors in acute myeloid leukemia, DCTH 4 (2016) 14-21, http://www.emaferesi.it/wp-content/uploads/2016/10/PDF_WEB_DTCH_1_2016.pdf .

[5] V. Bavetsias, S. Crumpler, C. Sun, S. Avery, B. Atrash, A. Faisal, A.S. Moore, M. Kosmopoulou, N. Brown, P.W. Sheldrake, K. Bush, A. Henley, G. Box, M. Valenti, B.A. de Haven, F.I. Raynaud, P. Workman, S.A. Eccles, R. Bayliss, S. Linardopoulos, J. Blagg, Optimization of Imidazo [4,5-b]pyridine-Based Kinase Inhibitors: Identification of a Dual FLT3/Aurora Kinase Inhibitor as an Orally Bioavailable Preclinical Development Candidate for the Treatment of Acute Myeloid Leukemia, J. Med. Chem. 55 (2012) 8721-8734, http://doi.org/10.1021/jm300952s.

[6] A.S. Moore, A. Faisal, G.D. de Castro, V. Bavetsias, C. Sun, B. Atrash, M. Valenti, B.A. de Haven, S. Avery, D. Mair, F. Mirabella, J. Swansbury, A.D. Pearson, P. Workman, J. Blagg, F.I. Raynaud, S.A. Eccles, S. Linardopoulos, Selective FLT3 inhibition of FLT3-ITD+ acute myeloid leukaemia resulting in secondary D835Y mutation: a model for emerging clinical resistance patterns, Leukemia 26 (2012) 1462-1470, http://doi.org/10.1038/leu.2012.52.

[7] F. Ma, P. Liu, M. Lei, J. Liu, H. Wang, S. Zhao, L. Hu, Design, synthesis and biological evaluation of indolin-2-one-based derivatives as potent, selective and efficacious inhibitors of FMS-like tyrosine kinase3 (FLT3), Eur. J. Med. Chem. 127 (2017) 72-86, http://doi.org/10.1016/j.ejmech.2016.12.038.

[8] P.P. Zarrinkar, R.N. Gunawardane, M.D. Cramer, M.F. Gardner, D. Brigham, B. Belli, M.W. Karaman, K.W. Pratz, G. Pallares, Q. Chao, K.G. Sprankle, H.K. Patel, M. Levis, R.C. Armstrong, J. James, S.S. Bhagwat, AC220 is a uniquely potent and selective inhibitor of FLT3 for the treatment of acute myeloid leukemia (AML), Blood 114 (2009) 2984-2992, http://doi.org/10.1182/blood-2009-05-222034.

[9] B. Nguyen, A.B. Williams, D.J. Young, H. Ma, L. Li, M. Levis, P. Brown, D. Small, FLT3 activating mutations display differential sensitivity to multiple tyrosine kinase inhibitors, Oncotarget, 8 (2017) 10931-10944, http://doi.org/10.18632/oncotarget.14539.

[10] I.A. Fernandes, T. Assis, I. Rosa, E. Cunha, E, Indolin-2-one Derivatives: Theoretical Studies Aimed at Finding More Potent Aurora B Kinase Inhibitors, Lett. Drug Des. Discov. 15 (2018), http://doi.org/10.2174/1570180815666180528090945.

[11] J.W. Chern, A.D. Jagtap, H.C. Wang, G.S. Chen, Indolin-2-one Derivatives as Protein Kinase Inhibitors. U.S. Patent 2013/158373 A1, October 24, 2013.

[12] Zorn, J.A., Wang, Q., Fujimura, E., Barros, T., Kuriyan, J., 2015. Crystal structure of the FLT3 kinase domain bound to the inhibitor Quizartinib (AC220). PLoS One. 10, e0121177. http://doi.org/10.1371/journal.pone.0121177.

[13] D.K. Gehlhaar, G.M. Verkhivker, P.A. Rejto, C.J. Sherman, D.R. Fogel, L.J. Fogel, S.T. Freer, Molecular Recognition of the Inhibitor AG-1343 by HIV-1 Protease: Conformationally Flexible Docking by Evolutionary Programming, Chem. Biol. 2 (1995) 317-324, https://doi.org/10.1016/1074-5521(95)90050-0.

[14] R. Thomsen, M.H. Christensen, MolDock: A New Technique for High-Accuracy Molecular Docking, J. Med. Chem. 49 (2006) 3315-3321, http://doi.org/10.1021/jm051197e.

[15] J.M. Yang, C.C. Chen. GEMDOCK: A Generic Evolutionary Method for Molecular Docking, Proteins. 55 (2004) 288-304, http://doi.org/ 10.1002/prot.20035.

[16] C.A. Nunes, M.P. Freitas, A.C.M. Pinheiro, S.C. Bastos. Chemoface: a novel free user-friendly interface for chemometrics, J. Braz. Chem. Soc. 23 (2012) 2003-2010, http://dx.doi.org/10.1590/S0103-50532012005000073.

[17] A.J. Hopfinger, S. Wang, J.S. Tokarski, B. Jin, M. Albuquerque, P.J. Madhav, C. Duraiswami, Construction of 3D-QSAR Models Using the 4D-QSAR Analysis Formalism, J. Am. Chem. Soc. 119 (1997) 10509-10524, http://doi.org/ 10.1021/ja9718937.

Theoretical studies aimed at finding FLT3 inhibitors and a promising compound and molecular pattern with dual Aurora B/FLT3 activity

Ítalo Antônio Fernandes[a]; Déborah Braga Resende[b]; Teodorico de Castro Ramalho[a]; Elaine Fontes Ferreira da Cunha[a*]

[a]Federal University of Lavras, Department of Chemistry, P.O. Box 3037, ZIP code 37200-000, Lavras-MG. italofernad@hotmail.com; teo@dqi.ufla.br; elaineffdacunha@gmail.com

[b]Federal University of Lavras, Department of Veterinary Medicine, P.O. Box 3037, ZIP code 37200-000, Lavras-MG. deborahbrr@gmail.com

*Corresponding author

elaineffdacunha@gmail.com

Elaine Fontes Ferreira da Cunha

Dept. of Chemistry (DQI)

UFLA - Federal University of Lavras

Campus Universitário, Caixa Postal 3037

Lavras – MG. 37200-000

Phone: + 55 35 38295129

Fig. 1. Chemical structures of Sunitinib, Quizartinib, Sorafenib, Midostaurin and Lestaurtinib.

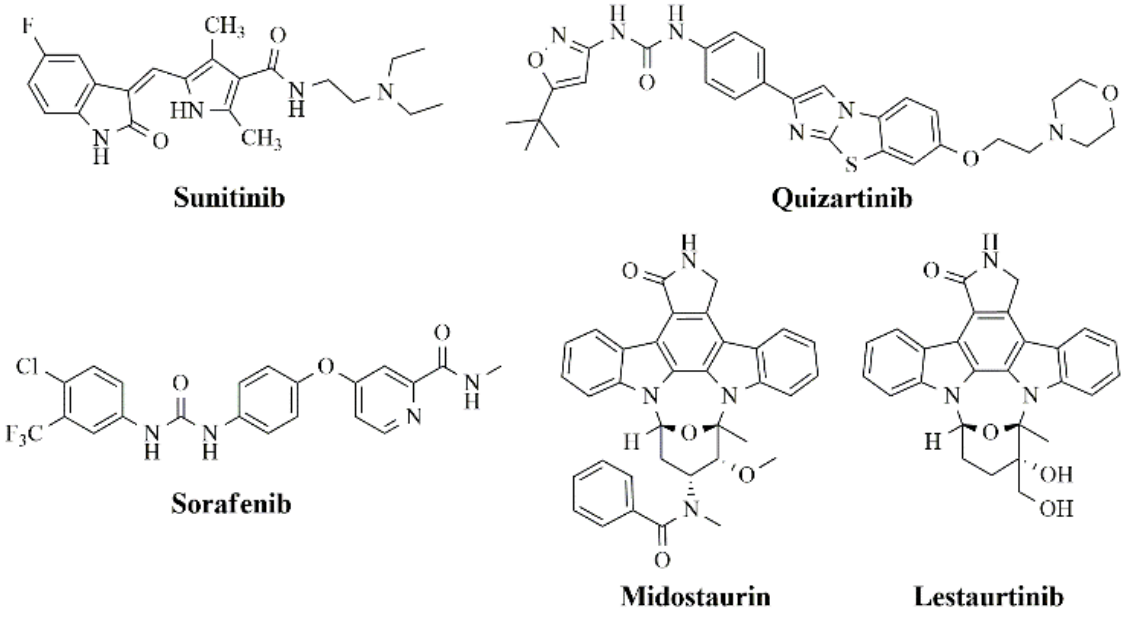

Fig. 2. Quizartinib into FLT3 interaction site. (**A**) Structure with yellow carbon atoms is the redocked quizartinib. (**B**) Hydrogen bonds evidenced for redocked quizartinib and amino acid residues located at a distance of 5Å.

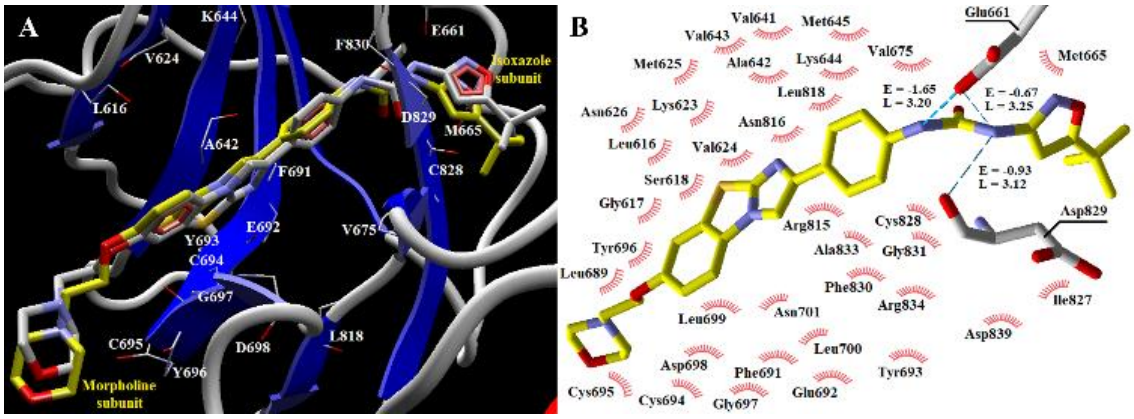

Fig. 3. Overlapped conformations of FLT3 inhibitors. Quizartinib is shown in yellow, and Sunitinib in purple.

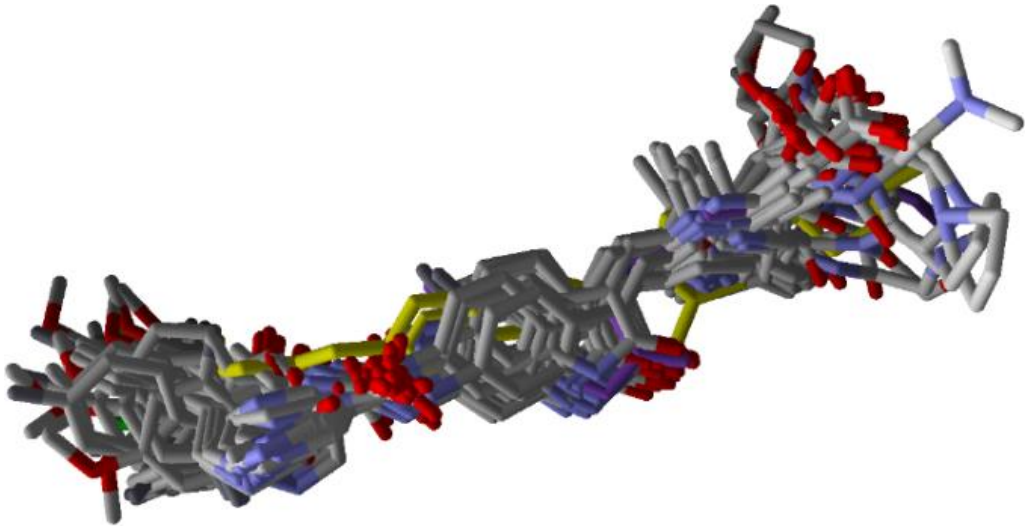

Fig. 4. Overlapped conformations of compounds: **1**, Quizartinib (yellow), and Sunitinib (purple).

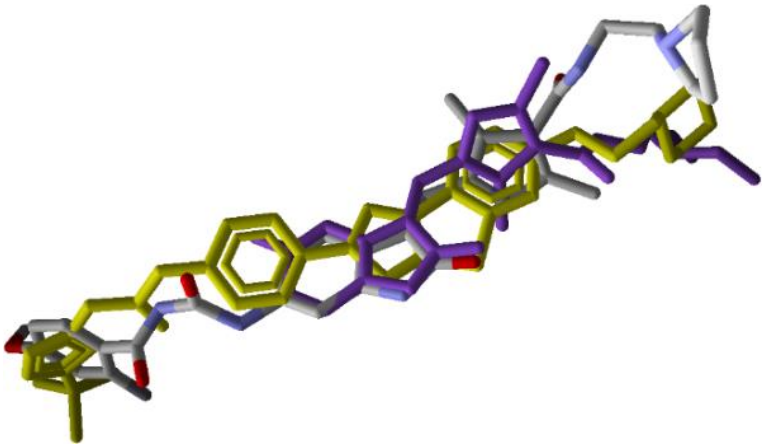

Fig. 5. Promising indolin-2-one molecular pattern to dual Aurora B/FLT3 activity.

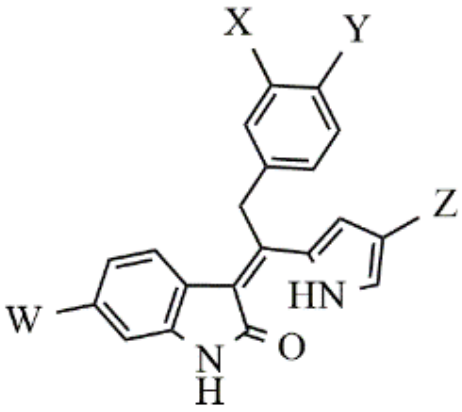

Theoretical studies aimed at finding FLT3 inhibitors and a promising compound and molecular pattern with dual Aurora B/FLT3 activity

Ítalo Antônio Fernandes[a]; Déborah Braga Resende[b]; Teodorico de Castro Ramalho[a]; Elaine Fontes Ferreira da Cunha[a*]

[a]Federal University of Lavras, Department of Chemistry, P.O. Box 3037, ZIP code 37200-000, Lavras-MG.
italofernad@hotmail.com; teo@dqi.ufla.br; elaineffdacunha@gmail.com

[b]Federal University of Lavras, Department of Veterinary Medicine, P.O. Box 3037, ZIP code 37200-000, Lavras-MG.
deborahbrr@gmail.com

SUPPLEMENTARY MATERIAL 1

MolDock Score, Rerank Score, Pose-Protein Interaction and H Bond energy values from each selected pose for **1-45**, Quizartinib, and Sunitinib compounds.

Compound	MolDock Score	Rerank Score	Pose-Protein Interaction	H Bond
1	-233.252	-182.465	-227.406	-7.274
2	-195.050	-166.924	-210.154	-5.678
3	-197.543	-162.841	-214.397	-6.742
4	-191.449	-136.830	-193.104	-10.123
5	-219.849	-184.435	-230.886	-6.491
6	-212.152	-175.088	-213.269	-9.546
7	-193.816	-159.317	-208.211	-4.882
8	-213.570	-171.751	-210.209	-8.513
9	-183.240	-158.294	-198.502	-4.705
10	-189.425	-119.396	-201.969	-4.879
11	-186.691	-125.637	-190.609	-10.482
12	-168.072	-137.521	-176.849	-9.540
13	-209.733	-174.497	-222.323	-4.986
14	-186.233	-134.548	-189.394	-5.775
15	-207.046	-164.561	-204.653	-9.026
16	-189.760	-135.853	-197.143	-7.793
17	-169.391	-140.976	-182.240	-7.786
18	-182.291	-133.341	-186.034	-3.354
19	-172.109	-139.140	-184.718	-7.110
20	-199.836	-166.128	-200.421	-5.895
21	-188.491	-154.188	-194.903	-9.045
22	-190.338	-164.517	-216.916	-4.791
23	-190.770	-116.834	-190.710	-8.307
24	-197.488	-160.606	-199.473	-9.381
25	-176.999	-143.114	-184.734	-3.865
26	-201.528	-163.944	-201.077	-5.251
27	-196.919	-158.127	-199.873	-4.806
28	-186.160	-164.744	-206.209	-2.874
29	-169.537	-145.653	-185.638	-2.471
30	-163.475	-141.236	-183.672	-4.298
31	-187.748	-149.773	-192.222	-10.722
32	-172.635	-131.196	-187.467	-6.771
33	-160.725	-135.099	-173.663	-3.303
34	-183.749	-134.630	-186.908	-7.718
35	-172.892	-132.504	-185.770	-6.962
36	-197.878	-161.967	-198.980	-3.458
37	-193.929	-158.383	-198.781	-7.160
38	-164.314	-129.142	-175.389	-4.418
39	-189.736	-137.183	-185.379	-9.090
40	-156.672	-130.662	-165.637	-7.204
41	-185.941	-146.981	-184.351	-7.105
42	-165.834	-102.511	-173.414	-6.100
43	-192.181	-161.437	-202.810	-2.398
44	-158.329	-123.751	-176.726	-4.152
45	-167.181	-136.765	-170.554	-3.526
Quizartinib	-204.591	-169.283	-212.101	-1.303
Sunitinib	-160.944	-127.131	-167.380	-1.398

Theoretical studies aimed at finding FLT3 inhibitors and a promising compound and molecular pattern with dual Aurora B/FLT3 activity

Ítalo Antônio Fernandes[a]; Déborah Braga Resende[b]; Teodorico de Castro Ramalho[a]; Elaine Fontes Ferreira da Cunha[a*]

[a]Federal University of Lavras, Department of Chemistry, P.O. Box 3037, ZIP code 37200-000, Lavras-MG.
italofernad@hotmail.com; teo@dqi.ufla.br; elaineffdacunha@gmail.com

[b]Federal University of Lavras, Department of Veterinary Medicine, P.O. Box 3037, ZIP code 37200-000, Lavras-MG.
deborahbrr@gmail.com

SUPPLEMENTARY MATERIAL 2

Measured and predicted pIC_{50}, and residual values for the training compounds.

Compound	Measured	Predicted	Residue
1	9.30	8.50	0.80
2	8.89	8.78	0.11
4	8.80	8.45	0.35
5	8.62	8.58	0.04
6	8.57	8.83	-0.26
7	8.57	8.43	0.14
8	8.57	8.55	0.01
9	8.54	8.21	0.33
10	8.54	8.47	0.07
11	8.46	8.64	-0.18
12	8.38	8.02	0.36
13	8.36	8.22	0.14
15	8.21	8.17	0.04
16	8.14	8.62	-0.48
17	8.12	7.76	0.36
18	8.09	8.38	-0.29
19	8.07	7.92	0.15
20	8.00	8.21	-0.21
21	8.00	8.11	-0.11
23	7.94	7.54	0.39
24	7.91	8.16	-0.26
25	7.81	7.84	-0.03
26	7.79	7.60	0.19
27	7.79	8.20	-0.41
28	7.61	7.75	-0.14
29	7.60	7.40	0.20
30	7.56	7.54	0.02
31	7.50	7.61	-0.11
32	7.46	7.72	-0.26
33	7.43	7.67	-0.25
34	7.42	7.12	0.30
35	7.42	7.54	-0.12
37	7.34	7.38	-0.03
38	7.32	7.70	-0.38
39	7.27	7.36	-0.10
41	7.13	7.01	0.12
42	7.06	7.21	-0.15
43	6.94	6.97	-0.03
44	6.83	7.14	-0.31
45	6.65	6.66	-0.01

Theoretical studies aimed at finding FLT3 inhibitors and a promising compound and molecular pattern with dual Aurora B/FLT3 activity

Ítalo Antônio Fernandes[a]; Déborah Braga Resende[b]; Teodorico de Castro Ramalho[a]; Elaine Fontes Ferreira da Cunha[a*]
[a]Federal University of Lavras, Department of Chemistry, P.O. Box 3037, ZIP code 37200-000, Lavras-MG.
italofernad@hotmail.com; teo@dqi.ufla.br; elaineffdacunha@gmail.com
[b]Federal University of Lavras, Department of Veterinary Medicine, P.O. Box 3037, ZIP code 37200-000, Lavras-MG. deborahbrr@gmail.com

SUPPLEMENTARY MATERIAL 3

Interaction energy values (kcal.mol^{-1}) of each amino acid residue for **1**-**45**, Quizartinib, and Sunitinib compounds.

Cpd/aa	*Ala642*	*Asp698*	*Asp829*	*Cys694*	*Cys695*	*Cys828*	*Glu661*	*Glu692*	*Gly697*	*Leu616*	*Leu818*	*Lys644*	*Met665*	*Phe691*	*Phe830*	*Tyr693*	*Tyr696*	*Val624*	*Val675*
1	-1.90	-1.91	-28.29	-12.11	-3.75	-18.82	-10.10	-4.10	-10.57	-23.07	-11.32	-1.91	4.22	-14.37	-8.25	-14.65	-4.19	-3.53	-10.21
2	-3.47	-2.52	-8.60	-11.61	-3.78	-8.46	11.60	-4.30	-9.89	-23.55	-12.07	-9.62	70.68	-12.02	-8.44	-12.14	-3.83	-5.74	-7.10
3	-3.18	-2.03	-14.63	-10.25	-8.59	-8.33	-21.14	-1.75	-10.32	-21.16	-13.13	-1.05	27.99	-12.19	-9.04	-13.02	-10.30	-4.48	-4.60
4	-2.06	-1.81	-12.19	-11.28	-8.05	-9.41	-15.47	-1.70	-9.61	-16.22	-14.06	-3.23	1.95	-4.00	-12.28	-13.12	-6.78	-5.76	-8.14
5	-3.93	-4.79	-28.56	-10.96	-3.05	-24.34	-7.84	-4.92	-11.72	-14.22	-12.61	-2.69	2.79	-14.80	-9.70	-10.11	-5.02	-5.04	-8.56
6	-3.72	-3.25	-19.77	-12.07	-2.87	-21.27	-4.86	-4.94	-9.70	-24.01	-11.81	-2.57	7.50	-12.93	-8.96	-10.96	-2.66	-5.69	-10.26
7	-3.58	-5.82	-9.43	-12.55	-3.54	-10.52	0.52	-2.20	-10.90	-17.27	-11.75	-7.18	77.63	-8.56	-7.08	-10.75	-6.27	-5.58	-4.75
8	-4.03	-5.13	-15.80	-12.87	-2.02	-23.44	-2.34	-5.47	-8.53	-20.14	-12.68	-1.61	9.50	-14.83	-8.84	-9.66	-2.13	-5.05	-7.23
9	-5.14	-2.17	-11.28	-8.87	-3.82	-6.94	3.47	-3.14	-10.13	-18.14	-9.58	-6.53	65.61	-12.54	-7.25	-11.71	-4.78	-8.17	-5.69
10	-2.30	-1.62	-12.27	-11.99	-3.68	-12.31	-9.30	-5.20	-9.17	-21.41	-11.99	-4.35	38.66	-3.53	-7.94	-12.27	-3.17	-3.58	-8.62
11	-2.39	-1.70	-13.05	-12.58	-9.24	-10.14	-16.87	-2.00	-9.45	-11.96	-14.02	-2.97	3.85	-2.70	-11.56	-15.15	-7.67	-5.44	-8.52
12	-4.28	-2.09	-12.71	-9.35	-3.91	-6.00	27.67	-3.86	-10.59	-18.13	-10.75	-6.04	9.85	-14.90	-7.70	-11.99	-4.87	-6.52	-6.58
13	-3.22	-9.77	-17.90	-10.84	-4.04	-11.92	-25.33	-3.83	-15.35	-15.56	-12.73	-4.41	15.24	-14.71	-9.85	-10.81	-7.82	-5.72	-6.56
14	-1.79	-1.59	-13.55	-10.83	-6.14	-11.91	-8.55	-2.41	-9.81	-15.30	-13.45	-5.53	-4.10	-2.98	-10.12	-15.00	-6.59	-5.87	-7.99
15	-2.15	-1.80	-25.45	-12.12	-3.52	-19.77	-8.72	-5.03	-9.32	-21.43	-11.89	-1.71	3.03	-16.56	-8.81	-12.82	-3.25	-3.42	-7.48
16	-2.66	-2.27	-10.52	-12.48	-4.21	-10.40	-1.77	-3.69	-10.22	-24.67	-12.05	-6.20	54.98	-1.02	-7.62	-11.22	-4.02	-3.64	-8.03
17	-2.77	-1.01	-16.21	-14.74	-2.24	-11.91	4.70	-5.36	-5.99	-11.54	-12.08	-7.04	28.74	-8.51	-6.83	-11.67	-1.20	-5.00	-8.43
18	-2.23	-1.92	-13.13	-13.07	-3.91	-10.60	-1.06	-4.51	-10.82	-17.85	-11.47	-5.12	39.50	-7.34	-7.64	-11.77	-4.50	-3.50	-9.17
19	-3.33	-0.91	-15.54	-14.26	-2.48	-12.12	8.11	-4.44	-6.15	-12.24	-11.87	-7.22	34.52	-3.82	-6.98	-12.19	-1.25	-5.27	-7.94
20	-3.48	-5.04	-20.27	-11.13	-2.16	-12.32	44.19	-1.95	-9.89	-22.54	-10.40	-2.13	-2.50	-18.51	-11.80	-7.48	-2.21	-4.43	-7.12
21	-2.15	-1.32	-25.70	-14.60	-2.07	-18.54	-9.08	-6.09	-6.94	-17.34	-11.95	-2.47	2.22	-16.83	-7.05	-12.42	-1.64	-4.73	-9.06
22	-2.94	-1.97	-12.01	-12.66	-6.93	-11.42	-17.81	-4.69	-14.44	-16.58	-10.88	-0.31	33.24	-20.81	-8.59	-11.82	-14.06	-2.89	5.41
23	-1.80	-1.48	-10.81	-11.82	-7.05	-11.32	-12.80	-1.94	-6.00	-19.99	-13.32	-4.11	-0.97	-3.64	-11.52	-6.08	-3.90	-6.15	-7.82
24	-3.61	-3.62	-25.94	-10.41	-3.73	-18.31	3.73	-5.12	-11.62	-15.53	-13.52	-6.86	-0.74	-17.03	-10.83	-12.29	-5.90	-3.21	-9.34
25	-1.70	-1.31	-12.20	-14.35	-1.81	-23.16	-2.52	-6.30	-4.04	-10.48	-11.75	-2.02	8.27	-13.68	-6.37	-10.84	-1.64	-5.55	-6.99
26	-2.59	-1.66	-18.36	-11.64	-3.54	-12.63	32.16	-3.09	-9.04	-13.48	-12.99	-7.69	-2.75	-19.03	-8.37	-14.20	-3.84	-3.67	-8.31
27	-3.79	-2.92	-13.91	-10.77	-4.62	-11.30	-19.02	-4.05	-12.08	-14.31	-12.35	-4.78	12.84	-14.90	-13.07	-11.54	-6.93	-6.75	-6.40
28	-4.49	-2.12	-13.80	-9.24	-3.64	-11.07	7.10	-3.21	-10.41	-18.62	-11.74	-9.56	27.49	-10.24	-8.61	-11.81	-4.27	-6.65	-7.45
29	-4.44	-1.16	-23.81	-11.81	-3.31	-11.65	2.30	-2.16	-4.03	-10.48	-12.26	-8.10	-1.23	11.81	-8.98	-11.76	-2.85	-6.58	-8.21
30	-3.46	-1.01	-17.06	-12.26	-2.70	-15.76	5.74	-1.79	-5.98	-10.60	-12.48	-3.40	50.76	-13.89	-7.20	-10.54	-2.08	-6.03	-1.60
31	-3.04	-1.25	-21.42	-10.60	-3.94	-11.96	-21.37	-4.68	-8.62	-15.67	-11.82	-4.61	-1.05	-14.40	-9.63	-16.59	-3.29	-6.16	-7.27
32	-1.88	-1.12	-16.49	-8.57	-6.61	-10.78	-7.95	-0.93	-7.19	-21.41	-10.72	-6.68	4.37	0.54	-9.77	-12.12	-4.89	-8.58	-7.27
33	-2.58	-0.85	-19.75	-12.76	-3.21	-10.32	12.68	-1.89	-6.22	-13.12	-11.82	-4.08	29.51	-12.09	-6.24	-12.57	-2.05	-6.41	-4.56
34	-1.89	-0.79	-14.09	-13.14	-2.10	-11.77	-6.60	-5.49	-5.51	-5.58	-12.82	-4.48	-4.64	-8.71	-11.04	-11.76	-1.12	-4.29	-7.49
35	-3.00	-0.67	-20.12	-13.76	-2.70	-11.78	-4.00	-4.92	-5.82	-10.84	-11.69	-6.47	-2.56	5.56	-7.77	-12.88	-1.14	-5.24	-8.90

36	-3.59	-2.33	-17.04	-10.53	-4.09	-15.48	-15.18	-1.60	-10.97	-18.08	-11.57	-1.90	6.44	-16.41	-8.20	-9.10	-5.18	-7.44	4.76
37	-2.96	-2.01	-14.00	-11.59	-3.68	-12.27	-21.55	-3.87	-10.00	-19.56	-12.71	-3.81	21.37	-16.47	-8.23	-12.49	-4.03	-4.28	-5.11
38	-2.04	-1.24	-14.85	-14.31	-2.46	-12.11	6.84	-5.96	-5.13	-8.97	-12.32	-5.81	27.07	-12.89	-6.44	-11.51	-1.79	-4.35	-8.87
39	-2.42	-1.55	-25.07	-11.15	-9.38	-18.03	-8.01	-2.73	-0.36	-13.27	-12.19	-1.68	-2.38	-15.94	-7.62	-16.61	-6.66	-4.76	-4.90
40	-2.07	-1.14	-14.32	-14.53	-1.87	-11.28	10.54	-5.39	-5.15	-8.90	-12.44	-7.02	2.20	-10.78	-7.14	-10.95	-1.30	-4.78	-8.37
41	-2.23	-1.22	-17.23	-14.97	-1.41	-20.78	-5.56	-6.80	-5.08	-10.34	-12.09	-2.18	4.18	-17.93	-6.69	-10.49	-1.07	-4.24	-0.69
42	-2.24	-1.51	-14.39	-10.47	-3.64	-11.66	-8.32	-5.08	-8.20	-11.91	-12.40	-4.53	-4.61	-5.64	-9.53	-11.34	-2.65	-3.94	-7.51
43	-3.53	-2.64	-19.41	-8.51	-2.35	-17.95	-11.74	-1.44	-9.49	-17.55	-10.16	-1.61	8.11	-16.42	-13.80	-6.79	-3.21	-8.19	2.66
44	-2.77	-0.98	-22.08	-12.72	-3.36	-7.88	4.48	-1.86	-6.34	-12.98	-12.08	-4.22	-1.32	-10.22	-5.81	-12.47	-2.26	-6.27	-7.50
45	-2.49	-0.95	-20.72	-11.88	-2.64	-16.45	-4.52	-3.07	-5.30	-8.81	-10.73	-1.48	-4.84	-15.70	-8.74	-10.91	-1.32	-7.52	1.07
Quizartinib	-4.48	-1.55	-18.63	-8.59	-7.63	-19.56	-11.13	-1.64	-10.93	-15.17	-9.37	-4.92	2.19	-9.99	-12.34	-10.03	-13.10	-7.47	-6.01
Sunitinib	-2.11	-1.65	-2.84	-10.80	-8.63	-0.98	–	-3.42	-9.61	-19.49	-12.80	–	–	-4.01	-10.82	-16.27	-19.13	-5.61	-3.63

Theoretical studies aimed at finding FLT3 inhibitors and a promising compound and molecular pattern with dual Aurora B/FLT3 activity

Ítalo Antônio Fernandes[a]; Déborah Braga Resende[b]; Teodorico de Castro Ramalho[a]; Elaine Fontes Ferreira da Cunha[a*]

[a]Federal University of Lavras, Department of Chemistry, P.O. Box 3037, ZIP code 37200-000, Lavras-MG.
italofernad@hotmail.com; teo@dqi.ufla.br; elaineffdacunha@gmail.com
[b]Federal University of Lavras, Department of Veterinary Medicine, P.O. Box 3037, ZIP code 37200-000, Lavras-MG.
deborahbrr@gmail.com

SUPPLEMENTARY MATERIAL 4

Chemical structures for compounds **IAF1-IAF100**.

IAF1 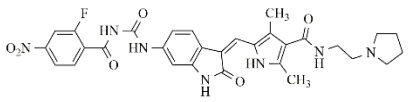	**IAF2** 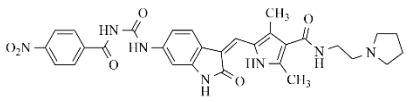	**IAF3** 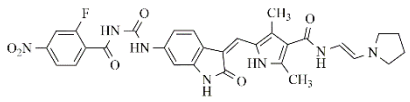
IAF4 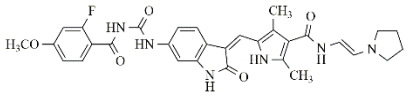	**IAF5** 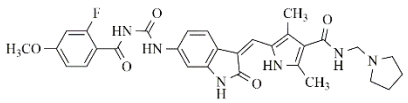	**IAF6** 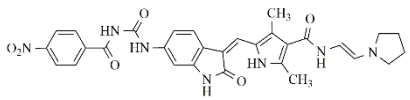
IAF7 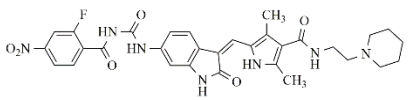	**IAF8** 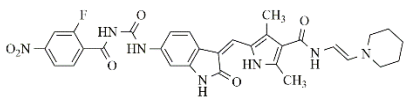	**IAF9** 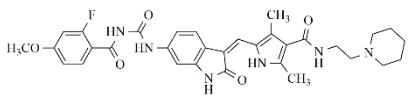
IAF10 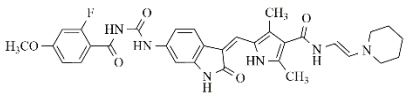	**IAF11** 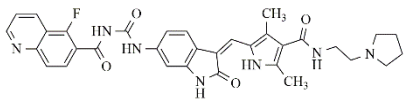	**IAF12** 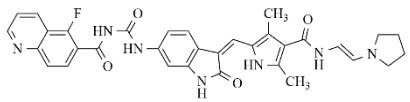
IAF13 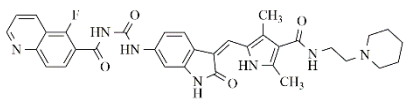	**IAF14** 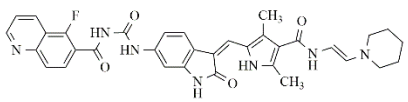	**IAF15** 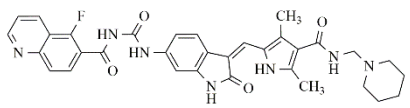
IAF16 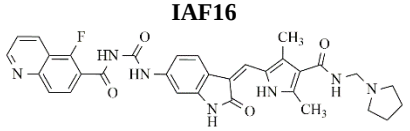	**IAF17** 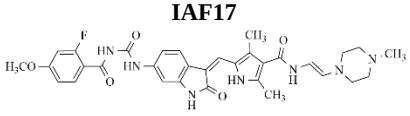	**IAF18** 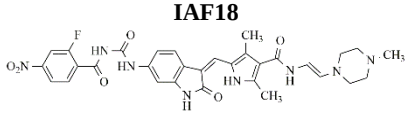
IAF19 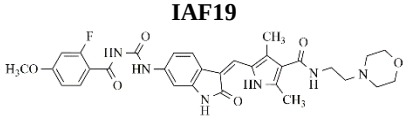	**IAF20** 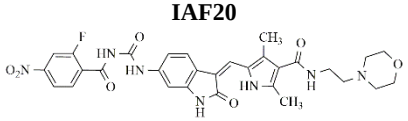	**IAF21** 
IAF22 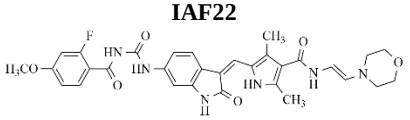	**IAF23** 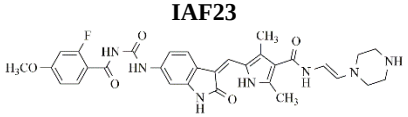	**IAF24** 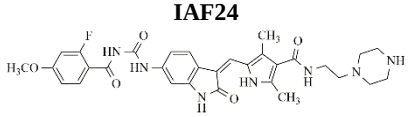
IAF25 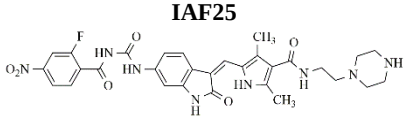	**IAF26** 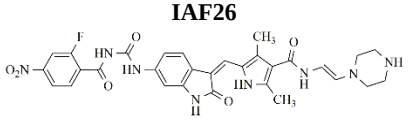	**IAF27** 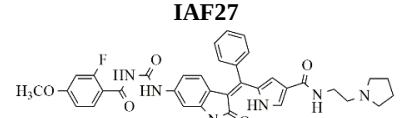
IAF28 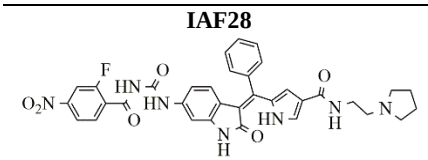	**IAF29** 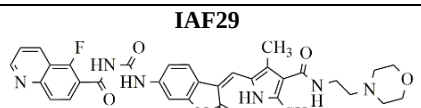	**IAF30** 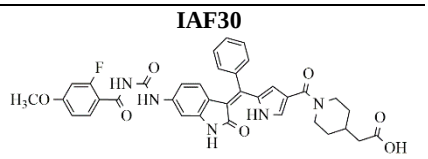

IAF31 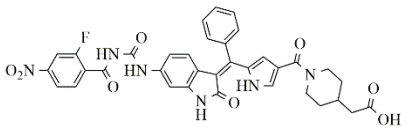	**IAF32** 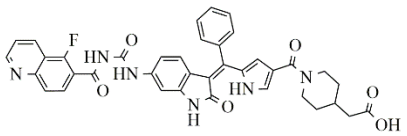	**IAF33** 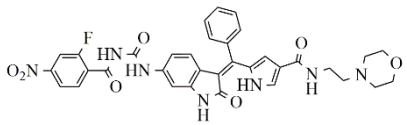
IAF34 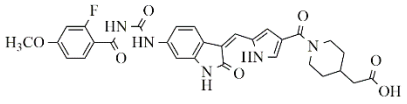	**IAF35** 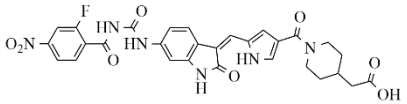	**IAF36** 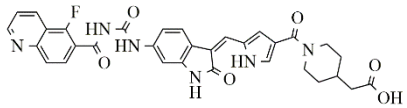
IAF37 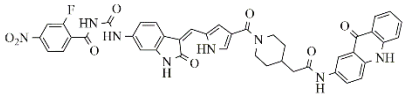	**IAF38** 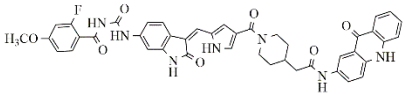	**IAF39** 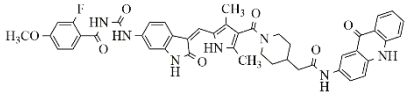
IAF40 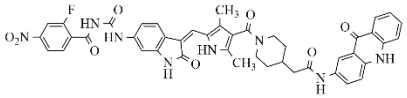	**IAF41** 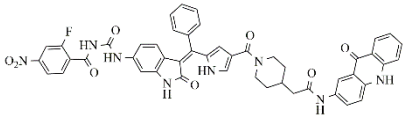	**IAF42** 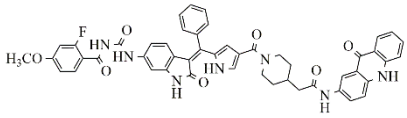
IAF43 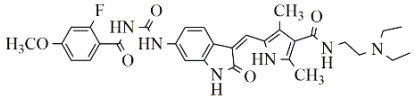	**IAF44** 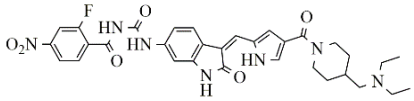	**IAF45** 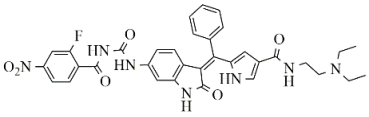
IAF46 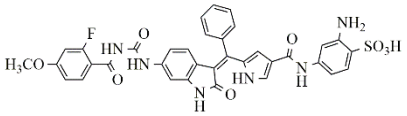	**IAF47** 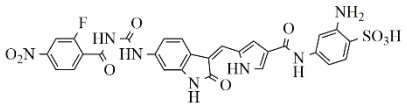	**IAF48** 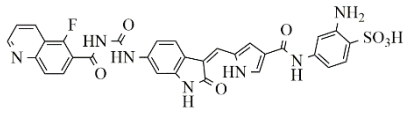
IAF49 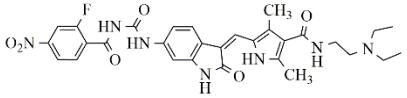	**IAF50** 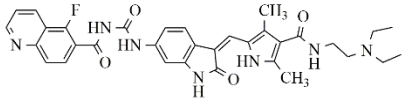	**IAF51** 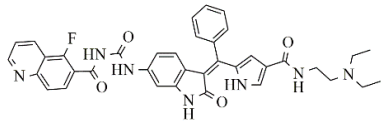
IAF52 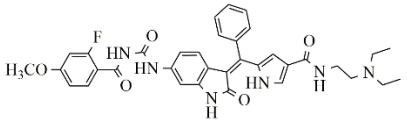	**IAF53** 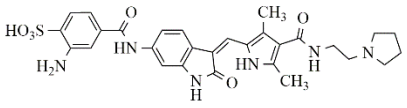	**IAF54** 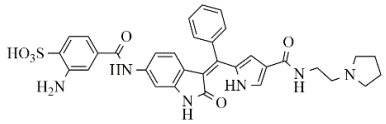
IAF55 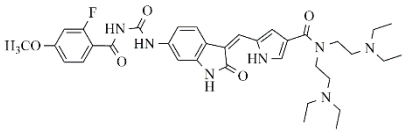	**IAF56** 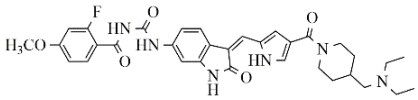	**IAF57** 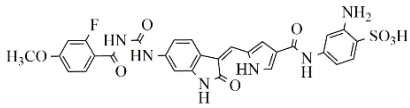
IAF58 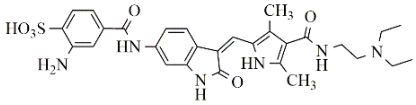	**IAF59** 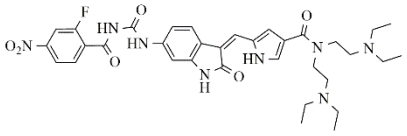	**IAF60** 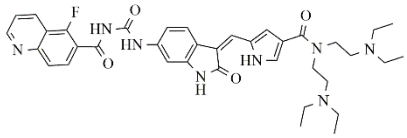
IAF61 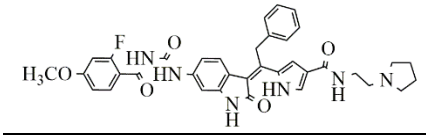	**IAF62** 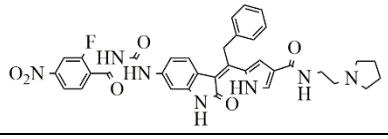	**IAF63** 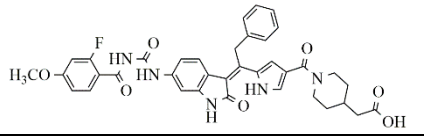
IAF64 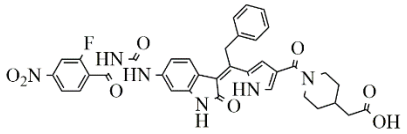	**IAF65** 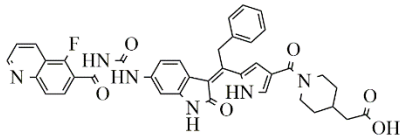	**IAF66** 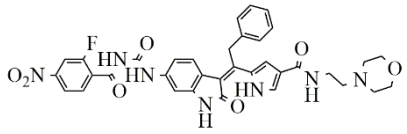

IAF67 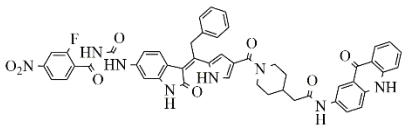	**IAF68** 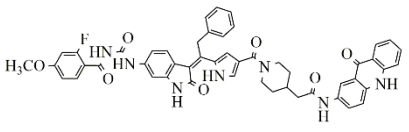	**IAF69** 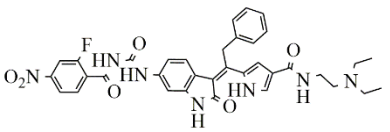
IAF70 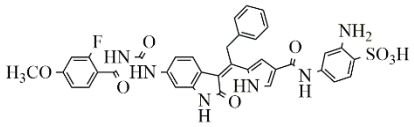	**IAF71** 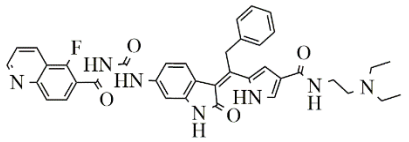	**IAF72** 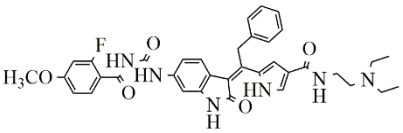
IAF73 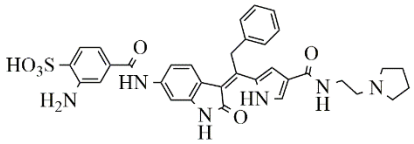	**IAF74** 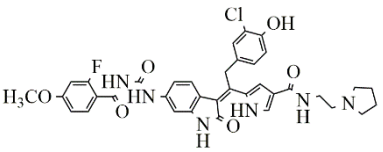	**IAF75** 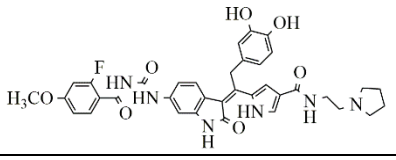
IAF76 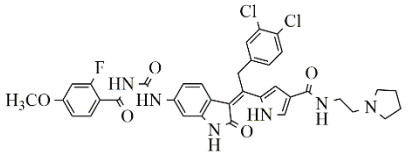	**IAF77** 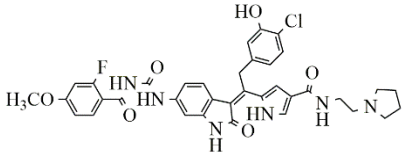	**IAF78** 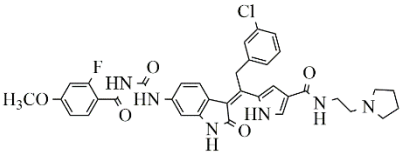
IAF79 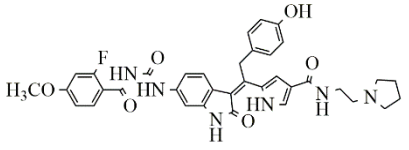	**IAF80** 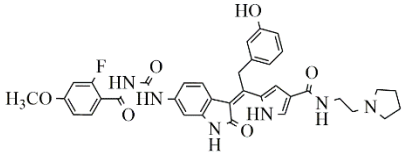	**IAF81** 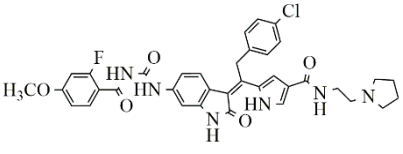
IAF82 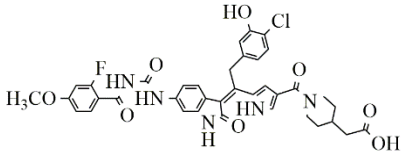	**IAF83** 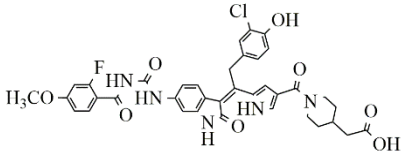	**IAF84** 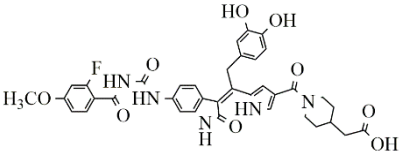
IAF85 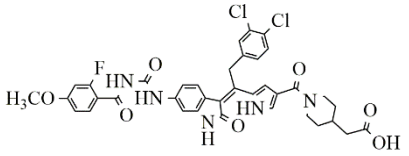	**IAF86** 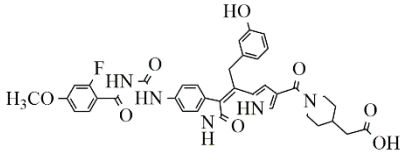	**IAF87** 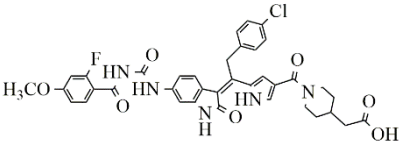
IAF88 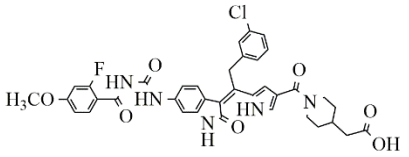	**IAF89** 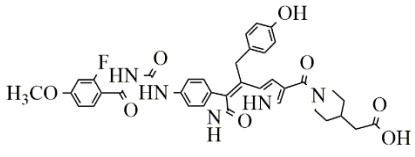	**IAF90** 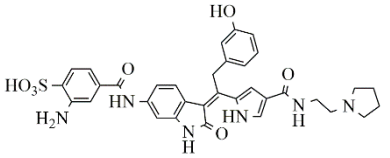
IAF91 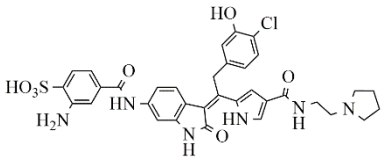	**IAF92** 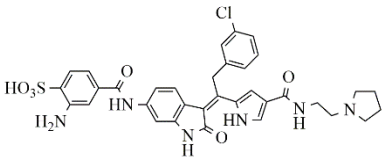	**IAF93** 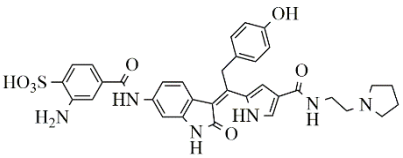
IAF94 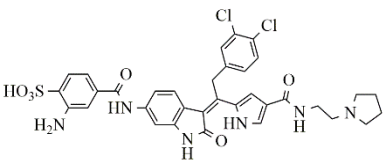	**IAF95** 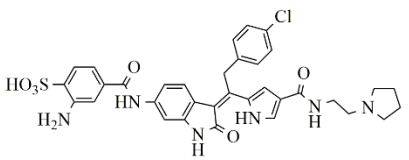	**IAF96** 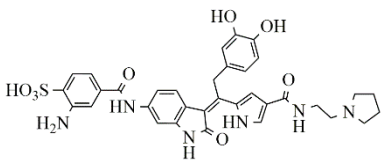

IAF97	IAF98	IAF99
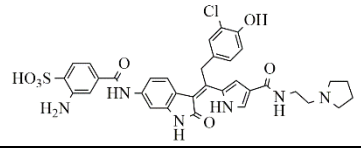	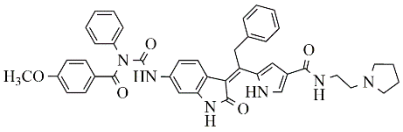	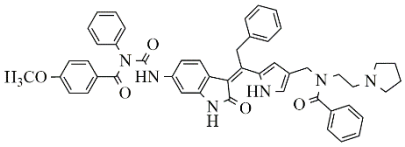

IAF100
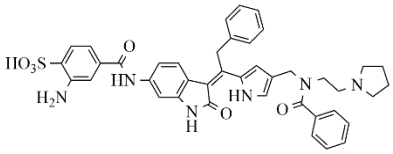

Theoretical studies aimed at finding FLT3 inhibitors and a promising compound and molecular pattern with dual Aurora B/FLT3 activity

Ítalo Antônio Fernandes[a]; Déborah Braga Resende[b]; Teodorico de Castro Ramalho[a]; Elaine Fontes Ferreira da Cunha[a*]

[a]Federal University of Lavras, Department of Chemistry, P.O. Box 3037, ZIP code 37200-000, Lavras-MG.
italofernad@hotmail.com; teo@dqi.ufla.br; elaineffdacunha@gmail.com

[b]Federal University of Lavras, Department of Veterinary Medicine, P.O. Box 3037, ZIP code 37200-000, Lavras-MG.
deborahbrr@gmail.com

SUPPLEMENTARY MATERIAL 5

MolDock Score, Rerank Score, Pose-Protein Interaction and H Bond energy values from each selected pose for compounds **IAF1-IAF100**.

Compound	MolDock Score	Rerank Score	Pose-Protein Interaction	H Bond Energy	Compound	MolDock Score	Rerank Score	Pose-Protein Interaction	H Bond Energy
IAF1	-218.71	-173.49	-228.28	-7.13	**IAF51**	-247.74	-197.72	-261.97	-7.96
IAF2	-227.41	-175.37	-226.68	-9.85	**IAF52**	-245.12	-194.27	-251.53	-6.85
IAF3	-226.77	-176.24	-223.40	-10.57	**IAF53**	-200.88	-149.71	-201.48	-7.27
IAF4	Pose not found				**IAF54**	Pose not found			
IAF5	-224.13	-173.28	-227.92	-7.33	**IAF55**	-227.88	-176.46	-230.46	-3.77
IAF6	-224.51	-177.83	-224.32	-9.44	**IAF56**	-215.21	-169.85	-229.46	-9.38
IAF7	-225.68	-185.62	-237.49	-10.95	**IAF57**	Pose not found			
IAF8	-226.08	-180.68	-232.02	-7.68	**IAF58**	-213.85	-167.47	-212.57	-7.18
IAF9	-214.47	-175.46	-225.32	-9.29	**IAF59**	-240.93	-193.60	-250.41	-7.36
IAF10	-217.41	-168.90	-224.71	-6.94	**IAF60**	-224.88	-184.53	-245.51	-5.49
IAF11	-217.76	-154.35	-227.71	-7.83	**IAF61**	-256.73	-194.61	-251.79	-10.54
IAF12	-231.60	-165.80	-234.06	-6.93	**IAF62**	-243.74	-159.94	-251.16	-4.03
IAF13	-233.87	-195.25	-251.31	-7.25	**IAF63**	-234.43	-157.50	-236.33	-5.98
IAF14	-221.89	-176.79	-238.93	-8.66	**IAF64**	-257.53	-201.03	-255.61	-6.56
IAF15	-217.02	-172.14	-231.46	-8.96	**IAF65**	-252.33	-194.88	-256.60	-8.45
IAF16	-221.80	-167.02	-230.00	-8.42	**IAF66**	Pose not found			
IAF17	-218.35	-170.45	-228.41	-7.26	**IAF67**	Pose not found			
IAF18	-217.21	-171.04	-222.94	-8.44	**IAF68**	Pose not found			
IAF19	-228.72	-190.09	-236.84	-6.83	**IAF69**	-234.87	-186.06	-251.50	-6.02
IAF20	-216.89	-166.12	-225.11	-7.69	**IAF70**	-236.96	-185.89	-249.26	-9.37
IAF21	-211.77	-158.14	-214.00	-5.97	**IAF71**	-244.66	-195.16	-256.71	-7.05
IAF22	-225.97	-180.38	-229.21	-9.03	**IAF72**	-238.17	-185.80	-251.73	-6.74
IAF23	-211.82	-166.97	-217.89	-7.16	**IAF73**	-219.36	-146.91	-231.75	-5.07
IAF24	-214.07	-157.78	-224.18	-6.28	**IAF74**	-243.56	-182.06	-243.35	-8.68
IAF25	-220.97	-170.55	-226.99	-7.11	**IAF75**	-257.27	-198.80	-254.38	-13.95
IAF26	-219.34	-170.79	-223.60	-3.42	**IAF76**	Pose not found			
IAF27	-238.36	-156.17	-244.37	-5.80	**IAF77**	-254.07	-193.16	-251.86	-7.89
IAF28	-253.32	-199.53	-255.47	-8.76	**IAF78**	-260.30	-189.16	-259.46	-4.99
IAF29	-233.30	-193.01	-246.36	-6.42	**IAF79**	-248.06	-192.85	-246.77	-8.35
IAF30	-255.64	-204.63	-258.28	-8.81	**IAF80**	-255.22	-194.42	-252.98	-11.75
IAF31	Pose not found				**IAF81**	-247.09	-194.20	-250.05	-10.01
IAF32	-239.04	-195.25	-263.71	-8.36	**IAF82**	-256.38	-191.53	-254.24	-10.89
IAF33	-230.34	-182.63	-256.41	-6.36	**IAF83**	-248.20	-174.04	-247.24	-8.34
IAF34	-208.54	-175.11	-224.91	-7.89	**IAF84**	-261.42	-194.15	-258.18	-11.16
IAF35	-217.99	-182.05	-232.77	-6.48	**IAF85**	Pose not found			
IAF36	-222.64	-188.03	-237.97	-7.69	**IAF86**	-260.19	-195.53	-255.07	-13.84
IAF37	Pose not found				**IAF87**	-238.91	-180.67	-238.61	-9.21
IAF38	Pose not found				**IAF88**	-254.29	-189.42	-250.82	-8.30
IAF39	Pose not found				**IAF89**	-237.51	-177.53	-234.88	-7.49
IAF40	Pose not found				**IAF90**	-225.09	-144.77	-236.59	-11.28
IAF41	Pose not found				**IAF91**	-239.52	-163.82	-245.80	-10.12
IAF42	Pose not found				**IAF92**	Pose not found			
IAF43	-233.85	-182.79	-234.72	-6.23	**IAF93**	-228.94	-182.35	-237.18	-8.83
IAF44	-222.12	-171.37	-228.99	-6.76	**IAF94**	-238.16	-182.91	-247.35	-4.97
IAF45	-236.67	-187.35	-252.04	-8.77	**IAF95**	-229.41	-161.10	-237.58	-7.04
IAF46	-255.93	-194.46	-254.41	-10.38	**IAF96**	-239.55	-158.95	-250.30	-12.49
IAF47	-207.95	-175.99	-223.11	-6.93	**IAF97**	Pose not found			
IAF48	-226.91	-184.16	-238.29	-15.22	**IAF98**	Pose not found			
IAF49	-228.67	-165.50	-227.00	-6.39	**IAF99**	Pose not found			
IAF50	-239.99	-197.19	-253.77	-8.15	**IAF100**	-236.74	-167.83	-236.07	-5.79

Theoretical studies aimed at finding FLT3 inhibitors and a promising compound and molecular pattern with dual Aurora B/FLT3 activity

Ítalo Antônio Fernandes[a]; Déborah Braga Resende[b]; Teodorico de Castro Ramalho[a]; Elaine Fontes Ferreira da Cunha[a*]
[a]Federal University of Lavras, Department of Chemistry, P.O. Box 3037, ZIP code 37200-000, Lavras-MG.
italofernad@hotmail.com; teo@dqi.ufla.br; elaineffdacunha@gmail.com
[b]Federal University of Lavras, Department of Veterinary Medicine, P.O. Box 3037, ZIP code 37200-000, Lavras-MG. deborahbrr@gmail.com

SUPPLEMENTARY MATERIAL 6

Interaction energy values (kcal.mol^{-1}) of each amino acid residue for compounds **IAF1-IAF100** with found poses.

Cpd/aa	*Ala642*	*Asp698*	*Asp829*	*Cys694*	*Cys695*	*Cys828*	*Glu661*	*Glu692*	*Gly697*	*Leu616*	*Leu818*	*Lys644*	*Met665*	*Phe691*	*Phe830*	*Tyr693*	*Tyr696*	*Val624*	*Val675*
IAF1	-2.02	-1.85	-27.20	-11.76	-2.89	-21.07	-5.91	-5.84	-9.41	-27.89	-12.79	-1.55	5.94	-17.68	-9.14	-11.28	-2.90	-4.36	-6.30
IAF2	-1.41	-1.85	-23.53	-8.69	-8.10	-19.73	-6.13	-2.33	-9.68	-18.95	-11.98	-1.67	2.81	-14.64	-8.67	-14.44	-16.97	-6.61	-7.29
IAF3	-0.92	-1.98	-29.83	-7.32	-8.74	-18.45	-10.14	-1.81	-9.83	-19.68	-12.31	-2.36	1.16	-14.16	-10.69	-12.57	-16.48	-7.12	-9.08
IAF5	-1.26	-1.89	-16.01	-12.26	-3.34	-24.22	-3.74	-6.00	-9.67	-24.87	-12.04	-1.39	9.61	-17.08	-7.34	-13.03	-4.00	-4.89	-8.11
IAF6	-1.21	-2.10	-25.64	-6.62	-9.37	-18.48	-6.85	-1.66	-11.27	-20.42	-12.59	-1.76	3.60	-14.51	-10.87	-11.55	-16.66	-6.93	-8.39
IAF7	-2.74	-1.50	-24.71	-12.51	-2.61	-21.86	-5.95	-6.39	-8.54	-24.53	-12.24	-1.44	5.87	-17.30	-8.51	-13.15	-2.12	-5.05	-5.62
IAF8	-1.76	-1.83	-21.47	-12.57	-10.92	-23.02	-5.36	-2.30	-7.38	-21.31	-12.34	-1.62	7.10	-15.18	-9.49	-6.39	-8.09	-6.86	-8.72
IAF9	-3.33	-3.09	-29.04	-12.15	-7.34	-18.41	-12.02	-5.64	-14.41	-16.73	-12.40	-2.92	2.08	-12.94	-9.14	-13.47	-15.82	-5.03	-9.55
IAF10	-2.21	-1.62	-17.22	-14.67	-12.83	-22.66	-3.58	-4.15	-6.16	-19.02	-12.73	-1.23	5.66	-17.72	-7.64	-6.54	-7.67	-6.03	-3.38
IAF11	-0.88	-1.62	-19.13	-14.66	-7.47	-23.93	-2.86	-4.59	-8.61	-19.08	-12.44	-0.73	6.52	-16.83	-6.33	-12.86	-8.04	-5.48	4.79
IAF12	-0.49	-1.98	-19.91	-7.92	-8.59	-22.76	-3.70	-2.17	-10.07	-19.31	-11.85	-1.25	5.27	-17.55	-8.35	-12.95	-15.25	-6.81	-6.34
IAF13	-3.09	-5.20	-18.63	-12.52	-5.66	-24.92	-3.27	-6.45	-13.76	-16.27	-12.26	-1.96	7.84	-14.53	-8.14	-12.48	-11.78	-5.12	-7.19
IAF14	-1.92	-1.41	-19.17	-12.52	-2.79	-24.04	-3.36	-6.26	-7.51	-26.81	-11.76	-0.81	8.22	-18.46	-7.13	-11.52	-2.81	-5.54	-2.89
IAF15	-1.40	-1.96	-24.95	-11.38	-5.93	-23.08	-5.78	-1.70	-4.94	-21.98	-12.27	-2.13	5.02	-14.69	-11.01	-9.35	-6.00	-7.38	-10.25
IAF16	-0.93	-1.60	-20.59	-11.60	-7.05	-24.67	-4.46	-2.13	-6.08	-21.11	-11.03	-2.52	6.17	-14.48	-9.18	-12.39	-6.79	-8.07	-8.02
IAF17	-1.86	-1.33	-15.62	-12.96	-2.83	-24.40	-3.32	-6.23	-7.72	-23.08	-11.65	-0.87	9.73	-18.02	-7.08	-11.75	-2.82	-5.69	-4.25
IAF18	-1.17	-2.23	-27.82	-8.04	-8.38	-20.51	-5.61	-1.04	-7.05	-18.51	-11.66	-2.38	4.54	-15.06	-12.09	-10.71	-15.75	-8.19	-9.12
IAF19	-4.48	-3.19	-17.34	-11.35	-6.48	-23.39	-3.89	-6.20	-14.13	-18.56	-11.80	-2.42	8.29	-13.12	-8.12	-12.48	-11.56	-5.80	-8.50
IAF20	-1.19	-1.98	-19.06	-8.23	-5.29	-23.37	-4.85	-1.94	-10.71	-19.62	-11.68	-1.54	5.75	-15.35	-9.07	-13.21	-19.62	-6.90	-6.59
IAF21	-1.23	-1.88	-25.97	-11.08	-14.27	-19.67	-6.51	-1.88	-7.32	-20.91	-12.81	-1.60	3.95	-14.56	-10.03	-1.73	-7.30	-6.38	-7.82
IAF22	-1.67	-1.99	-22.85	-8.78	-9.51	-21.48	-6.41	-1.58	-8.66	-19.68	-12.06	-1.70	7.29	-13.42	-9.69	-13.31	-17.11	-6.92	-7.42
IAF23	-1.57	-2.15	-22.97	-9.26	-9.27	-21.92	-3.70	-0.84	-8.01	-19.51	-11.34	-2.63	8.98	-14.09	-12.30	-3.92	-6.68	-8.17	-8.73
IAF24	-1.20	-2.06	-16.37	-6.28	-5.15	-23.58	-3.60	-1.59	-11.21	-19.74	-11.80	-1.28	8.03	-16.83	-9.63	-12.24	-17.24	-7.38	-5.32
IAF25	-1.32	-2.11	-16.64	-7.53	-6.10	-23.52	-3.90	-1.14	-10.50	-19.63	-10.95	-1.48	7.67	-15.28	-9.20	-11.55	-16.64	-7.94	-4.06
IAF26	-2.14	-2.20	-17.54	-8.12	-9.99	-22.71	-3.36	-0.75	-10.28	-19.08	-10.50	-2.32	6.49	-13.66	-10.71	-4.23	-9.52	-6.57	-3.55
IAF27	-5.48	-2.38	-16.65	-8.68	-2.37	-22.02	-4.20	-3.83	-7.11	-21.76	-11.50	-2.56	5.14	-10.96	6.94	-14.51	-1.66	-10.99	-3.33
IAF28	-3.24	-2.82	-16.79	-12.42	-4.28	-22.82	-3.98	-6.28	-6.38	-26.49	-12.48	-1.93	7.04	-16.18	7.30	-19.20	-2.35	-10.01	-6.07
IAF29	-2.98	-4.01	-19.62	-12.93	-2.27	-24.67	-2.47	-5.95	-9.68	-26.32	-12.23	-1.63	7.05	-13.41	-8.74	-10.42	-2.82	-4.88	-5.07
IAF30	-4.68	-1.88	-25.49	-13.62	-3.15	-20.04	-8.91	-4.41	-4.47	-28.73	-11.75	-1.89	5.26	-13.07	-1.71	-16.61	-2.09	-10.33	-10.29
IAF32	-5.43	-2.82	-16.61	-10.61	-4.74	-23.18	-0.80	-3.19	-7.76	-35.06	-11.76	-6.48	7.01	-9.46	2.00	-16.98	-2.81	-12.29	-6.48
IAF33	-3.61	-1.51	-17.61	-4.87	-8.57	-22.98	-3.14	-0.74	-9.46	-26.36	-8.93	-4.14	4.83	-9.26	0.72	-12.20	-7.03	-12.79	2.25
IAF34	-4.21	-3.09	-17.53	-14.13	-6.48	-22.97	-3.37	-4.05	-11.90	-13.08	-13.02	-1.59	7.59	-14.17	-9.87	-9.93	-11.78	-4.87	-6.60
IAF35	-4.56	-1.76	-17.21	-10.91	-6.48	-23.99	-4.22	-2.92	-9.97	-16.52	-12.25	-1.71	8.56	-12.89	-9.40	-11.27	-13.53	-5.98	-5.89
IAF36	-4.54	-1.35	-18.68	-12.22	-6.59	-24.39	-3.73	-2.39	-7.60	-20.69	-10.37	-1.57	5.12	-14.62	-9.19	-12.85	-15.42	-7.37	-2.65
IAF43	-4.27	-8.34	-16.53	-12.27	-2.05	-23.13	-2.76	-6.17	-8.68	-15.14	-12.07	-2.27	8.99	-13.89	-8.77	-10.77	-6.53	-5.71	-6.18
IAF44	-3.59	-1.38	-19.96	-14.28	-1.98	-22.77	-5.08	-6.29	2.09	-17.01	-12.34	-2.78	6.23	-12.79	-7.05	-15.85	-1.83	-5.74	-5.16

IAF45	-4.20	-2.47	-20.93	-10.81	-5.13	-21.64	-5.61	-5.85	-6.85	-20.68	-12.44	-2.35	4.93	-14.85	2.99	-17.38	-2.75	-10.47	-8.61
IAF46	-3.77	-6.10	-17.73	-6.25	-0.32	-21.35	-4.31	-0.92	-11.07	-14.45	-10.26	-2.63	3.89	-10.37	1.58	-3.09	-5.03	-12.14	-2.31
IAF47	-3.89	-9.79	-17.36	-6.58	-0.72	-23.80	-4.38	-1.63	-8.56	-10.78	-12.32	-1.80	6.49	-10.57	-11.85	-3.69	-7.78	-6.74	-3.36
IAF48	-3.36	-11.35	-25.93	-6.83	-0.31	-24.10	-5.34	-1.73	-4.52	-9.20	-12.21	-1.67	5.50	-13.58	-13.81	-3.37	-4.85	-6.54	-10.59
IAF49	-1.13	-2.05	-17.75	-11.13	-10.52	-22.84	-3.52	-1.89	-7.71	-20.45	-12.20	-1.44	4.98	-16.88	-9.73	-2.84	-6.50	-6.90	-2.98
IAF50	-2.91	-7.04	-22.57	-11.28	-2.25	-23.98	-4.78	-6.26	-15.54	-19.64	-11.20	-2.26	8.14	-14.04	-8.86	-10.06	-4.11	-5.64	-9.59
IAF51	-4.85	-2.81	-17.95	-10.58	-8.35	-24.03	-1.61	-6.23	-9.64	-22.35	-12.32	-2.68	6.89	-13.76	8.08	-18.63	-11.59	-10.30	-7.92
IAF52	-3.87	-1.35	-19.42	-10.38	-6.18	-21.76	-4.81	-1.07	-6.88	-25.00	-10.68	-2.38	2.80	-11.35	-2.70	-8.14	-8.06	-12.31	-1.91
IAF53	-3.05	-1.29	-15.56	-14.31	-3.79	-9.59	-4.65	-2.79	-8.64	-23.66	-10.89	-3.35	39.01	-18.27	-7.53	-11.24	-2.80	-3.50	-5.69
IAF55	-2.93	-7.64	-22.08	-6.98	-4.36	-24.12	-5.22	-1.75	-15.52	-17.99	-11.09	-1.78	2.67	-14.60	-10.20	-9.68	-15.83	-6.53	-1.41
IAF56	-1.85	-6.72	-27.84	-14.13	-3.25	-20.37	-9.81	-5.66	-10.96	-13.47	-11.85	-2.56	3.63	-16.98	-7.53	-13.17	-6.82	-4.20	-10.11
IAF58	-3.23	-1.12	-16.08	-9.23	-0.67	-11.35	-6.52	-1.92	-6.35	-24.59	-11.88	-2.77	12.65	-13.54	-15.27	-6.40	-0.42	-5.96	-8.08
IAF59	-2.08	-1.38	-16.47	-15.58	-6.23	-23.73	-3.24	-7.01	-10.70	-28.32	-10.84	-1.60	9.07	-16.48	-6.12	-14.34	-7.78	-5.48	-4.96
IAF60	-4.17	-9.55	-29.10	-12.90	-0.82	-23.47	-2.91	-2.68	-11.30	-24.89	-11.96	-3.03	2.39	-18.02	-8.73	-9.88	-2.56	-4.36	-7.38
IAF61	-2.94	-2.50	-26.20	-11.49	-3.54	-21.08	-7.60	-1.94	-8.46	-23.44	-12.55	-1.74	3.41	-13.53	2.87	-11.47	-6.05	-8.31	-7.64
IAF62	0.33	-3.82	-18.63	-12.10	-4.91	-22.62	-3.98	-4.40	-10.23	-13.79	-12.17	-1.98	5.80	-16.86	-3.65	-13.62	-8.12	-6.78	-7.57
IAF63	-4.93	-11.08	-17.97	-12.87	-3.48	-22.36	-4.09	-6.34	-12.89	-4.21	-11.35	-2.28	6.67	-15.21	-5.01	-13.15	-7.68	-8.72	-6.94
IAF64	-2.24	-7.53	-17.50	-12.27	-2.85	-22.69	-4.75	-5.26	-7.84	-24.10	-13.28	-1.67	5.68	-12.19	-12.16	-17.11	-2.75	-5.49	-5.59
IAF65	-3.04	-8.35	-22.13	-12.52	-3.42	-22.79	-4.81	-6.09	-7.95	-23.69	-14.28	-2.01	4.46	-15.41	-11.83	-18.02	-2.72	-5.18	-8.89
IAF69	-3.38	-8.21	-17.83	-11.56	-2.28	-22.65	-4.22	-5.34	-11.92	-16.04	-12.33	-2.77	7.36	-9.94	-12.99	-12.23	-7.07	-7.12	-9.10
IAF70	-2.69	-6.70	-16.39	-14.12	-2.81	-22.96	-1.66	-6.17	-8.48	-21.76	-14.69	-2.37	9.13	-13.54	-8.91	-16.60	-1.70	-6.43	-9.76
IAF71	-2.95	-7.33	-20.83	-14.62	-2.58	-24.63	-1.17	-5.52	-7.63	-29.11	-15.31	-3.10	9.26	-13.23	-4.85	-14.67	-1.69	-6.27	-11.61
IAF72	-3.92	-8.71	-20.07	-14.40	-3.09	-23.04	-5.87	-6.35	-13.11	-8.81	-13.15	-1.97	7.33	-15.89	-13.48	-13.00	-7.69	-6.58	-9.93
IAF73	-4.85	-11.49	-6.63	-12.98	-3.70	-15.12	-4.57	-5.76	-17.37	-7.16	-13.16	-1.50	7.07	-17.73	-7.78	-11.39	-8.06	-7.23	-7.10
IAF74	-2.36	-9.12	-18.19	-13.03	-3.00	-24.09	-4.44	-6.12	-8.92	-25.45	-14.53	-2.01	7.62	-15.26	-10.92	-17.51	-2.45	-5.21	-6.92
IAF75	-2.83	-13.64	-17.85	-11.29	-3.27	-22.60	-4.51	-6.18	-11.19	-30.74	-14.65	-1.93	6.75	-16.27	-10.32	-17.26	-2.56	-5.09	-8.26
IAF77	-1.98	-13.76	-18.29	-11.83	-2.61	-23.58	-4.77	-5.13	-9.74	-25.94	-13.30	-2.00	7.07	-12.99	-10.73	-13.40	-2.31	-5.84	-6.93
IAF78	-0.70	-4.75	-17.05	-13.57	-2.26	-24.85	-2.58	-4.75	-6.87	-26.86	-12.78	-1.87	10.67	-14.92	5.61	-13.87	-1.65	-8.57	-9.77
IAF79	-2.65	-7.84	-20.68	-11.09	-2.97	-22.82	-6.04	-5.64	-10.03	-20.23	-13.37	-2.58	6.44	-13.01	-12.88	-19.33	-2.45	-6.42	-6.16
IAF80	-1.77	-6.82	-18.81	-12.77	-3.19	-24.08	-4.25	-6.03	-10.29	-26.49	-14.51	-2.30	9.85	-14.37	-11.25	-17.94	-2.24	-5.51	-7.42
IAF81	-2.70	-8.15	-22.89	-10.93	-3.52	-20.70	-6.38	-6.05	-10.80	-26.20	-14.44	-2.98	7.34	-12.60	-9.75	-17.42	-2.23	-6.28	-7.67
IAF82	-2.31	-9.14	-16.17	-10.15	-4.89	-24.67	-1.46	-5.51	-8.52	-29.21	-14.96	-3.17	12.44	-13.51	-10.57	-18.81	-3.24	-5.97	-3.77
IAF83	-0.61	-8.70	-14.05	-10.06	-4.66	-24.51	-2.09	-4.86	-10.11	-24.94	-13.64	-3.08	8.44	-14.40	-12.84	-19.56	-2.87	-6.48	1.70
IAF84	-2.30	-9.21	-15.72	-10.78	-4.26	-24.89	-0.70	-6.02	-9.56	-32.12	-14.89	-2.95	9.54	-13.47	-8.23	-18.26	-2.53	-6.16	-5.29
IAF86	-2.20	-14.32	-15.94	-11.71	-4.15	-24.54	-0.96	-5.48	-8.66	-25.52	-14.41	-3.47	9.07	-12.90	-11.77	-18.15	-2.67	-6.78	-3.04
IAF87	-1.43	-8.64	-14.04	-10.31	-4.10	-21.84	-4.21	-5.28	-8.52	-23.04	-12.16	-3.04	5.49	-10.61	-12.96	-18.48	-2.56	-7.25	-6.52
IAF88	-1.84	-10.68	-14.71	-11.91	-4.48	-23.50	-3.78	-4.70	-7.34	-30.20	-13.77	-3.10	6.92	-11.76	-12.15	-17.63	-4.20	-6.36	-7.95
IAF89	-1.57	-9.80	-19.04	-11.41	-4.28	-21.90	-0.64	-5.02	-11.13	-29.86	-15.15	-4.33	12.54	-9.58	-4.65	-17.29	-2.75	-6.68	-5.44
IAF90	-4.26	-16.69	-5.57	-14.26	-4.01	-14.99	-10.26	-5.24	-13.44	-3.56	-14.14	-0.79	11.27	-18.05	-15.65	-11.72	-7.59	-6.59	-6.93
IAF91	-4.57	-21.01	-15.12	-14.37	-3.49	-12.03	-9.75	-4.61	-16.84	-3.41	-12.63	-2.84	10.69	-14.27	-15.79	-10.78	-4.42	-7.82	-7.23
IAF93	-4.33	-8.82	-15.62	-12.71	-2.25	-12.92	-10.61	-4.55	-9.53	-26.63	-13.37	-2.65	4.42	-16.10	-10.41	-11.38	-1.55	-7.05	-7.36
IAF94	-6.10	-5.18	-13.46	-12.62	-2.72	-11.33	-4.34	-3.35	-7.21	-27.47	-5.63	-4.29	-0.84	-18.95	-0.80	-9.95	-1.96	-7.27	-6.29
IAF95	-6.97	-9.06	-7.61	-14.10	-2.58	-13.93	-9.95	-4.42	-10.62	-11.00	-6.79	-1.46	19.40	-19.49	0.39	-10.25	-7.01	-7.52	-6.08
IAF96	0.94	-7.03	-12.79	-16.90	-4.96	-8.80	-10.95	-3.90	-14.67	-5.82	-13.04	-2.53	10.20	-15.89	8.27	-15.55	-8.01	-4.62	-8.82
IAF100	-4.34	-6.52	-15.38	-10.87	-0.81	-12.00	-8.65	-3.28	-8.37	-26.97	-12.30	-3.08	13.17	-11.45	-10.66	-10.63	-0.89	-7.69	-8.05